FLOODPLAIN INUNDATION MAPPING FOR ASSESSING THE IMPACTS OF CLIMATE CHANGE ON FLOOD EXTENT : A CASE OF CHIANG MAI MUNICIPALITY THAILAND

Kowit Boonrawd

A Thesis Submitted in Fulfillment of the Requirements for the Degree of Doctor of Philosophy in Civil Engineering

Suranaree University of Technology

Academic Year 2017

การทำแผนที่น้ำท่วมบนที่ราบน้ำท่วมสำหรับประเมินผลกระทบจากการเปลี่ยนแปลงภูมิอากาศต่อขอบเขตน้ำท่วม กรณีศึกษาเทศบาลนครเชียงใหม่

นายโกวิท บุญรอด

วิทยานิพนธ์นี้เป็นส่วนหนึ่งของการศึกษาตามหลักสูตรปริญญาวิศวกรรมศาสตรดุษฎีบัณฑิต

สาขาวิชาวิศวกรรมโยธา

มหาวิทยาลัยเทคโนโลยีสุรนารี

ปีการศึกษา 2560

FLOODPLAIN INUNDATION MAPPING FOR ASSESSING THE IMPACTS OF CLIMATE CHANGE ON FLOOD EXTENT : A CASE OF CHIANG MAI MUNICIPALITY THAILAND

Suranaree University of Technology has approved this thesis submitted in partial fulfillment of the requirements for the Degree of Doctor of Philosophy.

Thesis Examining Committee

(Asst. Prof. Dr. Kittiwet Kuntiyawichai)

Chairperson

(Assoc. Prof. Dr. Chatchai Jothityangkoon)

Member (Thesis Advisor)

(Asst. Prof. Dr. Preeyaphorn Kosa)

Member

(Asst. Prof. Dr. Pornpot Tanseng)

Member

(Asst. Prof. Dr. Mongkol Jiravacharadet)

Member

(Prof. Dr. Santi Maensiri)

Vice Rector for Academic Affairs

and Internationalization

(Assoc. Prof. Flt. Lt. Dr. Kontorn Chamniprasart)

Dean of Institute of Engineering

โกวิท บุญรอด : การทำแผนที่น้ำท่วมบนที่ราบน้ำท่วมสำหรับประเมินผลกระทบจากการเปลี่ยนแปลงภูมิอากาศต่อขอบเขตน้ำท่วม กรณีศึกษา เทศบาลนครเชียงใหม่ (FLOODPLAIN INUNDATION MAPPING FOR ASSESSING THE IMPACTS OF CLIMATE CHANGE ON FLOOD EXTENT : A CASE OF CHIANG MAI MUNICIPALITY THAILAND) อาจารย์ที่ปรึกษา : รองศาสตราจารย์ ดร.ฉัตรชัย โชติษฐยางกูร, 136 หน้า.

การประเมินผลกระทบจากการเปลี่ยนแปลงภูมิอากาศต่อขอบเขตน้ำท่วม ใช้ข้อมูลอนุกรมเวลาของฝนในอนาคต จากแบบจำลองภูมิอากาศระดับภูมิภาค (RCM) 2 ประเภท คือ Providing Regional Climates for Impacts Studies (PRECIS) and Meteorological Research Institute (MRI) ซึ่งมีความละเอียด 0.2 x 0.2 องศา (ขนาดกริด 20 x 20 ตารางกิโลเมตร) ข้อมูลรายวันในปี ค.ศ. 2015-2044 และสร้างจากแบบจำลองภูมิอากาศโลก รุ่นที่ 4 (ECHAM4) การปรับแก้ข้อมูลฝนในอนาคต ใช้แฟกเตอร์ปรับแก้ (AFs) บนพื้นฐานวิธี empirical quantile mapping โดยใช้ AFs ตามฤดูกาลรายเดือนร่วมกับ AFs รายวัน ปรับแก้ข้อมูลฝนในอนาคตทั้งจาก PRECIS และ MRI การทดสอบแบบจำลองแรสเตอร์กึ่ง 2 มิติ ประยุกต์ใช้ในการสร้างพื้นผิวน้ำและประมาณขอบเขตน้ำท่วม ที่สมจริงมากขึ้น แบบจำลองนี้นำมาประยุกต์ใช้สำหรับการสร้างแผนที่ขอบเขตน้ำท่วมรายชั่วโมง ของเขตเทศบาลเมืองเชียงใหม่ พัฒนาการเชื่อมต่อแบบจำลองสมดุลของน้ำและแบบจำลองน้ำท่วมบนที่ราบน้ำท่วมเข้าด้วยกันรับอนุกรมเวลาของฝนในอนาคต เปลี่ยนเป็นน้ำท่า เพื่อใช้สร้างแผนที่น้ำท่วมบนที่ราบน้ำท่วม ของเทศบาลเมืองเชียงใหม่ สำหรับประเมินผลกระทบจากการเปลี่ยนแปลงภูมิอากาศ การใช้ปริมาณฝนในอนาคตจากข้อมูล PRECIS พบว่าพื้นที่น้ำท่วมเพิ่มขึ้นร้อยละ 89.5, 20.8, 10.2 และ 7.0 ตามรอบการเกิดซ้ำที่ 10, 25 , 50, 100 ปีตามลำดับ สำหรับปริมาณฝนในอนาคตจากข้อมูล MRI มีแนวโน้มไปในทิศทางเดียวกัน แต่มีค่าสูงกว่า PRECIS โดยพื้นที่น้ำท่วมเพิ่มขึ้นร้อยละ 91.2, 30.4, 22.1 และ 21.5 ตามรอบการเกิดซ้ำที่ 10, 25 , 50, 100 ปีตามลำดับ เมื่อเทียบกับแผนที่น้ำท่วมในอดีต จากนั้นใช้ข้อมูลแบบจำลองระดับสูงเชิงเลข (DEM) ที่มีความละเอียดเชิงพื้นที่ 5 เมตร (ขนาดเซลล์ 5, 5) สามารถสร้างแผนที่น้ำท่วมที่ความน่าเชื่อถือมากขึ้นและนำมาประยุกต์ใช้กับการสร้างแผนที่ขอบเขตน้ำท่วมบนที่ราบน้ำท่วมสำหรับน้ำท่วมสูงสุดในแต่ละรอบการเกิดซ้ำ ของเทศบาลนครเชียงใหม่

สาขาวิชาวิศวกรรมโยธา ลายมือชื่อนักศึกษา ____________

ปีการศึกษา 2560 ลายมือชื่ออาจารย์ที่ปรึกษา ____________

KOWIT BOONRAWD : FLOODPLAIN INUNDATION MAPPING FOR ASSESSING THE IMPACTS OF CLIMATE CHANGE ON FLOOD EXTENT : A CASE OF CHIANG MAI MUNICIPALITY THAILAND. THESIS ADVISOR : ASSOC. PROF. CHATCHAI JOTHITYANGKOON, Ph.D., 136 PP.

RCMs/BIAS CORRECTION/ADJUSTMENT FACTOR/FLOOD INUNDATION MAP/CHIANG MAI MUNICIPALITY

To assess the impact of climate change on flood extent, a time series of future projection rainfall from two types of regional climate model (RCM); Providing Regional Climates for Impacts Studies (PRECIS) and Meteorological Research Institute (MRI) were used. They are RCM with resolution 0.2 x 0.2 degree (grid size 20 x 20 km) daily time step, from year 2015-2044 and generated from ECHAM 4 climate models. For bias correction of the projection rainfall, adjustment factor (AFs) based on empirical quantile mapping from a combination of seasonal monthly AF for monthly data and AFs for daily data is used to correct the future projection rainfall from both PRECIS and MRI. The quasi 2-D raster model was tested and applied to generate more realistic water surface and was used to estimate flood extent. The model was applied to the floodplains of Chiang Mai Municipality and used to estimate a time series of hourly flood maps. Coupling of water balance model and floodplain inundation model was developed to receive the projected rainfall time series to generate flood extent in flood plain and draw flood inundation map of Chiang Mai municipality. For PRECIS, the inundation area in Chiang Mai Municipality is increased by 89.5, 20.8, 10.2 and 7.0 % with 10, 25, 50, 100 years return period,

respectively. Similar trend occurs for MRI with higher percentage than PRECIS, increased by 91.2, 30.4, 22.1 and 21.5 % with 10, 25, 50, 100 years return period, respectively. Further when a fine spatial resolution of DEM was available based on spatial resolution of 5 meters (cell size 5, 5) data, then this data was used to simulate more reliable inundation map and applied to the whole flooding area of Chiang Mai municipality, including the assessment of flood inundation extent from flood peaks with return period.

School of Civil Engineering Student's Signature ________________

Academic Year 2017 Advisor's Signature Chatchai Joth

CHAPTER I

OVERVIEW

1.1 Introduction

Decision makers are increasingly demanded climate information at the national to local scale in order to address the risk posed by projected climate changes and their anticipated impacts. Readily available climate change projections are provided at global and continental spatial scales for the end of the 21st century (Intergovernmental Panel on Climate Change (IPCC), 2007). These projections, however, do not fit the needs of sub-national adaptation planning that requires regional and or local projections of likely conditions five to 10 years from now. Moreover, decision makers are interested in understanding the impacts of climate change on specific sectors, e.g., agricultural production, food security, disease prevalence, and population vulnerability.

In response to this demand, numerous impact and vulnerability assessments produced at different scales, from global to local, provide climate change impact results at spatial scales much finer than those at which projections are initially made. To produce such results, combinations of methods and indicators are often used, each with its own assumptions, advantages, and disadvantages. In reports, these essential factors may not be adequately communicated to the reader, thus leaving him/her without the ability to understand potential discrepancies between different reports.

Often, global or continental-scale information is directly used to produce local-scale impact maps, which is not appropriate since this large-scale information does not account for differences at the local scale. In order to derive climate projections at scales that decision makers desire, a process termed downscaling has been developed. The impact assessment studies of climate change in various basins different part of the world indicate changes in the amount of precipitation, its frequency and intensity affecting the magnitude and seasonal pattern of streamflow.

Flood inundation maps are a major tool for mitigating the effects of flooding. They provide predictions of flood extent and depth that are used in the development of spatially accurate hazard maps. These allow the assessment of risk to life and property in the floodplain, and the prioritization of either the maintenance of existing flood defenses or the construction of new ones. Flood plain maps indicate the geographical areas, which could be covered by a flood according to one or several probabilities: floods with a very low probability or extreme events scenarios; floods with a medium probability (likely return period ≈100y); floods with a high probability.

Flood hazard maps are detailed flood plain maps complemented with: type of flood, the flood extent; water depths or water level, flow velocity or the relevant water flow direction.

Flood risk maps indicate potential adverse consequences associated with floods under several probabilities, expressed in terms of the indicative number of inhabitants potentially affected type of economic activity of the area potentially affected installation which might cause accidental pollution in case of flooding; other information which the member state considers useful. To overcome some of the inconveniences of traditional flood risk assessment methods, a qualitative multi criteria index, called Flood Risk Index (FRI) is currently applied. This approach considers not only flood properties but also social-economic characteristics of the affected area and population (Zonensein et al. 2008).

Flood vulnerability maps present the degree of fragility of a (natural or socio-economic) community or a (natural socioeconomic) system towards natural hazards. It is a set of conditions and processes resulting from physical, social, economical and environmental factors, which increase the susceptibility of the impact and the consequences of natural hazards. Vulnerability is determined by the potential of a natural hazard, the resulting risk and the potential to react to and/or to withstand it, i.e. its adaptability, adaptive capacity and/or coping capacity.

Floods are destructive natural phenomena which can lead to serious problems in lowland regions, resulting in significant loss of human life and affecting fertility of natural resources and man-made properties. For example, during August and September 2005, the Chiang Mai Province had experienced at least 4 severe floods resulted from overbank flow from Ping River after having prolonged upstream intense rainfall. This event resulted in almost half of the municipal area was inundated for several days and was regarded as being worst flooding scenario ever seen in the province for almost 50 years. The total damage was estimated about more than 5 billion baths. At the peak flood, the water level recorded from gauge station P.1 at the Navarat Bridge was as high as 4.93 meter while the critical value for having flood (or overbank flow) was approximately at 3.70 meter only (Chatchawan, 2005).

Minyan et al., (2009) applied 1D flood model HEC-RAS for the Ping River and estimated the inundation area and flood depth for the year 2005 flood event in

Chiang Mai province. The sub objectives were to verify the model by comparing the flood inundation area and depth with the remote sensing image and surveyed data and prepared hazard map. HEC-GeoRAS was used as an interface between Arc-View and HEC-RAS. The final inundation map was visualized in ArcView GIS and used for hazard analysis. The general procedure adopted for inundation modeling consists basically of four steps; i) GeoRAS pre-processing to generate a HEC-RAS import file, ii) running of HEC-RAS to calculate water surface profiles, and iii) post-processing of HEC-RAS results, and iv) flood hazard mapping. The pre-processing phase included generation of DEM of the floodplain and the riverbed followed by centerline extraction of the river and creating cross-sections in the river. Geometric corrections of the floodplain and the river cross-sections in HEC-RAS were a part of the running of HEC-RAS phase. The post-processing comprised of the comparison of the model outputs with the extent and depth of satellite image and field data. Hazard analysis comprised of the using the model output for hazard zone in a GIS-based analysis. From the result, it was observed that the areas of 14 districts were inundated by the year 2005 flood, which was reasonably close to the base map classified from Landsat7 (ETM+) data acquired during the flood time. And the flood depth varies from 0 to 1.68 meter depth in the flood plain which is in conformity with the data taken during the field survey. The total area under hazard was 1,579 km^2. Out of this area, 274 km^2 was low hazard, 410 km^2 was medium hazard while 555 km^2 was high hazard and 338 km^2 was under very high hazard category. The numbers of schools, hospitals, factories affected by the 2005 flood were calculated by overlaying them with the final hazard map. And there are 590 numbers of schools, 142 numbers of hospitals, and 451 factories were affected by this flood event.

Duong et al., (2015) used runoff generation data from the MRI-AGCM3.2S dataset. This data was fed into distributed flow routing model 1K-FRM to project river discharge under a changing climate. Flow routing model 1K-FRM was developed in the Hydrology and Water Resources Research Laboratory, Kyoto University. The MRI-AGCM3.2S is the latest version of super-high-resolution atmospheric general circulation model which was jointly developed by Japan Meteorological Agency (JMA) and Meteorological Research Institute (MRI). Two river basins located in Kyushu (Japan) were selected as study areas, the Chikugo river basin and the Oyodo river basin. Since the observed runoff generation data is not available, the land surface model Simple Biosphere including Urban Canopy (SiBUC) was applied to reproduce runoff generation data to use in bias correction of the MRI-AGCM3.2S's output. SiBUC model was developed in the Disaster Prevention Research Institute, Kyoto University. Corrected runoff generation data were used to project river discharge and examined the changes in river discharge in those two basins under a changing climate.

Takahiro et al., (2015) presents a method to evaluate the impact of climate change by using GCM output and a Rainfall-Runoff-Inundation (RRI) model. The GCM used in this study is MRI-AGCM3.2S and 3.2H, the former one is the finest spatial resolution GCM in the world (20 km), while the latter one (60 km) is used to provide ensemble information with different cumulous schemes and sea surface temperature clusters to assess the uncertainty. In particular, this study focuses on flood inundation volumes in the Chao Phraya River basin in Thailand to evaluate how the frequency of devastating flooding like the one in 2011 will change in future under SRES-A1B scenario (2075-2099). The simulation results indicated the possible increase in average monsoon rainfall by approximately 1.1 times and the average flood inundation volume by 1.4 times, and accordingly shorten the return period of the large scale flooding in the future.

Pukongduean (2014) applied MIKE21 (2D hydrodynamic model) to generate urban flood severity map for Mueang Nakhon Ratchasima. Combining with the integration of physical, social, economic and environmental factors using GIS-based multiplication to generate urban flood vulnerability index and its classification map. From the result, simulated urban flood of reducing historical discharge in 2010 at Kud Hin Watergate by 10% was applied to simulate flood extent and economic value loss in different scenarios to optimize minimal flood extent and economic value loss for flood mitigation and prevention. Based on calibration process of MIKE 21 between the derived flood extent by model and flood record of Nakhon Ratchasima province in 2010 by Geo-Informatics and Space Technology Development Agency, it found that constant Manning's N is capable to give good comparable flood extent. Urban flood extent had represented the highest extent on 24 October 2010 with area of 88.36 km^2. The agricultural land is the main land use that was affected from flood with area of 76.89 km^2, followed by urban and built-up area of 7.74 km^2. The simulated flood depth during 14-27 October 2010 ranged between 0.10 and 3.91 m. while flood velocity varied from 0.00 to 2.06 m/s. Meanwhile, 8 days flood duration created the highest flooded area of 18.48 km^2. For urban flood severity analysis, the combination of the normalized of flood depth and velocity was classified into 5 classes: very low, low, moderate, high and very high using standard deviation classification method covered area of 29.27, 36.24, 16.76, 4.16 and 2.31 km^2, respectively. Meanwhile, urban flood vulnerability index values were classified into 5 classes: very low, low, moderate, high and very high using standard deviation classification covered area of 83.70, 2.17, 1.11, 0.66 and 1.13 km^2, respectively. Furthermore, urban flood simulation for flood mitigation and prevention had illustrated that when historical discharge in 2010 at Kud Hin Watergate was reduced by 60% or less than 17.82 m^3/s, it can mitigate urban flood and when discharge was reduced by 67% or less than 14.70 m^3/s, it can prevent urban flood in Mueang Nakhon Ratchasima district.

The objective of this work is to study the impacts of climate change on maximum annual discharges in the upper Ping River of Thailand and focusing on the future expansion of flood inundation in community area of Chiang Mai municipality and its vicinity, which is an initial step to develop flood hazard map (Osti, et al., 2008)

1.2 Aim and Significance

1.2.1 Develop bias corrected RCM data or distribution mapping based on derived Adjustment Factors (AF), which is the ratio between observed and simulated rainfall for a given frequency of occurrence.

1.2.2 Develop 1-D flood routing model and quasi 2-D floodplain inundation model which is applied for mapping space-time flood extent to the floodplains of Chiang Mai, north of Thailand and used to estimate a time series of hourly flood maps.

1.2.3 Construct future flood inundation map of Ching Mai Municipality as a consequence of climate change.

Flood inundation map with 100 years return period is a standard indicators for flood protection and mitigation. For Chiang Mai municipality, only observed flood extent from past floods was recorded to draw inundation map.

Reliable flood inundation map (100 years return period) which including the pact of climate changes is still not available for Chiang Mai municipality. This flood inundation map will be required for implementation and assessment of future flood protection measures for both structural and non-structural measures such as flood likes, diversion channel, building permits, environmental regulations and flood insurance.

1.3 Background

1.3.1 GCMs and RCMs data

(1) General Circulation Models

General or global circulation models (GCMs) simulate the Earth's climate via mathematical equations that describe atmospheric, oceanic, and biotic processes, interactions, and feedbacks. They are the primary tools that provide reasonably accurate global-, hemispheric-, and continental-scale climate information and are used to understand present climate and future climate scenarios under increased greenhouse gas concentrations.

A GCM is composed of many grid cells that represent horizontal and vertical areas on the Earth's surface (see Figure 1.1). In each of the cells, GCMs compute the following: water vapor and cloud atmospheric interactions, direct and indirect effects of aerosols on radiation and precipitation, changes in snow cover and sea ice, the storage of heat in soils and oceans, surfaces fluxes of heat and moisture,

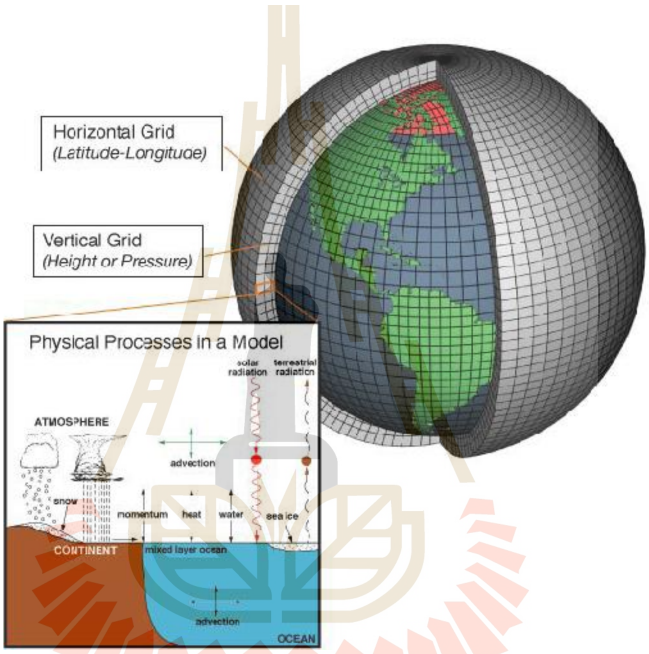
Horizontal Grid
(Latitude-Longitude)
Vertical Grid
(Height or Pressure)
Physical Processes in a Model
solar radiation
terrestrial radiation
ATMOSPHERE
advection
snow
momentum
heat
water
sea ice
CONTINENT
mixed layer ocean
advection
OCEAN

emissions. However, the magnitude of this increase varies from one model to another. Additionally, in certain regions, different models project opposite changes in rainfall amount, which highlights the uncertainty of future climate change projections even when sophisticated state-of-the art GCM tools are used.

There are four main sources of uncertainty in climate projections:

1. Uncertainty in future levels of anthropogenic emissions and natural forcings (e.g., volcanic eruptions);

2. Uncertainty linked to imperfect model representation of climate processes;

3. Imperfect knowledge of current climate conditions that serve as a starting point for projections; and

4. Difficulty in representing interannual and decadal variability in long-term projections.

Efforts are made to quantify these uncertainties. The future evolution of greenhouse gas emissions is highly uncertain due to socio-economic, demographic, and technological evolution. Alternative greenhouse gas emissions scenarios are used to drive GCMs in order to obtain a range of possible future outcomes. Additionally, models require initial conditions (Current state of the atmosphere.) to begin the forecast, and these are also not known with high accuracy. Therefore, projections are performed starting from slightly modified initial conditions to obtain a series of simulations, termed an ensemble. Finally, models cannot perfectly simulate all climate processes; therefore, simulations from multiple models are produced, and a multi-model ensemble mean or median (Different GCMs simulate certain climate processes accurately and others erroneously. Thus, a variety of GCMs are run, and the mean of this ensemble is determined to be the best estimate projection) is thought to be the most probable future climate trajectory. The spread among the individual simulations in a multi-model ensemble are an estimate of uncertainty due to sources 2 and 3 in the preceding list. It is important to communicate uncertainty in climate change projections and provide the following messages:

- Uncertainty does not mean that future projections are unknown or false.

- Uncertainty can be quantified.

- Decisions can be made in the face of uncertainty. For example, decisions are routinely made in the context of military operations and financial investments when uncertainty is greater than that of climate projections.

Figure 1.2 illustrates uncertainty in GCM simulation of historical global temperature change (IPCC, 2007). The black line represents observed temperature anomalies, and each yellow line is a simulation produced by an individual GCM with the red line being the multi-model ensemble mean. The spread between the simulations illustrates uncertainty. Note that although the individual GCM simulations provide different results, there is consensus and general agreement between the models.

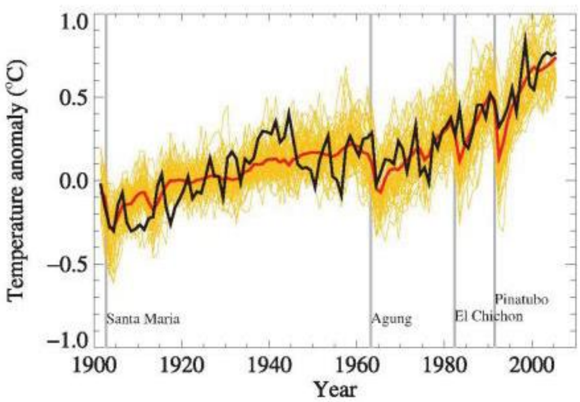

Temperature anomaly (°C)
1.0
0.5
0.0
−0.5
−1.0
1900
1920
1940
1960
1980
2000
Year
Santa Maria
Agung
El Chichon
Pinatubo

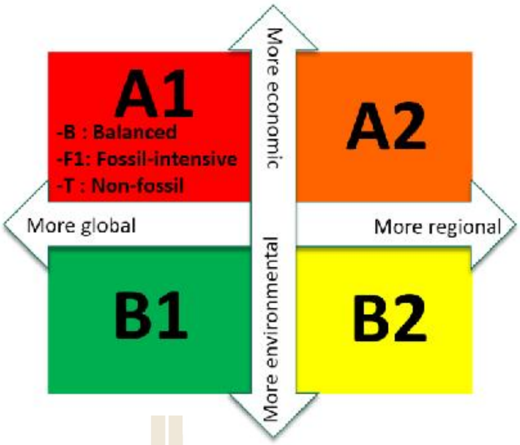
A1
-B : Balanced
-F1: Fossil-intensive
-T : Non-fossil
A2
B1
B2
More economic
More environmental
More global
More regional

fertility follows local historical traditions rather than patterns of developing countries. Global population does not peak in mid-century. Economic development is linked to regional rather than global patterns.

Scenario B1 has global population peaking around 2050 and declining thereafter. Economic growth is more globally linked but with introduction of clean and resource-efficient technologies. Social equity is emphasized with global attention to economic, social and environmental problems. However, there are no global restrictions on emissions of greenhouse gases.

Scenario B2 has an increasing global population, but somewhat less than A2, which does not peak in mid-century. Emphasis is on a local approaches to addressing economic, social, and environmental sustainability. Emphasis is on environmental protection and social equity through local approaches. Economic development is not as rapid as in B1 and A1 but with more diverse technological change.

(2) Regional Climate Model

Regional climate model (RCM), similar to a GCM in its principles but with high resolution. RCMs take the large-scale atmospheric information supplied by GCM output at the lateral boundaries and incorporate more complex topography, the land-sea contrast, surface heterogeneities, and detailed descriptions of physical processes in order to generate realistic climate information at a spatial resolution of approximately 20-50 kilometers (see Figure 1.4). Mean annual temperature is presented at 500 kilometer typical GCM grid cell; 50 kilometer typical RCM grid cell; and 1 meter, which requires statistical downscaling.

Figure 1.4 Mean annual temperature (1961–1990), Source: Daniels et al. (2012).

1.3.2 Downscaling technique

Although GCMs are valuable predictive tools, they cannot account for fine-scale heterogeneity of climate variability and change due to their coarse resolution. Numerous landscape features such as mountains, water bodies, infrastructure, land-cover characteristics, and components of the climate system such as convective clouds and coastal breezes, have scales that are much finer than 100-500 kilometers. Such heterogeneities are important for decision makers who require information on potential impacts on crop production, hydrology, species distribution, etc. at scales of 10-50 kilometers.

Various methods have been developed to bridge the gap between what GCMs can deliver and what society/businesses/stakeholders require for decision making. The derivation of fine-scale climate information is based on the assumption that the local climate is conditioned by interactions between large-scale atmospheric characteristics (circulation, temperature, moisture, etc.) and local features (water bodies, mountain ranges, land surface properties, etc.). It is possible to model these

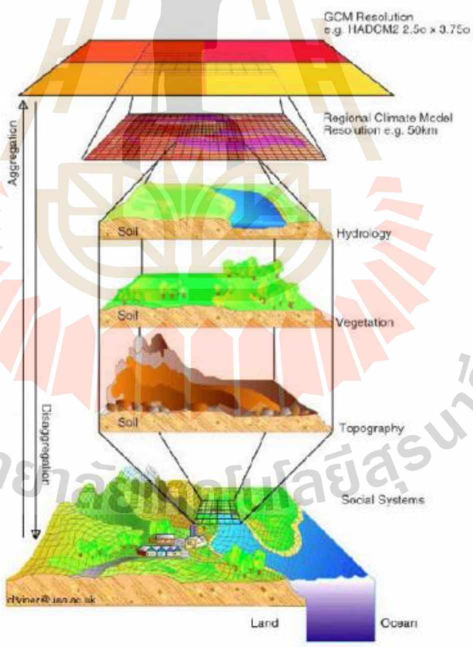
GCM Resolution
e.g. HADCM2 2.5o x 3.75o
Regional Climate Model
Resolution e.g. 50km
Aggregation
Soil
Hydrology
Soil
Vegetation
Soil
Topography
Disaggregation
Social Systems
Land
Ocean

spatial climate information from coarser-resolution GCM output, e.g., 500 kilometers grid cell GCM output to a 20 kilometers resolution, or even a specific location. Temporal downscaling refers to the derivation of fine-scale temporal information from coarser-scale temporal GCM output (e.g., daily rainfall sequences from monthly or seasonal rainfall amounts). Both approaches detailed below can be used to downscale monthly GCM output to localized daily information.

(1) Dynamical Downscaling

General Theory

Dynamical downscaling refers to the use of an RCM driven by a GCM to simulate regional climate. An RCM is similar to a GCM but has higher resolution and additional regional information, which enables it to better represent local landscape and possibly local atmospheric processes. The global model simulates the response of the global circulation to changes in atmospheric composition through a large number of processes, but some of them need to be approximated due to the coarse resolution of the models. On the other hand, at the resolution of 25-50 km for portions of the globe, the RCM is able to capture some of those smaller-scale processes more realistically. Atmospheric fields (e.g., surface pressure, wind, temperature, and humidity) simulated by a GCM are fed into the vertical and horizontal boundaries of the RCM. Locally specific data and physics-based equations are then used to process this information and obtain regional climate outputs. The primary advantage of RCMs is their ability to model atmospheric processes and land cover changes explicitly.

Assumptions and Caveats

Although there has been great advancement during the past decade in the technical ability of RCMs to simulate regional climate, significant challenges and concerns still exist. Since smaller grid cells, more surface information, and often more processes are included in an RCM, the number of computations might be as large, if not larger, than in a GCM that covers the entire globe. Thus, RCMs are computationally demanding and may require as much processing time as a GCM to compute projections (Wilby et al., 2009). They also require a substantial amount of input, e.g., surface properties and high-frequency GCM information. In addition, complex calibration procedures are often needed to make realistic simulations.

Just like GCMs, RCMs have difficulty accurately simulating convective precipitation, which is a major concern for tropical regions. Most RCMs also do not accurately simulate extreme precipitation. A systematic bias that can worsen as the resolution is increased. Statistical bias corrections often need to be performed to better match the model output to the observations (Brown et al., 2008). In some cases, fine adjustments to the convective schemes can improve the realism of simulated rainfall, but these adjustments require substantial expertise and reduce geographic portability

Regional Climate Models and Application

RCMs are developed by research institutions that have sufficient computational capacity and technical expertise. Various RCMs differ in their numerical, physical, and technical aspects. The most commonly used RCMs in climate change downscaling studies include the U.S. Regional Climate Model Version 3 (RegCM3); Canadian Regional Climate Model (CRCM); UK Met Office Hadley Centre’s Regional Climate Model Version 3 (HadRM3); German Regional Climate Model (REMO); Dutch Regional Atmospheric Climate Model (RACMO); and German HIRHAM, which combines the dynamics of the High Resolution Limited Area Model (HIRLAM) and European Centre-Hamburg (ECHAM) models.

Although the above models have been developed primarily over North America and Europe, they can be adapted to any region of the globe by incorporating appropriate information on terrain, land-cover, hydrology, and so on; hence, several RCM can be used over a given region. However, downscaled results can differ depending on which RCM(s) is used. It is important to recognize that a single RCM will most likely not provide 'accurate' results; therefore, researchers, practitioners, and decision makers should utilize the results with caution, keeping in mind dynamical downscaling assumptions and caveats.

Most intensive downscaling studies and projects utilize various RCMs to produce a multi-model ensemble and further validate results against observations. A variety of climate change assessment projects have been established to provide high-resolution climate change scenarios for specific regions. They are usually multi-country, multi-institutional, large-scale projects. They are an important source of regional projections as well as of additional information about RCMs, methods, and even characteristics of current regional climate.

(2) Statistical Downscaling

General Theory

Statistical downscaling involves the establishment of empirical relationships between historical large-scale atmospheric and local climate characteristics. Once a relationship has been determined and validated, future large-scale atmospheric conditions projected by GCMs are used to predict future local climate characteristics. In other words, large-scale GCM outputs are used as predictors to obtain local variables or predictands. Statistical downscaling encompasses a heterogeneous group of methods that vary in sophistication and applicability (see Table 1.1).

Statistical downscaling methods are computationally inexpensive in comparison to RCMs that require complex modeling of physical processes. Thus, they are a viable and sometimes advantageous alternative for institutions that do not have the computational capacity and technical expertise required for dynamical downscaling. Unlike RCMs, which produce downscaled projections at a spatial scale of 20-50 kilometers, statistical methods can provide station-scale climate information.

Assumptions and Caveats

Although statistical downscaling is efficient, computationally inexpensive, and consists of a diverse group of methods, it contains the following inherent assumptions:

1. The statistical relationship between the predictor and predictand does not change over time.

2. The predictor carries the climate change signal.

3. There is a strong relationship between the predictor and predictand.

4. GCMs accurately simulate the predictor.

The first point is known as the stationarity assumption and postulates that the statistical relationship between the predictor and predictand remains stable into the future. Whether relationships based on present associations will be upheld under future climate conditions is unknown. The second is the assumption that the large-scale variable represents the climate system and captures any change that may occur in the future. Assumption three implies that the strength of the relationship should be initially evaluated to determine its validity. Assumption four relates to the ability of a

GCM to simulate climate variables observed in the past as well as their future evolution. Predictor validations are usually performed prior to a given GCM's use in downscaling schemes.

Main Categories

Statistical downscaling consists of a heterogeneous group of methods that vary in sophistication and applicability. They are all relatively simple to implement but require a sufficient amount of high-quality observational data.

Methods can be classified into three main categories:

1. Linear methods: Establish linear relationships (i.e., some type of proportionality), between predictor(s) and predictand. Linear methods are very straightforward and widely used, and they can be applied to a single predictor-predictand pair or spatial fields of predictors-predictands. The greatest constraint is the requirement of a normal distribution of the predictor and the predictand values, which means that it cannot be used to predict the distribution of daily rainfall because it is typically non-normal (frequent small amounts of rainfall and a few heavy events generally make the distribution not symmetrical). These methods are primarily used for spatial downscaling.

2. Weather classifications: The local variable is predicted based on large-scale atmospheric states. The states can be identifiable synoptic weather patterns or hidden, complex systems. The future atmospheric state, simulated by a GCM, is matched with its most similar historical atmospheric state. The selected historic atmospheric state then corresponds to a value or a class of values of the local variable, which are then replicated under the future atmospheric state. These methods are particularly well suited for downscaling non-normal distributions, such as daily

rainfall. However, a large amount of observational daily data (e.g., 30 years of daily data for the region of interest) is required in order to evaluate all possible weather conditions. In addition, these methods are more computationally demanding in comparison to linear ones, due to the large amount of daily data analyzed and generated.

3. Weather generators: These statistical methods are typically used in temporal downscaling. For example, they are used to generate daily sequences of weather variables (e.g., precipitation, maximum and minimum temperature, humidity, etc.) that correspond to monthly or annual averages or amounts. Temporal downscaling is necessary for some impact models that require local spatial data at a daily resolution, which GCMs cannot reliably provide. Weather generators produce sequences of daily values, but since different weather sequences may be associated with a given set of, for example, monthly values, multiple sequences commonly are generated to be further used in impact models. Weather generators are data-intensive, require long sequences of daily data, and are sensitive to missing or erroneous data in the calibration set (Wilby et al., 2009). In addition, only some weather generators have the ability to account for the coherency among variables when multiple variables are predicted, e.g., to generate a daily sequence of insolation that matches the generated daily sequence of rainy and dry days.

Table 1.1 identifies various statistical downscaling methods under the linear, weather classification, and weather generator categories, along with particular variable requirements, advantages, and disadvantages.

Table 1.1 Statistical downscaling category, method, predictor and predictand variables, advantages, and disadvantages.

Category & Method		**Predictor& predictand**	**Advantages**	**Disadvantages**
Linear Methods spatial	Delta method	Same type of variable (e.g., both monthly temperature, both monthly precipitation)	- Relatively straight-forward to apply - Employs full range of available predictor variables	- Requires normality of data (e.g., monthly temperature, monthly precipitation, long-term average temperature) - Cannot be applied to non-normal distributions (e.g., daily rainfall) - Not suitable for extreme events
	Simple and multiple linear regression	Variables can be of the same type or different (e.g., both monthly temperature or one monthly wind and the other monthly precipitation)		
	CCA& SVD			
Weather Classification Spatial and temporal	Analog method	Variables can be of the same type or different (e.g., both monthly temperature, one large-scale atmospheric pressure field and the other daily rainfall)	- Yields physically interpret-able linkages to surface climate - Versatile, i.e., can be applied to both normally and non-normally distributed data	- Requires additional step of weather type classification - Requires large amount of data and some computational resources - Incapable of predicting new values that are outside the range of the historical data
	Cluster analysis			
	ANN			
	SOM			

Table 1.1 Statistical downscaling category, method, predictor and predictand variables, advantages, and disadvantages (cont.).

<table>
<tr><th colspan="2">Category & Method</th><th>Predictor& predictand</th><th>Advantages</th><th>Disadvantages</th></tr>
<tr><td>Weather Generator
Spatial and temporal</td><td>LARS-WG</td><td rowspan="2">Same type of variable, different temporal scales (e.g., predictor is monthly precipitation and predictand is daily precipitation)</td><td rowspan="3">- Able to simulate length of wet and dry spells
- Produces large number of series, which is valuable for uncertainty analysis
- Production of novel scenarios</td><td rowspan="4">- Data-intensive
- Sensitive to missing or erroneous data in the calibration set
- Only some weathers generators can check for the coherency between multiple variables (e.g., high insolation should not be predicted on a rainy day)
- Requires generation of multiple time-series and statistical post-processing of results</td></tr>
<tr><td></td><td>Mark Sim GCM</td></tr>
<tr><td></td><td>NHMM</td><td>Variables can be of the same type or different (e.g., both monthly temperature, one large-scale atmospheric pressure and the other daily rainfall)</td></tr>
<tr><td colspan="4">CCA: Canonical Correlation Analysis
SVD: Singular Value Decomposition
ANN: Artificial Neural Network
SOM: Self-Organizing Map
LARS-WG: Long Ashton Research Station Weather Generator
GCM: General Circulation Model
NHMM: Nonhomogeneous Hidden Markov Model</td></tr>
</table>

Summary of Downscaling Approaches

Table 1.2 attempts to summarize and compare different aspects of the dynamical and statistical downscaling approaches.

Table 1.2 Advantages, disadvantages, outputs, requirements, and applications of dynamical and statistical downscaling.

	Dynamical downscaling	**Statistical downscaling**
Provides	- 20-50 km grid cell information -Information at sites with no observational data -Daily time-series -Monthly time-series -Scenarios for extreme events	-Any scale, down to station-level information -Daily time-series (only some methods) -Monthly time-series -Scenarios for extreme events (only some methods) -Scenarios for any consistently observed variable
Requires	-High computational resources and expertise -High volume of data inputs -Reliable GCM simulations	-Medium/low computational resources -Medium/low volume of data inputs -Sufficient amount of good quality observational data -Reliable GCM simulations
Advantages	-Based on consistent, physical mechanism -Resolves atmospheric and surface processes occurring at sub-GCM grid scale -Not constrained by historical record so that novel scenarios can be simulated -Experiments involving an ensemble of RCMs are becoming available for uncertainty analysis	-Computationally inexpensive and efficient, which allows for many different emissions scenarios and GCM pairings -Methods range from simple to elaborate and are flexible enough to tailor for specific purposes -The same method can be applied across regions or the entire globe, which facilitates comparisons across different case studies -Relies on the observed climate as a basis for driving future projections -Can provide point-scale climatic variables for GCM-scale output -Tools are freely available and easy to implement and interpret; some methods can capture extreme events

Table 1.2 Advantages, disadvantages, outputs, requirements, and applications of dynamical and statistical downscaling (cont.).

	Dynamical downscaling	**Statistical downscaling**
Disadvantages	-Computationally intensive -Due to computational demands, RCMs are typically driven by only one or two GMC/emission scenario simulations -Limited number of RCMs available and no model results for many parts of the globe -May require further downscaling and bias correction of RCM outputs -Results depend on RCM assumptions; different RCMs will give different results -Affected by bias of driving GCM	-High quality observed data may be unavailable for many areas or variables -Assumes that relationships between large and local-scale processes will remain the same in the future (stationarity assumptions) -The simplest methods may only provide projections at a monthly resolution
Applications	-Country or regional level (e.g., European Union) assessments with significant government support and resources -Future planning by government agencies across multiple sectors -Impact studies that involve various geographic areas	-Weather generators in widespread use for crop-yield, water, and other natural resource modeling and management -Delta or change factor method can be applied for most adaptation activities

Sources: STARDEX, 2005; Fowler et al., 2007; Wilby et al., 2009; and Daniels et al., 2012.

Since the RCM is nested in a GCM, the overall quality of dynamically downscaled RCM output is tied to the accuracy of the large-scale forcing of the GCM and its biases (Seaby et al., 2013). Despite recovering important regional-scale features that are underestimated in coarse-resolution GCMs, RCM outputs are still subject to systematic errors and therefore often require a bias correction as well as further downscaling to a higher resolution.

Statistical downscaling involves the establishment of empirical relationships between historical and/or current large-scale atmospheric and local climate variables. Once a relationship has been determined and validated, future atmospheric variables that GCMs project are used to predict future local climate variables. Statistical downscaling can produce site-specific climate projections, which RCMs cannot provide since they are computationally limited to a 20-50 kilometers spatial resolution. However, this approach relies on the critical assumption that the relationship between present large-scale circulation and local climate remains valid under different forcing conditions of possible future climates (Zorita and von Storch, 1999). It is unknown whether present-day statistical relationships between large- and regional-scale variables will be upheld in the future climate system.

Oftentimes, dynamical and statistical approaches are used in conjunction. Dynamical-statistical downscaling involves the use of an RCM to downscale GCM output before statistical equations are used to further downscale RCM output to a finer resolution. Dynamical downscaling improves specific aspects of regional climate modeling and provides better predictors for further statistical downscaling to higher-resolution output (Guyennon et al., 2013). Statistical-dynamical downscaling is a somewhat more complex approach but is less computationally demanding in comparison to dynamical downscaling. This method statistically pre-filters GCM outputs into a few characteristic states that are further used in RCM simulations (Fuentes and Heimann, 2000).

Downscaling consists of a variety of methods, each with their own merits and limitations. International organizations or national governments currently provide no official guidance that assists researchers, practitioners, and decision makers in determining climate projection parameters, downscaling methods, and data sources that best meet their needs.

1.3.3 Rainfall-Runoff model

The development and the application of rainfall-runoff models have been a corner-stone of hydrological research for many decades. In general, the purpose of the development of these models is a two-fold. The first is to advance our understanding and state of knowledge about the hydrological processes involved in the rainfall-runoff transformation. The second is to provide practical solutions to many of the related environmental and water resources management problems.

Progress in the development of rainfall-runoff models has been accelerated by the fast advancement in the technology of digital computers which has allowed the storage and the processing of long records of data. These technological advances have provided fertile ground for the development of what might now be called a glut of rainfall-runoff models. Common features of all of these developed models are that, each is a simplified form of the real-world system and that all such models are to a greater or lesser extent, in error. Depending on the degree of the physical abstraction from the real world system, the rainfall-runoff model structures may be classified into three broad types (Clarke, 1994).

Distributed Physically-based Models which are based on the complex law of physics generally expressed as systems of non-linear partial differential equations.

Systems-Based (Black or Grey box) Models which make little or no attempt to simulate the individual constituent hydrologic processes and which rely heavily on systems theory developed in other branches of engineering science. The essence of these models is the empirical discovery of transfer functions which interrelate in the time domain the input (usually rainfall) and the output (usually discharges) functions.

Quasi-Physical Conceptual Models which occupy an intermediate position between the other two types of models in terms of complexity, disaggregation and data requirements.

The physically-based distributed models are well suited to solving problems such as predicting the effects of land use changes and studying the hazards of pollution (Beven, 1989). However, their implementation in practice has many difficulties, most notably, their intense data requirements and the estimation of meaningful values of the parameters. The other two more conventional types of models are often too primitive to present scientifically sound solutions to such problems. Nevertheless, these last two types of models have often proved to be effective in the solution of a wide spectrum of important hydrological problems, such as river flow forecasting and the extension of hydrological records.

1.3.4 Flood routing model

The term flood routing refers to procedures to determine the outflow hydrograph at a point downstream in a river (or reservoir) as a function of the inflow hydrograph at a point upstream. As flood waves travel downstream they are attenuated and delayed. That is, the peak flow of the hydrograph decreases and the time base of the hydrograph increases. The shape of the outflow hydrograph depends upon the channel geometry and roughness, bed slope, length of channel reach, and initial and boundary flow conditions.

The propagation of flood waves in a channel is a gradually varied unsteady flow process, which is governed by conservation of mass and momentum equations. The solution of these equations in a distributed manner is referred to as distributed routing of flood waves. When no spatial variability is taken into account and when the channel reach or reservoir is considered as a black box, the corresponding routing procedure is referred to as lumped routing.

Jothityangkoon and Sivapalan, 2013 formulated a routing model a based on a non-linear storage-discharge relationship which is converted from an observed and synthetic rating curve. To draw the rating curve, required parameters for each reaches are estimated from hydraulic properties, floodplain geometry and vegetation and building cover of compound channels. Boonrawd and Jothityangkoon, 2015(b) defined the shape of the floodplain by using fitting exercise based on the reverse approach between past and simulated inundation flood extent, to solve the current problem of inadequate topographic input data for floodplain.

1.3.5 Floodplain inundation model

Flood inundation models are a major tool for mitigating the effects of flooding. They provide predictions of flood extent and depth that are used in the development of spatially accurate hazard maps. These allow the assessment of risk to life and property in the floodplain, and the prioritisation of either the maintenance of existing flood defences or the construction of new ones.

There have been significant advances in flood inundation modelling over the past decade. Progress has been made in the understanding of the processes controlling runoff and flood wave propagation, in simulation techniques, in low cost high power computing, in uncertainty handling, and in the provision of new data sources.

One of the main drivers for this advancement is the veritable explosion of data that have become available to parameterise and validate the models. The acquisition of the vast majority of these new data has been made possible by developments in the field of remote sensing (Smith et al., 2006; Schumann et al, 2008a). Remote sensing, from both satellites and aircraft, allows the collection of spatially distributed data over large areas rapidly and reduces the need for costly ground survey. The two-dimensional synoptic nature of remotely sensed data has allowed the growth of two- and higher-dimensional inundation models, which require 2D data for their parameterisation and validation. The situation has moved from a scenario in which there were often too few data for sensible modelling to proceed, to one in which (with some important exceptions) it can be difficult to make full use of all the available data in the modelling process.

One dimensional (1-D) hydraulic modeling of full St.Venant equation is a standard practice to generate the space-time variation of flood depth and magnitudes. The drawback of this approach is that flood inundation extent is drawn by linear interpolation between each cross section. Recent advance of remotely sensed topographic data and high computational capacity, encourages two dimensional (2-D) hydraulic models flood inundation modeling to overcome the limitation over 1-D modeling (Horritt and Bates, 2002; Merwade, 2008). Recently, 2-D hydraulic models become practical tools to estimate floodplain inundation characteristic (Bates and De Roo, 2000).

The data requirements of flood inundation models have been reviewed by Smith et al. (2006). They fall into four distinct categories, (a) topographic data of the channel and floodplain to act as model bathymetry, (b) time series of bulk flow rates and stage data to provide model input and output boundary conditions, (c) roughness coefficients for channel and floodplain, which may be spatially distributed, and (d) data for model calibration, validation and assimilation.

The basic topographic data requirement is for a high quality Digital Terrain Model (DTM) representing the ground surface with surface objects removed. For rural floodplain modelling, modelers require that the DTM has vertical accuracy of about 0.5m and a spatial resolution of at least 10 m. (David et al, 2010). Whilst this level of accuracy and spatial scale is insufficient to represent the micro-topography of relict channels and drainage ditches existing on the floodplain that control its initial wetting, at higher flood depths inundation is controlled mainly by the larger scale valley morphology, and detailed knowledge of the micro-topography becomes less critical (Horritt and Bates, 2002) Important exceptions are features such as embankments and levees controlling overbank flow, for which a higher accuracy and spatial scale are required (~10cm vertical accuracy and 2m spatial resolution) (Smith et al., 2006). This also applies to the topography of the river channels themselves. On the other hand, for modelling over urban floodplains knowledge of the micro-topography over large areas becomes much more important, and a vertical accuracy of 5cm with a spatial resolution of 0.5m is needed to resolve gaps between buildings (Smith et al., 2006). Modellers also require a variety of features present on the ground surface to be measured and retained as separate Geographic Information System (GIS) layers to be used for tasks such as determining distributed floodplain roughness coefficients. Layers of particular interest include buildings, vegetation, embankments, bridges, culverts and hedges. One important use for these is for adding to the DTM critical features influencing flow paths during flooding, such as buildings, hedges and walls. A further use is the identification and removal of false blockages to flows which may be present in the DTM, such as bridges and culverts. It should be borne in mind that different modelling applications may have different requirements for a DTM as well as other data, with wide area inundation models used for high level assessment of flood risk requiring lower resolution data than more detailed models used for the design of remedial works or for planning emergency response.

Flood inundation models also require discharge and stage data to provide model boundary conditions. The data are usually acquired from gauging stations spaced 10-60km apart on the river network, which provide input to flood warning systems. Modelers ideally require gauged flow rates to be accurate to 5% for all flow rates, with all significant tributaries in a catchment gauged. However, problems with the rating curve extrapolation to high flows and gauge bypassing may mean discharge measurement errors may be much higher than this acceptable value during floods. At such times gauged flow rates are likely only to be accurate to 10% at best, and at many sites errors of 20% will be much more common. At a few sites where the gauge installation is significantly bypassed at high flow errors may even be as large as 50%. The data requirements of an alternative scenario in which input flow rates are predicted by a hydrological model using rainfall data as an input, rather than being measured by a gauge.

Estimates of bottom roughness coefficients in the channel and floodplain are also required. The role of these coefficients is to parameterise those energy losses not represented explicitly in the model equations. In practice, they are usually estimated by calibration, which often results in them compensating for model structural and input flow errors. As a result, it can be difficult to disentangle the contribution due to friction from that attributable to compensation. The simplest method of calibration is to calibrate using two separate global coefficients, one for the channel and the other for the floodplain. However, ideally friction data need to reflect the spatial variability of friction that is actually present in the channel and floodplain, and be calculable explicitly from physical or biological variables.

A final requirement is for suitable data for model calibration, validation and assimilation. If a model can be successfully validated using independent data, this gives confidence in its predictions for future events of similar magnitude under similar conditions. Until recently, validation data for hydraulic models consisted mainly of bulk flow measurements taken at a small number of points in the model domain, often including the catchment outlet. However, the comparison of spatially distributed model output with only a small number of observations met with only mixed success (Lane et al., 1999). The 2D nature of modern distributed models requires spatially distributed observational data at a scale commensurate with model predictions for successful validation. The observations may be synoptic maps of inundation extent, water depth or flow velocity. If sequences of such observations can be acquired over the course of a flood event, this allows the possibility of applying data assimilation techniques to further improve model predictions.

For mapping space-time flood extent of Chiang Mai floods, Boonrawd and Jothityangkoon, 2015(b) developed a coupling of a 1-D flood routing model and quasi 2-D floodplain inundation model to simulated temporal extent of flood area.

1.3.6 Hydrologic Modeling System HEC-RAS

Mapping a floodplain requires a forecasting of the behavior of the stream in question for various recurrence interval storm events and the ability to translate the forecasted results into a plan-view extent of flooding. The Hydrologic Engineering Center's River Analysis System (HEC-RAS) was developed by the U.S. Army Corps of Engineers (USACE) led by Gary W. Brunner. HEC-RAS has the ability to model flood events and produce water surface profiles over the length of the modeled stream. With the companion GIS utility, HEC-GeoRAS, those water surface profiles can easily be converted to flood inundation maps. This software allows the user to perform one-dimensional steady flow, one and two-dimensional unsteady flow calculations, sediment transport/mobile bed computations, and water temperature/water quality modeling.

HEC-RAS is a Hydrologic Modeling System that is designed to describe the physical properties of streams and rivers, and to route flows through them. Given the discharge computed by HEC-HMS or by other means, HEC-RAS computes the resulting water surface elevation. Using a program HEC-GeoRAS, these elevations can be mapped in ArcGIS to form a flood inundation map. In this exercise, we can run a HEC-RAS model and use ArcGIS to create the corresponding floodplain map. The geometric data required to define in HEC-RAS includes:

- Cross-section data
- Reach lengths (measured between cross sections)
- Stream junction information (Reach lengths a cross junctions and tributary angles)

HEC-GeoRAS is a GIS extension that provides the user with a set of procedures, tools, and utilities for the preparation of GIS data for import into HEC-RAS and generation of GIS data from RAS output. While the GeoRAS extension is designed for users with limited geographic information systems (GIS) experience, knowledge of GIS is advantageous. Users, however, must have experience modeling with HEC-RAS and have a thorough understanding of river hydraulics to properly create and interpret GIS data sets.

1.4 Methodological steps

Overview of a conceptual framework of this research methodology and processes is presented in Figure 1.6

1.4.1 Data preparation

The observed flood inundation area from past floods was defined based on relationship between flood level at P1 and flood depth measured in the city during past flood events. Flood warning system for Chiang Mai city was set up in the form of flood hazard maps by Civil Engineering Natural Disaster Research Unit (CENDRU).

The water level, channel cross section, channel profile, floodplain characteristics, inundation area, rating curve and the other field data are provided by The Thai Meteorological Department, Royal Irrigation Department and google map.

The topography of land surface substantially influence on the magnitude and dynamics of surface runoff. To illustrate the shape of land surface, The Digital Elevation Model (DEM) can be used to generate topographic map. DEM contains spatially distributed elevation information to allow an automatic delineation of watershed boundary. Topographic data from the Land Development Department is formatted are converted to text/shape file by ArcGIS, HEC-RAS, MATLAB and Microsoft Excel

1.4.2 Data correction

Bias correction can be used to reduce uncertainty and risk of projection bias of regional climate model (RCM) simulation in climate change studies. Many bias correction approaches have been developed to manage these biases. The simple one is distribution mapping based on derived adjustment factors (AF), which is the ratio between observed and simulated rainfall for a given frequency of occurrence. Five methods are used to estimate the distribution between adjustment factors and exceedance probability.

1.4.3 Simulated and calculated processes

The future projection rainfall from a time series of corrected future rainfall from a grid that give the shortest distance between the centroid of RCM grid and the subcatchment is assigned to the subcatchment.

This part contributes to generating of flood maps for study area during October's flood 2010 based on the simulated flood extent map. A flood extent map is simulated by flood map model which is developed from rainfall-runoff, flood routing, and floodplain inundation model. A hydrologic model is used development a flood map model based on the original lumped model detailed in Jothityangkoon et al. (2001; 2013) as showing in chapter 3. The model is developed with ArcGIS/Erdas/ MATLAB software packet. The simulated flood extent map are compared with the observed flood extent map (of the same event) calibrated with surveying data and collecting data. The result to be re-developed until outcome is significant and acceptable. If the result of flood extent map is acceptable, the product can use to generate projection flood map. This rainfall-runoff model and inundation model are used to receive future projection rainfall after bias correction and to delineate flood map in this study.

1.4.4 Prediction scenarios

Projection flood maps in 2D/3D are generated and constructed based on different scenarios (rain frequency, land use change and climate change) and flood management (Diversion channel and Retention basin).

Adaptation measures will be further studied based on the consequences of climatic impact with baseline period from year 1985-2014 (30 years) and future projection period from year 2015-2074 (60 years). The first scenario is climate change for the simulation covers the Intergovernmental Panel on Climate Change (IPCC) emission scenarios A2 and B2. The second scenario is based on the extreme condition 10, 25, 50, 100 years return periods. The finally scenario is land use change in the Upper Ping River catchment.

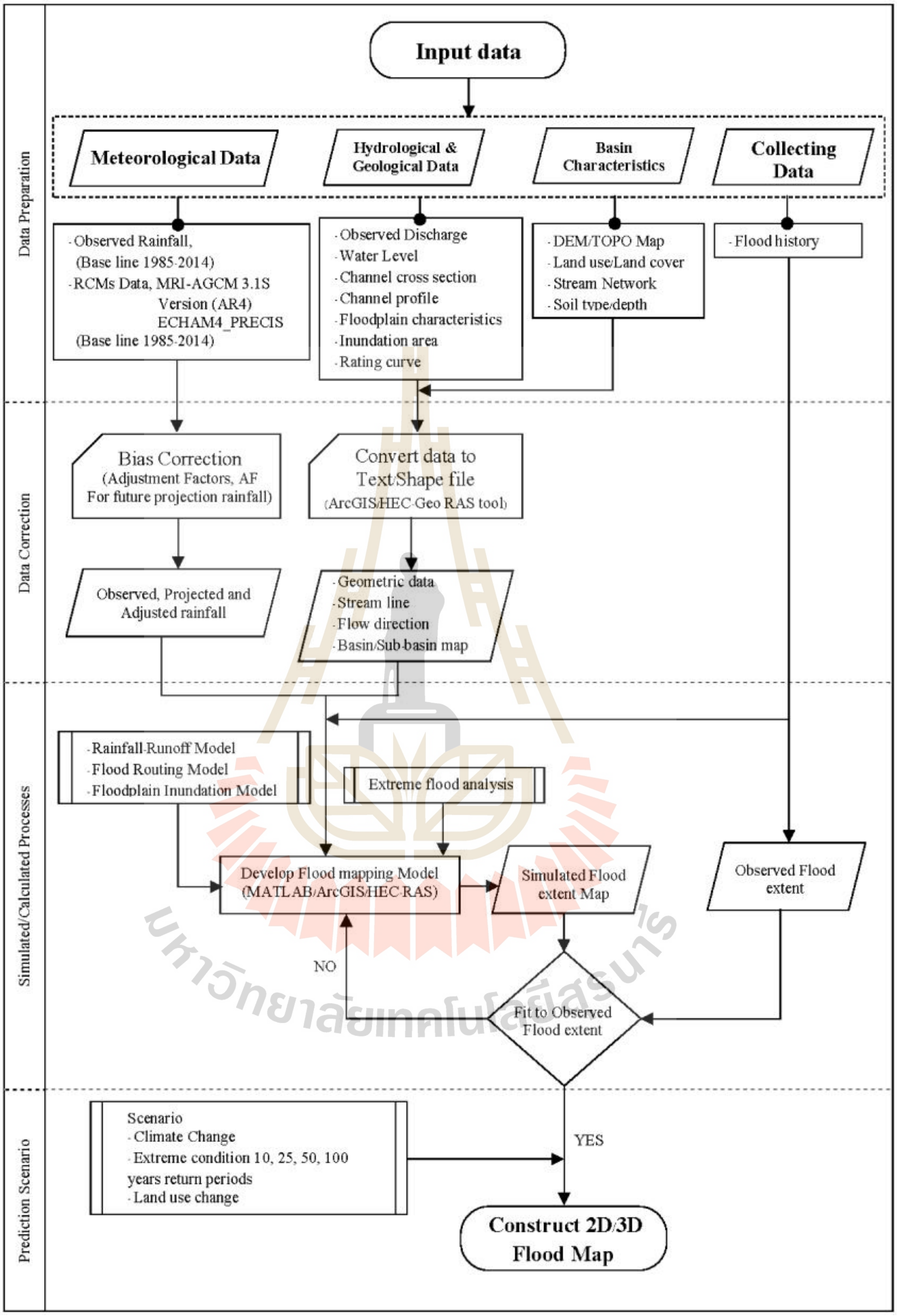
Data Preparation
Data Correction
Simulated/Calculated Processes
Prediction Scenario
Input data
Meteorological Data
Hydrological & Geological Data
Basin Characteristics
Collecting Data
- Observed Rainfall, (Base line 1985-2014)
- RCMs Data, MRI-AGCM 3.1S Version (AR4) ECHAM4_PRECIS (Base line 1985-2014)
- Observed Discharge
- Water Level
- Channel cross section
- Channel profile
- Floodplain characteristics
- Inundation area
- Rating curve
- DEM/TOPO Map
- Land use/Land cover
- Stream Network
- Soil type/depth
- Flood history
Bias Correction (Adjustment Factors, AF For future projection rainfall)
Convert data to Text/Shape file (ArcGIS/HEC-Geo RAS tool)
Observed, Projected and Adjusted rainfall
- Geometric data
- Stream line
- Flow direction
- Basin/Sub-basin map
- Rainfall-Runoff Model
- Flood Routing Model
- Floodplain Inundation Model
Extreme flood analysis
Develop Flood mapping Model (MATLAB/ArcGIS/HEC-RAS)
Simulated Flood extent Map
Observed Flood extent
NO
Fit to Observed Flood extent
YES
Scenario
- Climate Change
- Extreme condition 10, 25, 50, 100 years return periods
- Land use change
Construct 2D/3D Flood Map

1.5 Summary of results

Coupling of water balance model and floodplain inundation model was developed to receive projected rainfall time series from two types of regional climate model (RCM); Providing Regional Climates for Impacts Studies (PRECIS) and Meteorological Research Institute (MRI). They are RCM with resolution 0.2 x 0.2 degree (grid size 20 x 20 km) daily time step, from year 2015-2044 and generated from ECHAM 4 climate models.

For chapter 2 empirical quantile mapping is used for bias correction of projection rainfall that its adjustment factors (AFs) are estimated from comparison between observed and past projection rainfall from base-time period, year 1985-2014. AFs in the first step are applied to correct seasonal pattern of monthly rainfall within a year and applied to correct daily rainfall intensity in the second step. Results further show that whereas bias correction does not seem to affect the change signals in rainfall means, it can introduce extra uncertainty to the change signals in high and low rainfall amounts, and consequently, in runoff.

For chapter 3 the quasi 2-D raster model is tested and applied to generate more realistic water surface and is used to estimate flood extent. The model is applied to the floodplains of Chiang Mai, north of Thailand and used to estimate a time series of hourly flood maps. Extending from daily to hourly flood extent, mapping development provides more details of flood inundation extent and depth.

For chapter 4 by using a synthetic rating curve for compound channel which includes the effect of trees and buildings distribution on floodplain, floodplain inundation model based on flat water surface assumption can be formulated with a number of selected channel cross sections. Although the vertical resolution of existing

DEM (based on scale 1:50,000) for the floodplain of Chiang Mai Municipality is too low to represent any change of flood level, the assumed shape of floodplain can be defined and tested from a good fit between observed and simulated flood extent using the reverse engineering approach. This model can be used with confidence to construct a daily flood extent map. The shape of the floodplain is defined by using fitting exercise based on the reverse approach between past and simulated inundation flood extent, to solve the current problem of inadequate topographic input data for floodplain. Mapping of daily flood can be generated relying on flat water levels. This model receives peak runoffs as results from the water balance model, and generate flood extent in flood plain and draw flood inundation map of Chiang Mai municipality with different return periods. These expected results show the increase of flood inundation extent as a consequence of climate change.

The limitations of flood plain inundation mapping delineate areas which are assessed as being subject to inundation along the generated relying on flat water levels. The maps do not show real time flooding from unsteady flow model. The flood mapping are based on channel cross sections survey, hydrological and hydraulic modelling to an accuracy sufficient only for broad scale floodplain inundation mapping. This simplified floodplain inundation modeling are potential and alternative tools for developing countries where no spatial input data with high resolution are available.

Further simulation from chapter 4 when a fine spatial resolution of DEM are available based on spatial resolution of 5 meters (cell size 5, 5) data in Figure 1.7, then this data can be used to simulate more reliable inundation map and apply to the whole flooding area of Chiang Mai municipality, including the assessment of flood

Floodplain inundation mapping : Chiang Mai municipality

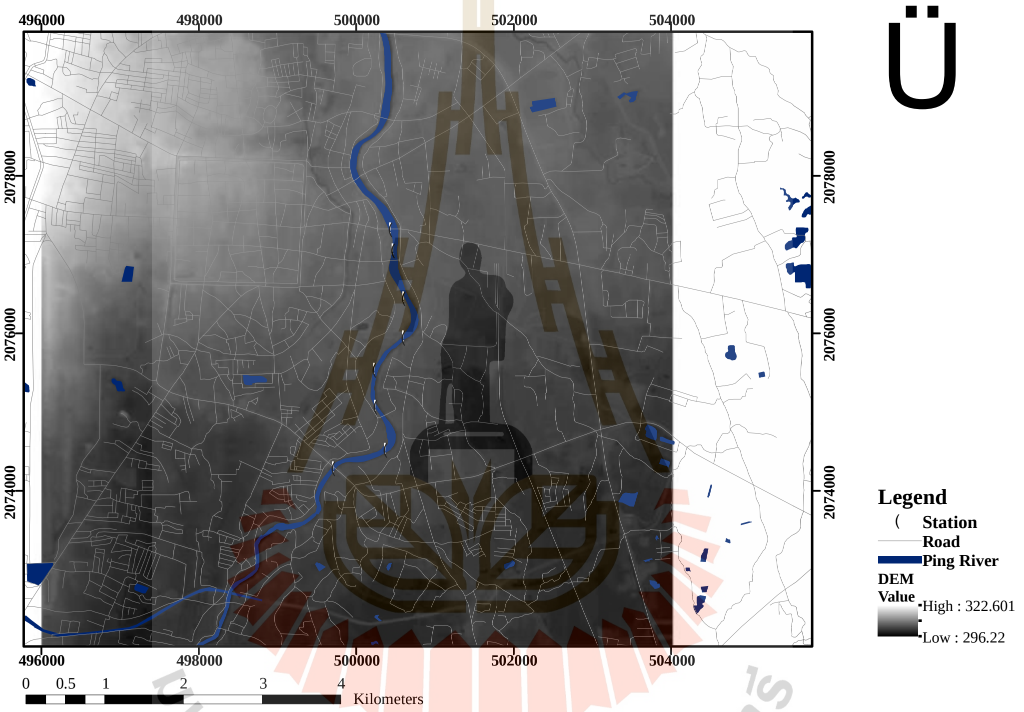

Floodplain inundation mapping : Chiang Mai municipality

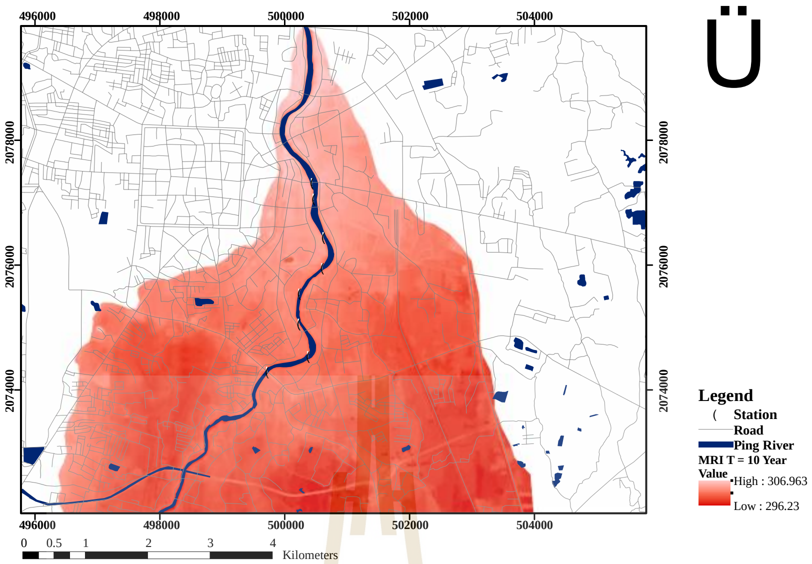

Floodplain inundation mapping : Chiang Mai municipality

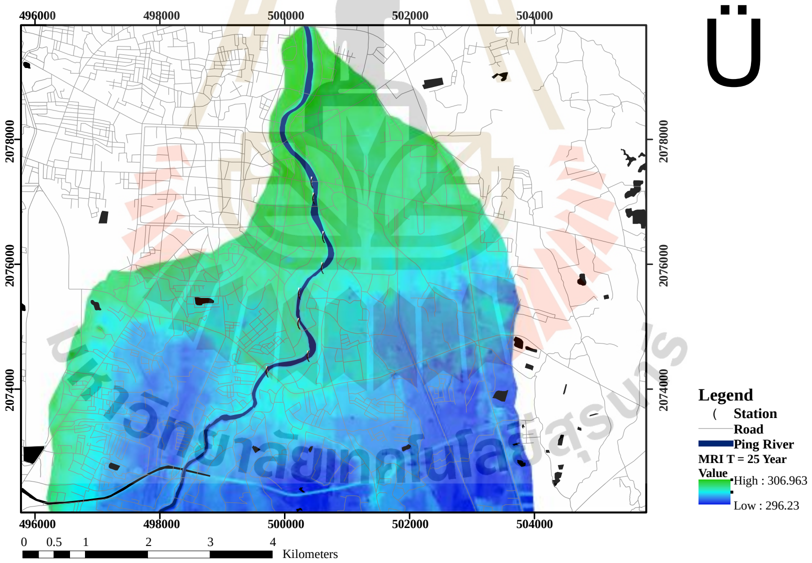

Floodplain inundation mapping : Chiang Mai municipality

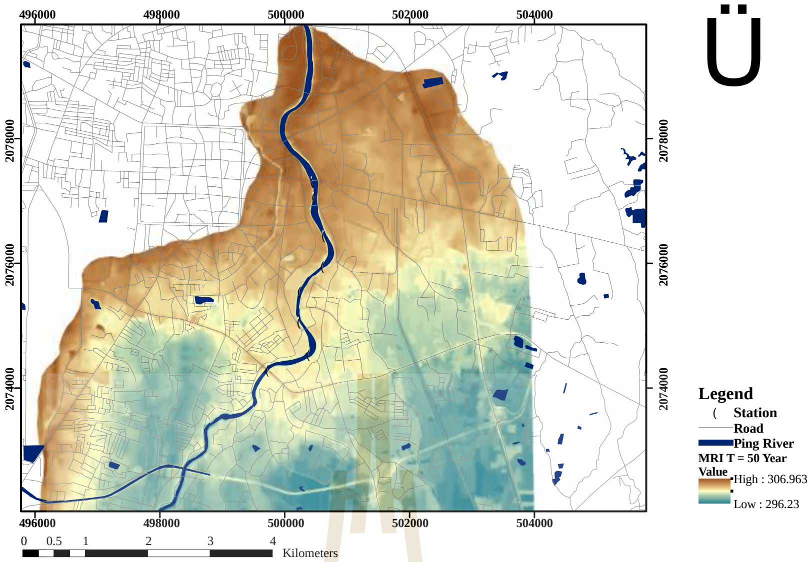

Floodplain inundation mapping : Chiang Mai municipality

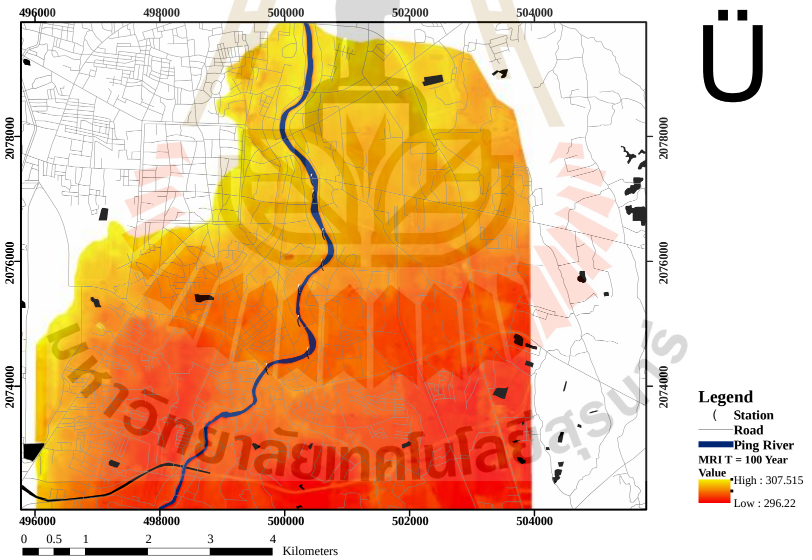

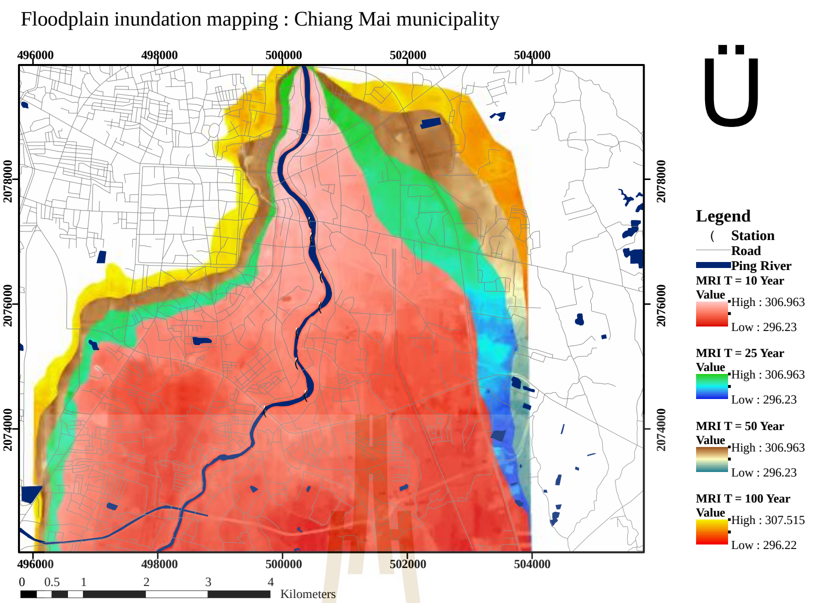
Floodplain inundation mapping : Chiang Mai municipality
496000
498000
500000
502000
504000
2078000
2076000
2074000
0 0.5 1 2 3 4 Kilometers
Legend
Station
Road
Ping River
MRI T = 10 Year
Value
High : 306.963
Low : 296.23
MRI T = 25 Year
Value
High : 306.963
Low : 296.23
MRI T = 50 Year
Value
High : 306.963
Low : 296.23
MRI T = 100 Year
Value
High : 307.515
Low : 296.22

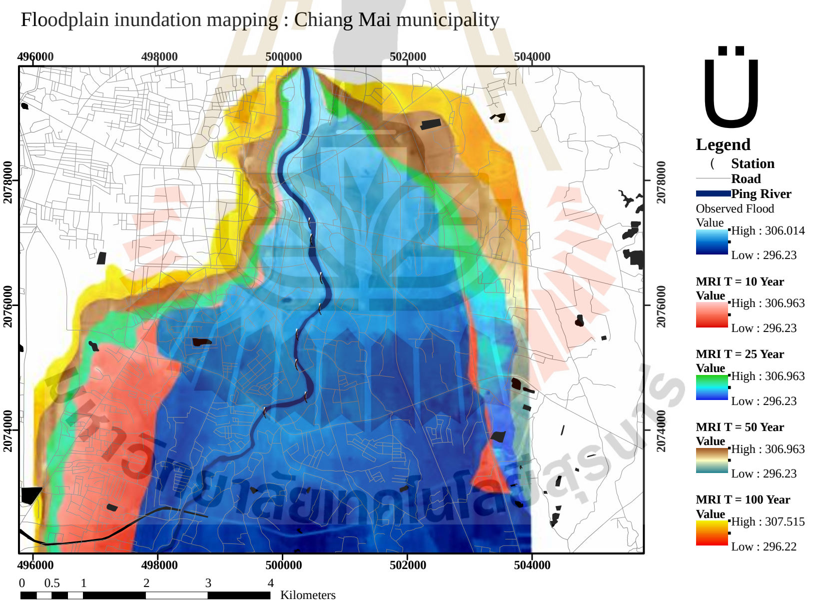
Floodplain inundation mapping : Chiang Mai municipality
496000
498000
500000
502000
504000
2078000
2076000
2074000
0 0.5 1 2 3 4 Kilometers
Legend
Station
Road
Ping River
Observed Flood
Value
High : 306.014
Low : 296.23
MRI T = 10 Year
Value
High : 306.963
Low : 296.23
MRI T = 25 Year
Value
High : 306.963
Low : 296.23
MRI T = 50 Year
Value
High : 306.963
Low : 296.23
MRI T = 100 Year
Value
High : 307.515
Low : 296.22

1.6 Recommendation for future research

1. If digital elevation data at a fine spatial resolution are available from an airborne laser altimetry survey or LiDAR data, then this data can be used to simulate more reliable inundation map by using the quasi 2-D raster model and apply to the whole flooding area of Chiang Mai municipality, including the assessment of flood inundation extent from flood peaks with different exceedance probability or return period (Yin et al., 2013). The accuracy of flow patterns on floodplain depends on land surface characteristics and properties which can be interpreted from high resolution topographic information such as LiDAR data.

2. Future research will continue to examine the implications of climate change mitigation for sustainable development, scenarios depending on these behavioral patterns of future societies as described in the IPCC’s Fifth Assessment Report (AR5)

AR5, The extremely likely (>95% confidence) that human influence has been the dominant cause of the observed warming since the middle 20th century from the Summary for Policy Makers (SPM AR5)

1.7 References

Bates P. D. and De Roo A. P. J., 2000. A simple raster-based model for flood inundation

simulation. Journal of Hydrology. 236, 54-77.

Beven, K., 1989. Changing Ideas in Hydrology – The Case of Physically- Based

Models. J. Hydrol., 105: 157-172.

Brown, C., Greene, A., Block P., Giannini, A. (2008). Review of Downscaling

Methodologies for Africa Climate Applications, International Research

Institute for Climate and Society Columbia University, 15 April 2008 IRI Technical Report 08-05: IRI Downscaling Report.

Boonrawd K. and Jothityangkoon C., 2015(a). Bias correction test of simulated rainfall

from PRECIS using adjustment factors based on distribution mapping, THA 2015 international conference on climate change and environmental management in Monsoon Asia, 28-30 January 2015, Swissotel Concorde, Bangkok, Thailand, Thai Hydrologist Association (THA).

Boonrawd K. and Jothityangkoon C., 2015(b). Mapping temporal extent of Chiang Mai

floods using coupled 1-D and quasi 2-D floodplain inundation models, Songklanakarin Journal of Science and Technology, 37(2), 171-181, 2015.

Chatchawan S., 2005. Report of flood situation and management in Chiang Mai municipal area 2005 (in Thai). [Online]. Available: http://www.thaienvimonitor.net/ News/CHANGMAI.pdf.

Clarke R.T., 1994. Statistical Modelling in Hydrology. John Wiley and Sons.

Daniels A. E., Morrison J. F., Joyce L. A., Crookston N. L., Chen S. C. & McNully S. G.,2012. Climate projections FAQ. General Technical Report. Fort Collins, CO,

U.S. Department of Agriculture, Forest Service, Rocky Mountain Research Station: 1-32.

Duong D. T., Tachikawa Y. and Yorozu K., 2015. Application of a Land Surface Model for Bias Correction of Runoff Generation Data from MRI-AGCM3.2S Dataset,

THA 2015 international conference on climate change and environmental management in Monsoon Asia, 28-30 January 2015, Swissotel Concorde, Bangkok, Thailand, Thai Hydrologist Association (THA).

Fowler H. J., Blenkinsop S. and Tebaldi C., 2007. Linking climate change modelling to impacts studies: recent advances in downscaling techniques for hydrological modelling. International Journal of Climatology 27(12), 1547-1578.

Fuentes, U. and Heimann, D., 2000. An improved statistical-dynamical downscaling scheme and its application to the alpine precipitation climatology. Theoretical and Applied Climatology 65, 119-135.

Guyennon, N., Romano, E., Portoghese, I., Salerno, F., Calmanti, S., Perangeli, A.B., Tartari, G., & Copetti, D., 2013. Benefits from using combined dynamical-statistical downscaling approaches – lessons from a case study in the Mediterranean region. Hydrology and Earth System Sciences 17(2), 705-720.

Horritt, M.S., Bates, P.D., 2002. Evaluation of 1D and 2D numerical models for predicting river flood inundation, Journal of Hydrology, 268, 87-99.

IPCC, 2001. Climate Change 2001: Synthesis Report. A contribution of Working Groups I, II, and III to the Third Assessment Report of the Intergovernmental Panel on Climate Change (Watson, R.T. and the Core Writing Team (eds.)). Cambridge University Press, Cambridge, United Kingdom, and New York, NY, USA, 398 pp.

IPCC, 2007. Fourth Assessment Report: Climate Change 2007. Contribution of Working Group I to the Fourth Assessment Report of the Intergovermental Panel on Climate Change. D. Q. S. Solomon, M. Manning, Z. Chen, M. Marquis, K.B. Averyt, M. Tignor and H.L. Miller. Cambridge, United Kingdom and New York, NY, USA: IPCC.

Jensen K.H., 2013. Assessment of robustness and significance of climate change signals for an ensemble of distribution-based scaled climate projections. Journal of Hydrology 486(0), 479-493.

Jothityangkoon C., Sivapalan M. and Farmer D. L., 2001. Process controls of water balance variability in a large semi-arid catchment: Downward approach to hydrological model development, Journal of Hydrology, 254, 174-198.

Jothityangkoon C., Hirunteeyakul C., Boonrawd K. and Sivapalan M., 2013. Assessing the impact of climate and land use changes on extreme floods in a large tropical catchment, Journal of Hydrology, 490, 88-105,

Lane S.N., Bradbrook K.F., Richards K.S., Biron P.M. and Roy A.G., 1999. The application of computational fluid dynamics to natural river channels: three-dimensional versus two-dimensional approaches. Geomorphology, 29, 1-20.

Mason, D. C., Schumann, G. J-P. and Bates, P.D., 2011. Data utilization in flood inundation modelling. In: Pender, G. and Faulkner, H. (eds.) Flood risk science and management. Wiley-Blackwell, pp. 211-233. ISBN 9781405186575

Merwade V.M., Olivera F., Arabi M.and Edleman S., 2008. Uncertainty in flood inundation Mapping-current issues and future direction. ASCE Journal of Hydrologic Engineering. 13(7), 608-620.

Minyan D., J. Zhang., Z. Liu and A. Aekakkararungroj., 2009. Use of Remote Sensing

and GIS for Flood Hazard Mapping in Chiang Mai Province, Northern Thailand, ISPRS Archives-Volume XXXVIII-7/C4, 2009. International Conference on Geo-spatial Solutions for Emergency Management and the 50th

Anniversary of the Chinese Academy of Surveying and Mapping 14-16 September 2009 Beijing, China.

Osti R., Tanaka S. and Tokioka T., 2008. Flood hazard mapping in developing countries: problems and prospects, Disaster Prevention and Management, 17(1),

2008, 104-113.

Pukongduean P., 2014. Mapping of urban flood severity and vulnerability using MIKE

21: A case of Mueang Nakhon Ratchasima, Thailand. (Doctoral thesis in Geoinformatics), School of Remote Sensing, Suranaree University of Technology.

Schumann, G., Bates, P. D., Horritt, M.S., Matgen, P. and Pappenberger, F. (2008a). Progress in integration of remote sensing derived flood extent and stage data and hydraulic models. Reviews of Geophysics. In press.

http://www.agu.org/journals/pip/rg/2008RG000274-pip.pdf.

Seaby L. P., Refsgaard J. C., Sonnenborg T.O., Stisen S., Christensen J. H., and Jensen,

K.H., 2013. Assessment of robustness and significance of climate change

signals for an ensemble of distribution-based scaled climate projections. Journal

of Hydrology 486(0), 479-493.

Smith M.J., Edwards E.P., Priestnall G. and Bates P.D., 2006. Exploitation of new data

types to create Digital Surface Models for flood inundation modelling. FRMRC

Research report UR3, June 2006. 78pp

STARDEX., 2005. Downscaling climate extremes. Final Report: 1-21.

Takahiro S., Yusuke Y., Yuya T., Akira H. and Yoichi I., 2015. Assessment of climate

change impact on large scale flooding – a case

study in the Chao Phraya River Basin via new modeling technology, THA 2015 international conference on climate change and environmental management in Monsoon Asia, 28-30 January 2015, Swissotel Concorde, Bangkok, Thailand, Thai Hydrologist Association (THA).

Viner D., 2012. Spatial Downscaling. Retrieved from http://www.cccsn.ec.gc.ca/

Wilby R. L., Troni, J., Biot, Y., Tedd, L., B. C. Hewitson, D. M. Smith, & R. T. Sutton,

2009. A review of climate risk information for adaptation and development planning. International Journal of Climatology 29(9), 1193-1215.

Zonensein, M.G, Miguez, L.P.C.de Magalhaes, M.G.Valentin and F.C.B.Mascarenhas,

2008. Flood Risk Index as an Urban Management Tool. 11th International Conference on Urban Drainage, Edinburgh, Scotland, UK.

Zorita E. and Von Storch H., 1999. The analog method as a simple statistical downscaling technique: comparison with more complicated methods. Journal of Climate 12(8), 2474-2489.

CHAPTER II

BIAS CORRECTION TEST OF SIMULATED RAINFALL FROM PRECIS USING ADJUSTMENT FACTORS BASED ON DISTRIBUTION MAPPING

2.1 Summary

To reduce uncertainty and risk of projection bias of regional climate model (RCM) simulation in climate change studies, many bias correction approaches have been developed to manage these biases. The simple one is distribution mapping based on derived adjustment factors (AF), which is the ratio between observed and simulated rainfall for a given frequency of occurrence. Five methods are used to estimate the distribution between adjustment factors and exceedance probability. Method 1, AFs are derived from all daily rainfall data and used to shift distribution of daily rainfall intensity. Method 2, temporal scaling of input rainfall data is changed from daily to monthly. Method 3 is similar to Method 2, the difference is AFs are used to adjust distribution of daily rainfall. For Method 4, seasonal AFs are derived from monthly rainfall data for each month of all years and used to shift distribution of monthly rainfall of each month. Method 5 is the combination of Method 4 for the first step and Method 1 for the second step. These methods are tested to correct simulated rainfall from Providing Regional

Thai Hydrologist Association, THA 2015 International Conference

Climates for Impacts Studies (PRECIS) and ECHAM4 climate models with resolution 0.2 x 0.2 degree (grid size 20x20 km) daily time step, baseline period from year 1982-2005. The performance of all methods is evaluated by using the plot of inter-annual variability, intra-annual variability and daily intensity distribution against exceedance probability. The best improvement of simulated rainfall is achieved with Method 5.

2.2 Introduction

Hydrological modeling of climate change impact studies, large-scale climate variables for current and future conditions are generally provided by global climate models (GCMs). To resolve processes and features relevant to hydrology at the catchment scale, regional climate models (RCMs) are commonly used to transfer coarse-resolution GCM data to a higher resolution.

Downscaling is a technique commonly used in hydrology when investigating the impact of climate change. It is a way of bridging the gap between low spatial resolution global climate models (GCMs) and the catchment- or regional-scale hydrological models (Fowler et al., 2007).

Hydrological simulations driven with the higher-skill bias corrected RCM data performed generally better than corresponding simulations driven with lower-skill bias-corrected RCM data.

The higher-skill bias corrected RCM data or distribution mapping based on derived adjustment factors (AF), which is the ratio between observed and simulated rainfall for a given frequency of occurrence. It corrects most of the statistical characteristics and has the narrowest variability ranges, combined with the best fit of the ensemble median.

2.3 Study area

The Study area covers Upper Ping River basin, Thailand is located in the northern region of Thailand. The main stream of the river flows through Chiang Mai, one of the most popular tourist destination of the northern Thailand. It flows to Bhumibol Dam on the south of the basin. The catchment area upstream of Bhumibol Dam is 26,386 km^2. Observed precipitation dataset extends over Upper Ping River basin and covers the period 1982–2005, selected a 24 years sequence of daily rainfall time series were used in this study. Projected rainfall from grid points shown in Figure 2.1 Are compared to observed data from selected 42 rain gauges.

2.4 RCM data

These methods are tested to correct simulated and projected rainfall from Providing Regional Climates for Impacts Studies (PRECIS) which receives input data from ECHAM4 climate models with resolution 0.2 x 0.2 degree (grid size 20x20 km) daily time step, baseline period from year 1982-2005. (Chinvanno et.al., 2009)

The simulation covers the Intergovernmental Panel on Climate Change (IPCC) emission scenarios A2 and B2.

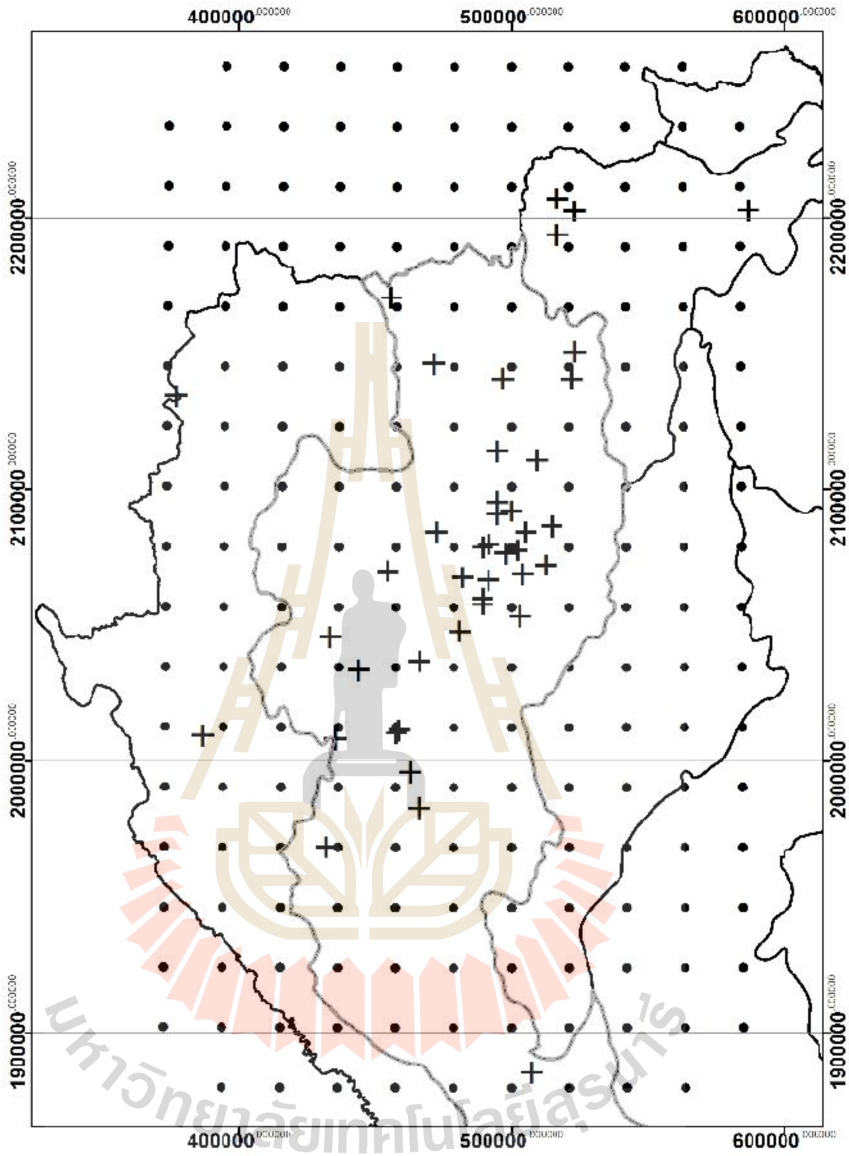
400000
500000
600000
2200000
2100000
2000000
1900000

2.5 Methodology

Bias correction method

A solution to the problem of RCM misrepresentation of precipitation is to pre-process the RCM output through bias correction a number of bias correction methods to adjust RCM simulations were utilized (1) linear scaling, (2) local intensity scaling, (3) power transformation, (4) variance scaling, (5) distribution mapping and (6) delta-change approach. Bias correction approaches is given in Table 2.1. (Gudmundsson et al.2012)

When using the linear scaling method, RCM daily rainfall amounts, P are transformed into $P*$ such that

$$P^* = aP \tag{2.1}$$

Using an adjustment factor a,

$$a = \frac{O'}{P'} \tag{2.2}$$

Where O' and P' are Observed and RCM simulated daily or monthly rainfall data with the same frequency from 20x20 km grid size, respectively. Here, the daily, monthly adjustment factors and combination of them are applied to each uncorrected daily observation of that month, generating the corrected daily time series. The linear correction method belongs to the same family as the factor of change or delta change method. This method has the advantage of simplicity and modest data requirements.

When using the distribution mapping method, to describe the probability distribution of a random variable X, we use a cumulative distribution function. The value of this function $F_X(X)$ is simply the probability P of the event that the random variable takes on value equal to or less than the argument such that

$$F_X(X) = P[X \leq x] \tag{2.3}$$

However, correcting only the monthly mean precipitation can distort the relative variability of the inter-monthly precipitation distribution, and may adversely affect other moments of the probability distribution of daily precipitations. For bias correction test in this study, the complexity of derived AFs is added in 5 steps (5 methods)

Method 1, AFs are derived from all daily rainfall data and used to shift distribution of daily rainfall intensity.

Method 2, temporal scaling of input rainfall data is changed from daily to monthly.

Method 3 is similar to Method 2, the difference is AFs are used to adjust distribution of daily rainfall.

Method 4, seasonal AFs are derived from monthly rainfall data for each month of all years and used to shift distribution of monthly rainfall of each month.

Method 5 is the combination of Method 4 for the first step and Method 1 for the second step. The comparison of observed, projected and adjusted rainfall station using frequency analysis of its distribution based on exceedance probability.

Table 2.1. Overview of methods used to correct RCM-simulated precipitation (P) and/or temperature (T) data.

Methods	Short Description	
linear scaling	P,T	adjusts RCM time series with correction values based on the relationship between long-term monthly mean observed and RCM control run valuesprecipitation is typically corrected with a factor and temperature with an additive term
local intensity scaling	P	combines a precipitation threshold with linear scaling (both described above)
power transformation	P	is a non-linear correction in an exponential form (a*Pb) that combines the correction of the coefficient of variation (CV) with linear scaling
variance scaling	T	combines standard linear scaling with a scaling based on standard deviations
distribution mapping	P,T	matches the distribution functions of observations and RCM-simulated climate values. a precipitation threshold can be introduced to avoid substantial distortion of the distribution caused by too many drizzle days (i.e., very low but non-zero precipitation) also known as quartile - quartile mapping, probability mapping, statistical downscaling or histogram equalization.
delta-change approach	P,T	·RCM-simulated future change signals (anomalies) are superimposed upon observational time series ·usually done with a multiplicative correction for precipitation and an additive correction for temperature

2.6 Results and Discussion

For Method 1, AFs is applied to projected daily rainfall with the same frequency (Figure 2.2 (a)). Distribution of adjusted daily rainfall is shifted to give a perfect fit to distribution of observed rainfall (Figure 2.2(b)).

After these adjusted rainfalls are accumulated to annual and monthly rainfall. The distribution of annual and monthly rainfall present a little improvement. Under-estimate annual rainfall for wet years and over-estimate annual rainfall for dry years are still exist (Figure 2.2 (c)). Seasonal pattern of average monthly rainfall is far different from the pattern of observed rainfall (Figure 2.2(d)).

Second trial for Method 2, AFs are estimated for projected monthly rainfall with the same frequency (Figure 2.3(a)). Although, distribution of adjusted monthly rainfall is shifted to give a perfect fit to the distribution of observed monthly rainfall, discrepancy between adjusted annual and monthly rainfall and observed rainfall is found. Compare to Method 1, better results of seasonal patterns of average monthly rainfall are presented.

Third trial for Method 3, AFs are estimated similar to Method 2 but applied for projected daily rainfall with the same frequency. Shitted distribution of adjusted daily rainfall show a good agreement with distribution of observed daily rainfall (Figure 2.3(b)). However, the difference between adjusted annual and monthly rainfall and observed rainfall is not resolved fitting. Results are the same as the previous results from Method 2.

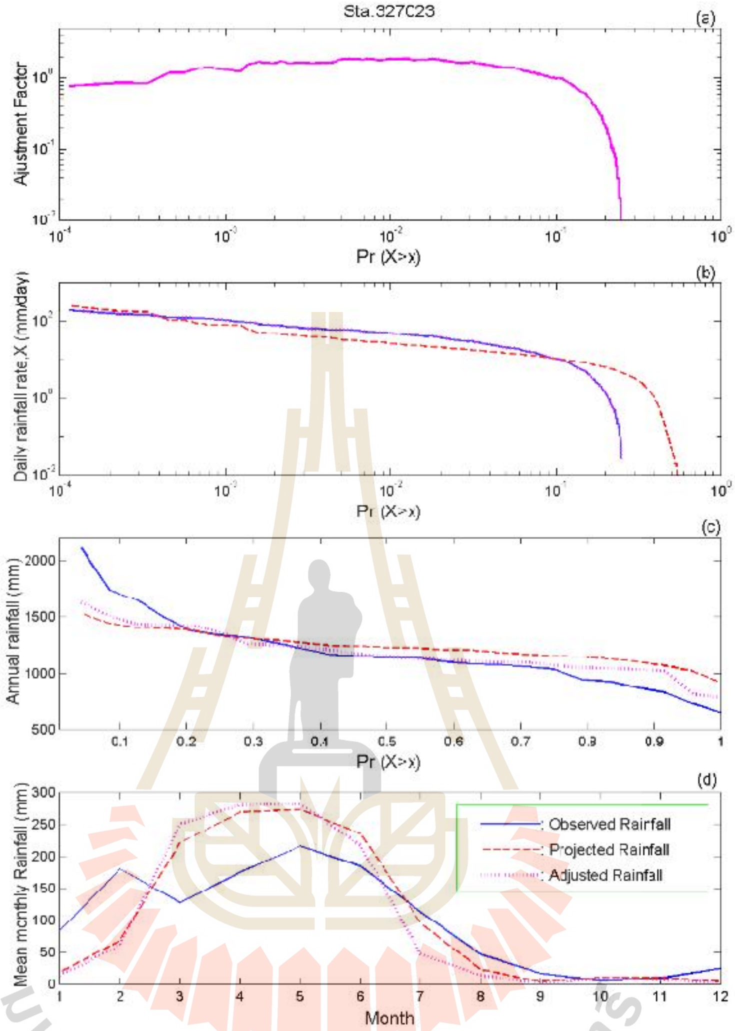

Sta.327023
(a)
Ajustment Factor
Pr (X>x)
(b)
Daily rainfall rate, X (mm/day)
Pr (X>x)
(c)
Annual rainfall (mm)
Pr (X>x)
(d)
Mean monthly Rainfall (mm)
Month
Observed Rainfall
Projected Rainfall
Adjusted Rainfall

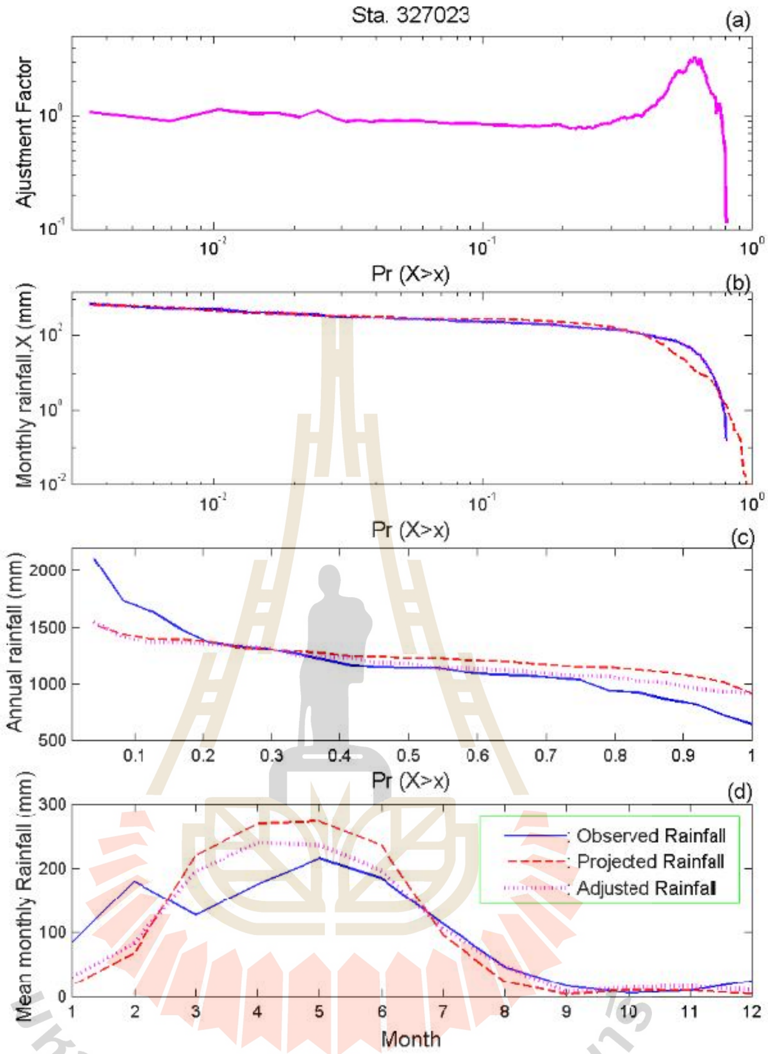

Sta. 327023
(a)
Ajustment Factor
Pr (X>x)
(b)
Monthly rainfall,X (mm)
Pr (X>x)
(c)
Annual rainfall (mm)
Pr (X>x)
(d)
Mean monthly Rainfall (mm)
Month
: Observed Rainfall
: Projected Rainfall
: Adjusted Rainfall

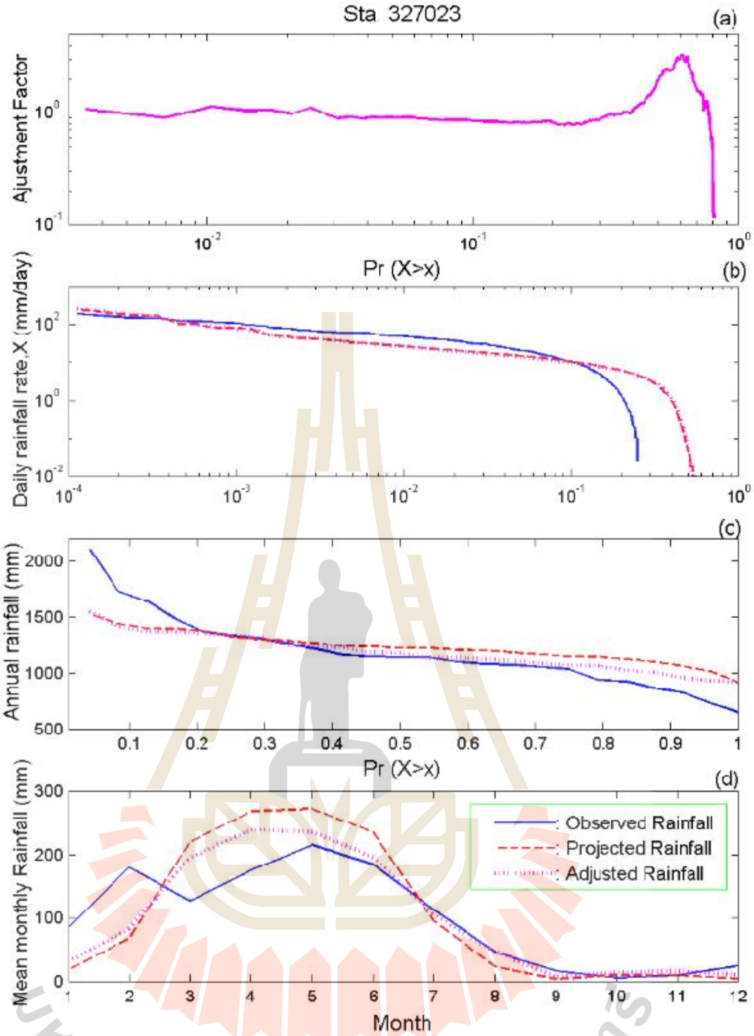
Sta 327023
(a)
Ajustment Factor
Pr (X>x)
(b)
Daily rainfall rate, X (mm/day)
(c)
Annual rainfall (mm)
Pr (X>x)
(d)
Mean monthly Rainfall (mm)
Month
: Observed Rainfall
: Projected Rainfall
: Adjusted Rainfall

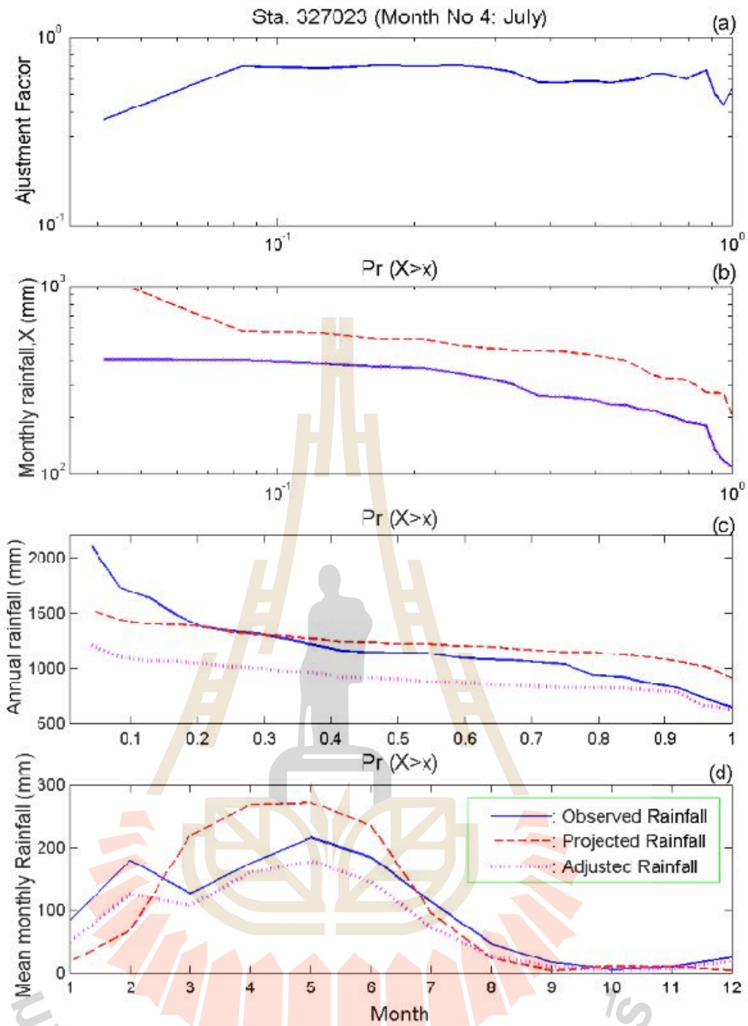

Sta. 327023 (Month No 4: July)
(a)
Ajustment Factor
Pr (X>x)
(b)
Monthly rainfall, X (mm)
Pr (X>x)
(c)
Annual rainfall (mm)
Pr (X>x)
(d)
Mean monthly Rainfall (mm)
Month
Observed Rainfall
Projected Rainfall
Adjustec Rainfall

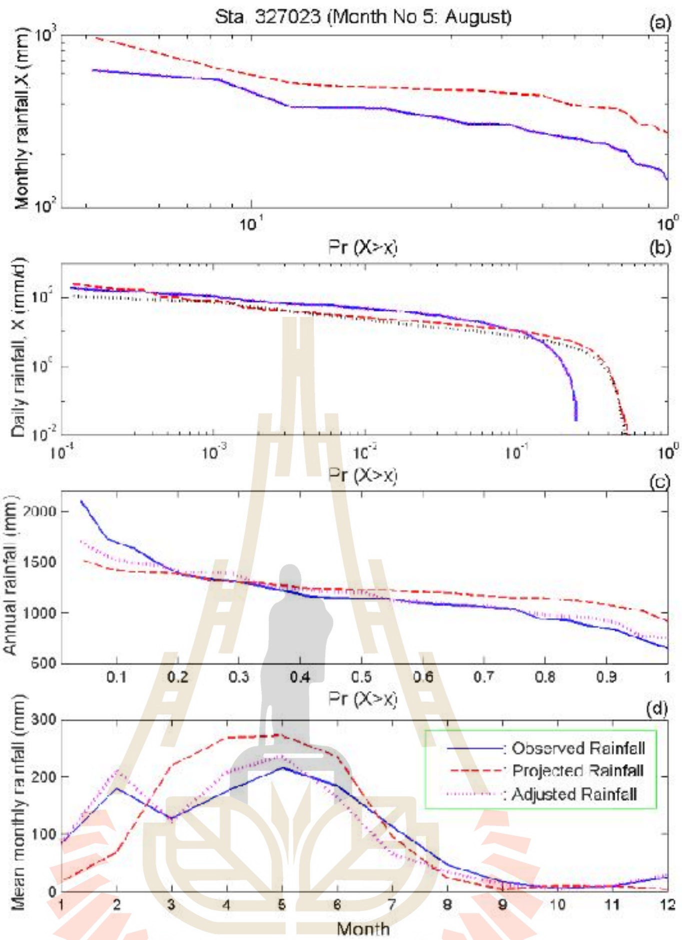
Sta. 327023 (Month No 5: August)
(a)
Monthly rainfall, X (mm)
Pr (X>x)
(b)
Daily rainfall, X (mm/d)
Pr (X>x)
(c)
Annual rainfall (mm)
Pr (X>x)
(d)
Mean monthly rainfall (mm)
Month
: Observed Rainfall
: Projected Rainfall
: Adjusted Rainfall

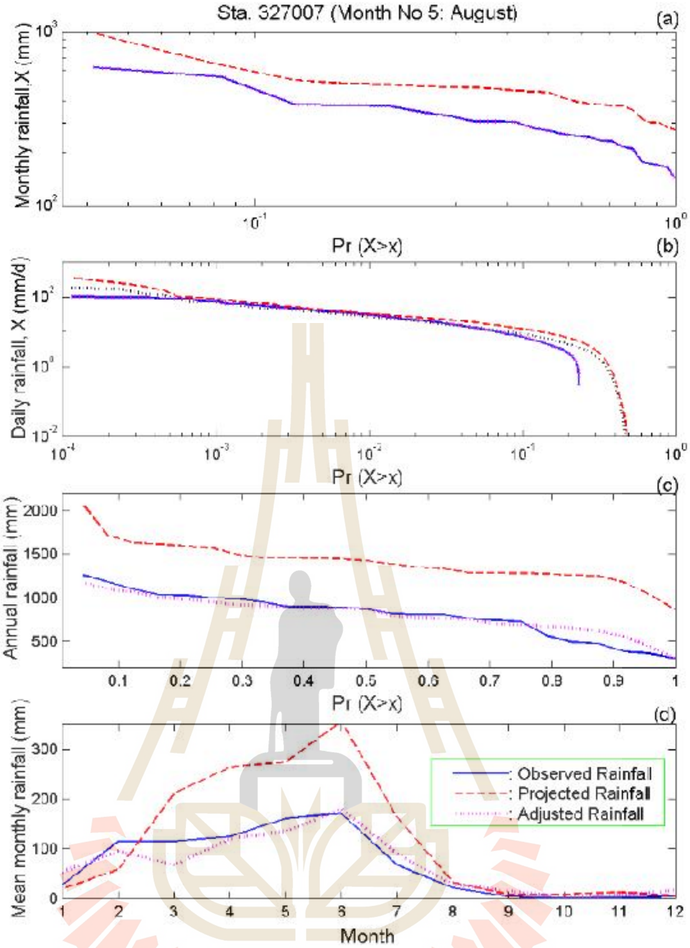

Sta. 327007 (Month No 5: August)
(a)
Monthly rainfall,X (mm)
Pr (X>x)
(b)
Daily rainfall, X (mm/d)
Pr (X>x)
(c)
Annual rainfall (mm)
Pr (X>x)
(c)
Mean monthly rainfall (mm)
Month
: Observed Rainfall
: Projected Rainfall
: Adjusted Rainfall

Fourth trial for Method 4, Seasonal AFs are estimated from monthly rainfall for each month of the year and applied for projected monthly rainfall. AFs for July in Figure 2.5(a), can shift the distribution of adjusted July rainfall and give a perfect fit to observed July rainfall (Figure 2.5(b)). However, when this method is used for every months of the year, annual adjusted rainfall show under-estimated results for the whole annual series. Seasonal pattern of adjusted monthly rainfall is shifted close to observed monthly pattern (Figure 2.5(d)).

Final trial for Method 5, two steps of AFs estimation from Method 1 and Method 4 are combined. Distribution of adjusted daily, monthly and annual rainfall are shifted to give a better fit to distribution of observed rainfall, compare to the other method (Figure 2.6 (b)-(d)).

To confirm the accuracy of Method 5, this bias correction test is applied to many locations of available observed rainfall. Figure 2.6 and 2.7 present an example of this test. Projected rainfall data from 2 grid points close to rain gauge station sta. 327023 and 327007 can be shifted its distribution close to observed rainfall data with satisfied results.

2.7 Conclusion

The performance of all methods is evaluated by using the plot of inter-annual variability, intra-annual variability and daily intensity distribution against exceedance probability. The best improvement of projected rainfall using AFs is achieved with Method 5. AFs in the first step are applied to correct seasonal pattern of monthly rainfall within a year and applied to correct daily rainfall intensity in the second step.

Results further show that whereas bias correction does not seem to affect the change signals in rainfall means, it can introduce extra uncertainty to the change signals in high and low rainfall amounts, and consequently, in runoff. Future climate change impact studies need to take this into account when deciding whether to use raw or bias corrected RCM results. Nevertheless, the bias in RCM simulations will continue to reduce as RCM accuracy is improved and RCMs will become increasingly useful for hydrological studies.

2.8 Acknowledgement

This study was partly funded by the Institute of Research and Development, Suranaree University of Technology for the first author.

2.9 References

Chinvanno S., Laung-Aram V., Sangmanee C., Thanakitmetavut J., 2009. Future Climate Projection for Thailand and Mainland Southeast Asia Using PRECIS and ECHAM4 Climate Models., **Southeast Asia START Regional Center Technical Report** No. 18.

Fowler H. J., Blenkinsop S., and Tebaldi C., 2007. Linking climate change modelling to impacts studies: recent advances in downscaling techniques for hydrological modelling, **Int. J. Climatol.**, 27, 1547–1578, doi:10.1002/joc.1556.

Gudmundsson L., J. B. Bremnes, J. E. Haugen, and T. Engen-Skaugen., 2012. Technical

Note: Downscaling RCM precipitation to the station scale using statistical transformations - a comparison of methods, **Hydrol Earth Syst Sci,** 16(9), 3383–3390, doi: 10.5194/hess-16-3383-2012.

CHAPTER III

MAPPING TEMPORAL EXTENT OF CHIANG MAI FLOOD USING COUPLED 1-D AND QUASI 2-D FLOODPLAIN INUNDATION MODELS

3.1 Summary

A coupling of a 1-D flood routing model and quasi 2-D floodplain inundation model is applied for mapping space-time flood extent. The routing model is formulated based on a non-linear storage-discharge relationship which is converted from an observed and synthetic rating curve. To draw the rating curve, required parameters for each reaches are estimated from hydraulic properties, floodplain geometry and vegetation and building cover of compound channels. The shape of the floodplain is defined by using fitting exercise based on the reverse approach between past and simulated inundation flood extent, to solve the current problem of inadequate topographic input data for floodplain. Mapping of daily flood can be generated relying on flat water levels. The quasi 2-D raster model is tested and applied to generate more realistic water surface and is used to estimate flood extent. The model is applied to the floodplains of Chiang Mai, north of Thailand and used to estimate a time series of hourly flood maps. Extending from daily to

hourly flood extent, mapping development provides more details of flood inundation extent and depth.

3.2 Introduction

To assess an impact of severe flood and at the same time mitigate economic and social losses, mapping of floodplain inundation extent including flood depth and flood duration is an import ant tool for the improvement of flood management systems. Extrapolation work from historical to future potential flood mapping under different possibilities and scenarios are necessary information for stake holders in choosing appropriate measures to reduce flood risks. The magnitude and frequency of floods possibly tend to increase in near future which is the consequence of climate and human induced changes (IPCC, 2007).

The devastating results of past floods in Chiang Mai City, particularly in the core economic and residential zones, has brought great public concern about the performance of flood protection and warning systems managed by local authorities. Questions are also being raised by the local people on what are the potential impacts of future land use changes, the forest loss to agricultural plantation, and the uncontrolled urban expansion (Chatchawan, 2005; CENDRU, 2013).

Flood inundation mapping can be formulated in a number of ways including historical flood investigation through field survey and/or remote sensing survey, using hydrological or hydraulic modeling or their combination. Compared to different approaches, hydraulic modeling gives advantages over other methods. It incorporates spatial terrain data and generates the space-time variation of flood depth and magnitudes. One dimensional (1-D) hydraulic modeling of full St. Venant equation is still a standard practice. By receiving design flood inputs, it can simulate flood magnitude and depth downstream and convert to flood inundation extent such as MIKE, HEC (Fread, 1993; Ervine and MacLeod 1999; De Kok and Grossmann, 2010). The limitation of this method is that the map of flood inundation extent is drawn by linear interpolation of flood characteristics between each cross section. Recently, many cases of uncertainties are studied in form of probabilistic flood inundation map (Merwade et al., 2008; Sarhadi et al., 2012)). To overcome this limitation, two dimensional (2-D) hydraulic models have been proposed to have advantages over 1-D modeling (Horritt and Bates, 2002; Tayefi et al., 2007; Cook and Merwade, 2009). Recent advances in availability of remotely sensed topographic data and high computational capability, allows 2-D flood inundation modeling based on finite difference and finite element numerical method to become practical tools to estimate floodplain inundation extent, flood depth and depth-averaged velocity vector for each node and time step (Bates and De Roo, 2000).

However, the application of the complex 2-D models require massive input data together with consuming high computational cost and time which makes this model less attractive for large-scale floodplain analysis. Application of simplified raster-based hydraulic model is widely used due to some advantages over full 2-D model to simulate dynamic flood inundation (Bradbrook et al., 2004; Yu and Lane, 2006). The raster based model can simply integrate spatial topographic data and process them with high computational efficiency. These models consist of coupling the 1-D and 2-D model representing channel flow and flow over the floodplain (Bates and De Roo, 2000; Yin, et al., 2013). The raster-based storage model is developed further to adaptive time step diffusion model (Hunter et al., 2005), including inertial term (Bates et al., 2010) for high efficiency of computation with stable solutions. To improve the quality of river flood inundation prediction with given high resolution of topographic data, comparison study of different hydraulic models were examined for different topographic complexity (Tayefi et al., 2007). However, scarcity of high resolution and detailed topographic data for floodplain, i.e. Lidar and synthetic aperture radar (SAR), still exists in developing countries.

3.3 Approaches for floodplain inundation model

3.3.1 Storage-discharge approach

The 1-D channel routing model proposed here is based on a conceptualization of each channel link in the network as non-linear storages. The water balance of each channel reach is modeled by solving equation $dS_c/dt=I(t)-Q(t)$, combined with a non-linear storage (S_c) to discharge (Q). The storage-discharge relationship expresses as a power function $S_c = kQ^m$ where k and m are model parameters, $I(t)$ represents the summation of upstream channel reaches and lateral inflow. The parameter k and m are estimated a priori for each of the stream reaches. These parameters reflect different physical properties of river flow transition from normal to extreme floods or from in-bank to over-bank flow (Jothityangkoon and Sivapalan, 2003; Jothityangkoon et al., 2013).

For estimation of k and m in study river, recorded stage-discharge curve (rating curve) are used, together with surveyed data on the geometry of main channel, cross section of floodplain and length of the river reach. The estimation of the rating curves beyond recorded data can be achieved by a simple hydraulic approach. The compound channel is subdivided to main channels and floodplain sections, and discharges in each section are estimated separately. For the main channel, the measured rating curve can be used and estimated Manning coefficient given cross section area and slope of the channel at this stream gauge. At the other cross sections without measured rating curve, synthetic rating curves can be estimated given cross section area, slope of the channel and simulated Manning coefficient from neighbor cross section. Details of this procedure are described by Jothityangkoon and Sivapalan (2003) and Jothityangkoon et al. (2013). To capture the effect of houses and other buildings on the floodplain, the flow resistance in floodplain due to its size and spacing is considered in the same manner as the case of vegetation on the floodplain.

3.3.2 Raster based storage cell approach

(1) Diffusive model

The advantages of the storage cell formulation are that (i) it is a simple concept to calculate flow rate. Computational times and costs are much lower than solving numerical solution of full shallow water equations, (ii) this method interface well with a regular grid-based cell representing topographic characteristics generating from current remote sensing technology. For these reasons, this method is popular for floodplain inundation modeling (Hunt et al., 2007). The volumetric flow rate between floodplain cells is calculated by using Manning equation,

$$Q_x^{i,j} = \frac{h_f^{5/3}}{n}\left(\frac{h^{i-1,j} - h^{i,j}}{\Delta x}\right)^{1/2} \Delta y \tag{3.1}$$

where is the flow rate in x direction at node (i, j), $h^{i,j}$ is the elevation of free water surface at node (i, j), ax and ay are the cell dimensions on rectangular coordinate *[L]*, n is the Manning's friction coefficient [$L^{-1/3}T$], *hf* is the difference between the highest free water surface from two cells and the highest elevation of floodplain bed between nodes.

Interaction between inflow outflow and water surface height within a cell can be explained by water balance or continuity equation of the storage cell $\Delta h / \Delta t = \Delta Q / (\Delta x \Delta y)$. Using finite difference method, this equation is solved to,

$$\frac{{}^{t+\Delta t}h^{i,j} - {}^{t}h^{i,j}}{\Delta t} = \frac{{}^{t}Q_x^{i-1,j} - {}^{t}Q_x^{i,j} + {}^{t}Q_y^{i,j-1} - {}^{t}Q_y^{i,j}}{\Delta x \Delta y} \tag{3.2}$$

where ${}^{t}h$ and ${}^{t+\Delta t}h$ are flow depth at time t and t+at, ${}^{t}Q_x^{i,j}$, is flow rate at time t and at is the time step.

Assuming that the depth-averaged velocity u is constant with steady and uniform flow in x direction, 1D Saint-Venant equation or momentum equation is simplified to an ordinary non-linear differential equation (neglecting acceleration and advection term),

$$S_0 + \frac{\partial h_f}{\partial x} + \frac{n^2 u^2}{h_f^{4/3}} = 0 \tag{3.3}$$

where S_0 is the bed slope, if flood wave propagates over flat plane, $S_0 = 0$, analytical solution can be derived (Hunter et al., 2005),

$$h(x,t) = \left[\frac{7}{3}\left(C - n^2u^2\left(x - ut\right)\right)\right]^{\frac{3}{7}} \tag{3.4}$$

where h is the water depth which is a function of location on space x and at any time t, C is a constant depending on the initial condition form integration results.

(2) Inertial Model

For inertial model formulation, only advection term is neglected from 1-D Saint-Venant equation. By assuming flow in a rectangular channel a momentum equation in term of flow per unit width (q) [L^2T^{-1}] is:

$$\frac{\partial q}{\partial t} + \frac{gh\partial(h+z)}{\partial x} + \frac{gn^2q^2}{R^{4/3}h} = 0 \tag{3.5}$$

where z is the bed elevation [L], R is the hydraulic radius [L], g is the gravity acceleration [LT^{-2}]. For wide shallow flow, R is assumed equal h. Equation 5 can be discretize with respect to the time step Δt and q_t in the friction term is replaced by a $q_{t+\Delta t}$

(the third term in Equation 3.5). Equation 3.5 is rearranged to give flows at the next time step, derived by Bates et al. (2010):

$$q_{t+\Delta t} = \frac{q_t - gh_t \Delta t \frac{\partial(h_t+z)}{\partial x}}{1 + gh_t \Delta t n^2 q_t / h_t^{10/3}} \tag{3.6}$$

3.3.3 Reverse engineering approach

For some developing countries with inadequate available hydrological input data, Hagen et al. (2010) proposed a parsimonious model based on the reverse engineering approach to generate nationwide flood hazard maps from past inundation extents. Motivated by this study, floodplain characteristics can be defined from the map of observed flood extent and depth for lacking good quality of DEM. To evaluate the quality of flood inundation estimation, observed and simulated inundation maps are compared by considering fit index (F).

$$F = 100 * \left(\frac{A_{op}}{A_o + A_p - A_{op}} \right) \tag{3.7}$$

where A_{op} is the inundated area where both observed and simulated flood extent are completely are overlaid, A_o is the total observed area of inundation, and A_p is the total simulated area of inundation. F varies between zeros to 100; zero means no overlap between simulated and observed inundated area and 100 means a perfect match.

3.4 Application to Chiang Mai Municipality

3.4.1 Study area

The Upper Ping River catchment is located in the north of Thailand (see Figure 3.1). The river flows southward through the valley of Chiang Mai. The catchment area upstream of stream gauge station P1 (Navarat Bridge) and P68 (Ban Nam Tong) are 6,350 and 6,430 km^2, respectively. The flood study area covers about half of Chiang Mai municipality (40.2km^2) and two districts (Pa Daet, 25 km^2 and Nong Hoi, 3.67 km^2) which lie on the floodplain of the Upper Ping River.

3.4.2 Historical flood map and flood warning system

The severe floods usually arrive during August and September. The recent ones (in the past 20 years) occurred in 1994, 1995, 2001, 2005, and 2011 with maximum water levels at the P1 station of 4.43, 4.27, 4.18, 4.93 and 4.94 m, respectively. From an experience in observed flood routing from past flooding events between input flood hydrograph at stream gauge P.67 (Ban Mae Tae, 32 km upstream of P1) and output hydrograph at P1, it was found that if the maximum depth of flood at P.67 equals 4.70 m, the maximum depth of flood at P.1 equals 3.7 m, within about 7-8 hrs later (Chatchawan, 2005). Based on this correlation and observed relationship between flood level at P1 and flood depth measured in the city during flood events, flood warning system for Chiang Mai city was set up in the form of flood hazard maps. Chiang Mai flood maps given by Civil Engineering Natural Disaster Research Unit (CENDRU) Chiang Mai University divides inundation areas into seven zones depending on upstream referenced water level at P1 (Chatchawan, 2005; CENDRU, 2013).

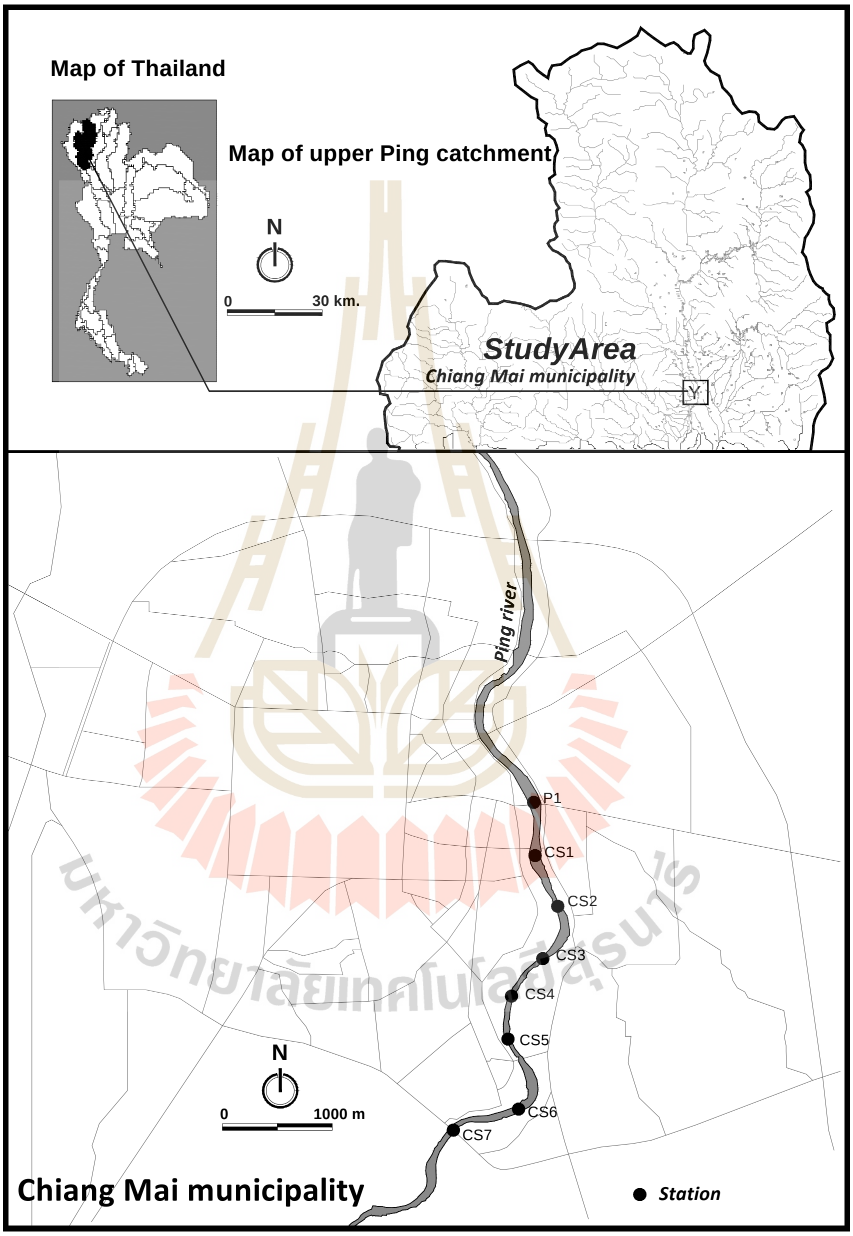

Figure 3.1 Location map of the Upper Ping River Basin, study reach and floodplain of Chiang Mai Municipality.

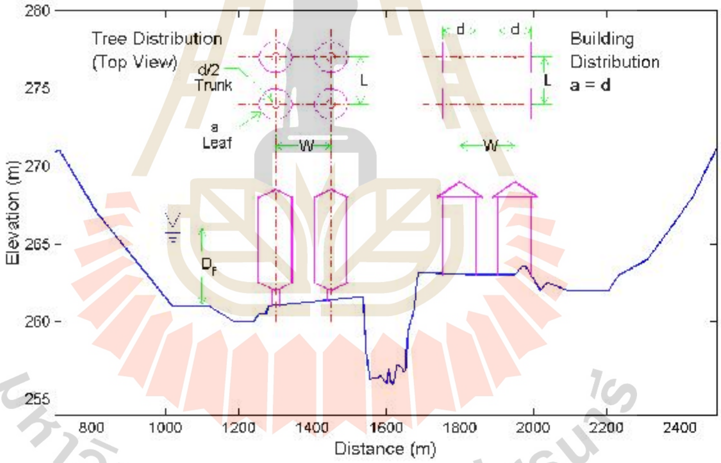

Tree Distribution
(Top View)
d/2
Trunk
a
Leaf
L
W
d
d
L
Building
Distribution
a = d
W
D_F
Elevation (m)
Distance (m)

3.4.4 Application of the model for flood extent estimation

Estimation procedures consist of four main steps (Figure 3.4).

(1) Formulate 1-D floodplain inundation model by fitting the simulated to observe flood extent maps based on assumed floodplain cross section (step 1-6 in Figure 3.4), upstream boundary condition and inputs are observed flood peaks at station P1.

(2) Convert input flood hydrograph to daily flood extent maps using 1-D flood routing model and flat water level assumption (step 7 in Figure 3.4).

(3) Simulate a time series of hourly flood extent maps by using 1D raster model (step 8-9 in Figure 3.4). After channel cross sections are converted to grid based-storage cells in series and given water surface elevation in main channel of the river, flow rates from Equation 1 and water surface elevations from Equation 3.2 are simultaneously calculated for each time step to generate water surface elevation on floodplain for each cross section. Upstream boundary condition and inputs are water surface elevations in the main channel at each cross section.

(4) Generate a pilot map of 3-D floodplain inundation extent 2-D raster model (step 10 in Figure 3.4). Similar to the previous step, except the flow rates are determined on both directions (x: on floodplain, y: along main channel). Water surface elevation are generate for floodplain at each cross section and between cross sections.

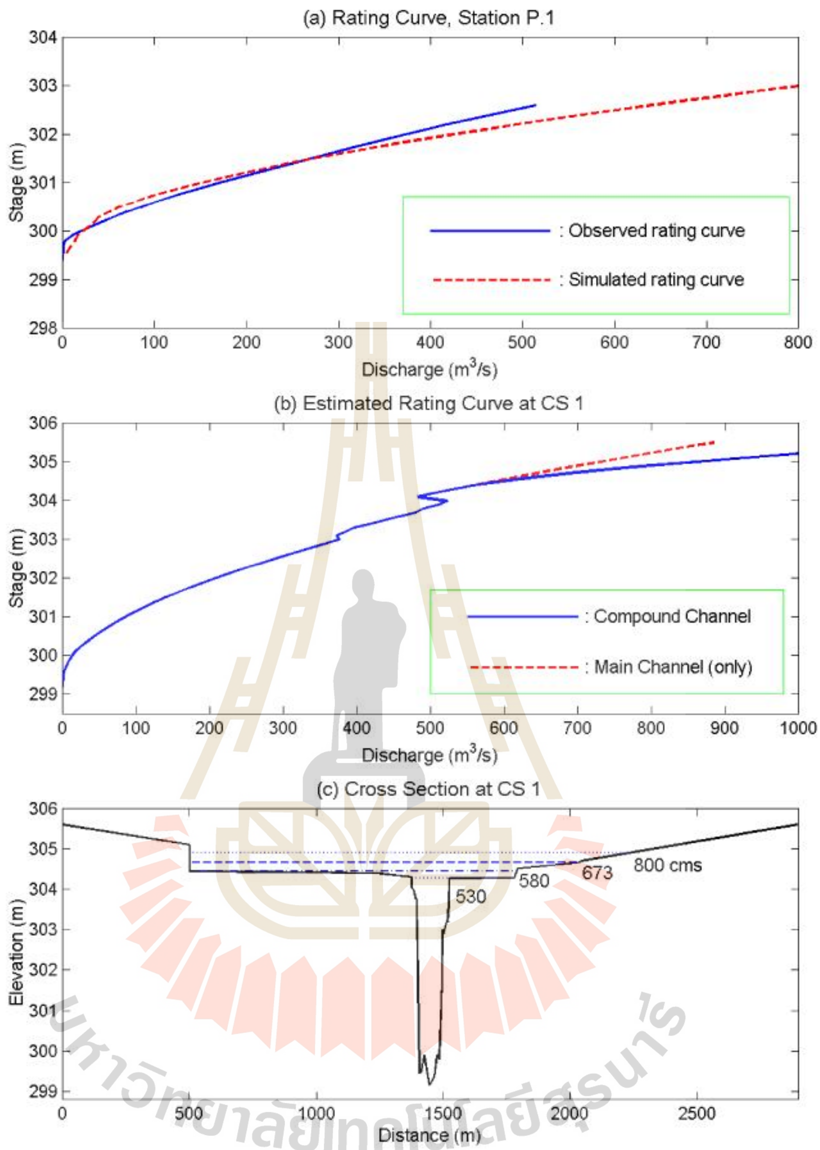

(a) Rating Curve, Station P.1
Stage (m)
Discharge (m3/s)
: Observed rating curve
: Simulated rating curve
(b) Estimated Rating Curve at CS 1
Stage (m)
Discharge (m3/s)
: Compound Channel
: Main Channel (only)
(c) Cross Section at CS 1
Elevation (m)
Distance (m)
530
580
673
800 cms

3.4.5 Approach to estimate 3-D flood map

Hourly flood extent mapping from previous section is generated from the interpolation of water surface level from seven cross sections of floodplain. To test whether the raster models are able to simulate 2-D flood propagation over more realistic floodplain topography, grid-based storage cell from step 10 in Figure 3.4 is generated again from 1-D to 2-D in a short interval of a floodplain cross section.

3.5 Results and Discussion

3.5.1 Synthetic rating curves and flood extent for different water levels and flood peaks

Given surveyed cross section and channel slope of Ping River at stream gauge P1 (slope = 0.0087), simulated rating curve fit to observed rating curve can be drawn with assumed Manning n=0.065 for in-bank flow in main channel (Figure 3.3a). Figure 3.3b presents an example of estimated rating curves at cross section CS1 for two cases: (i) main channel only, (ii) compound channel including the effect of trees and/or building distribution. The parameter m and k from calculated storage-discharge curve for seven cross sections are in the range of m=0.66-0.72 (for main channel) 1.55-2.15 (for floodplain) and k = 18417-4536 (main channel) and 0.19-20.35 (floodplain).

The next cross section (CS1) is about 450 m downstream of P1 where there is no stream gauge; a synthetic rating curve is drawn by using n the same as P1 and surveyed cross sections from the profile and cross section surveying project along Ping River for Chiang Mai's flood warning, completed in 2007 by the Royal Irrigation

Department. The rating curve is extended to over-bank flows on floodplain based on trial and error processes until assumed shape of floodplain provides a good fit between estimated and observed flood extent and inundation depth in the form of flood inundation mapping (see Figure 3.4). Final shape of compound channel at CS1 is shown in Figure 3.3c. Over-bank flow occurs when Q>510 m^3/s. For Q=530 m^3/s, water level, inundation extent from left and right river bank are 304.28, 1, and 255 m (line of sight toward downstream). The estimated distance of inundation extent for Q=530 m^3/s can be plotted on the map in Figure 3.5b. Plan view of the flood map shows that there is no over-bank flow on the right bank of Ping River but over-bank is found on the left bank. Estimated and observed flood extents on the left bank are identical. Inundation extents for the other Qs are estimated and plotted in the flood map; see Figure 3.5c, d, e, and f. By using the method similar to CS1 step 1 to 6 in Figure 3.4, water level and inundation extent from the river bank are calculated for the other six cross sections (CS2-CS7) downstream of CS1. The estimated distant of inundation extent for all cross sections with the same Q is plotted in the same map to present the boundary and area of inundation cover. These maps present a good agreement between observed and simulated flood extent where the fit index is higher than 75%. Some discrepancies between estimated and observed inundation extent are found, for example, at CS2, Q=580 m^3/s and at CS5, Q=600 m^3/s, mostly are underestimations.

3.5.2 Daily flood extent mapping

Flood plain inundation modeling from a snap shot of inundation extent on floodplain can be used to simulate a time series of flood extent. Moderate daily flood events during 19-22 September 2005 with Q=164, 543, 679 and 472 m^3/s are selected as an input to the proposed floodplain inundation model and used to generate daily floodplain inundation extents. Figure 3.6 presents a time series of daily flood map showing an expansion and contraction of flood extent along both sides of the Ping River. However, verification of these results with satellite images during this flood event is required. The results of flood routing model show that the simulated flood hydrograph from each river reaches are almost identical. This indicates that the attenuation of hydrograph due to the effect of routing in short channel storages (3,850 m from P1 to CS7) with some lateral inflows is not significant.

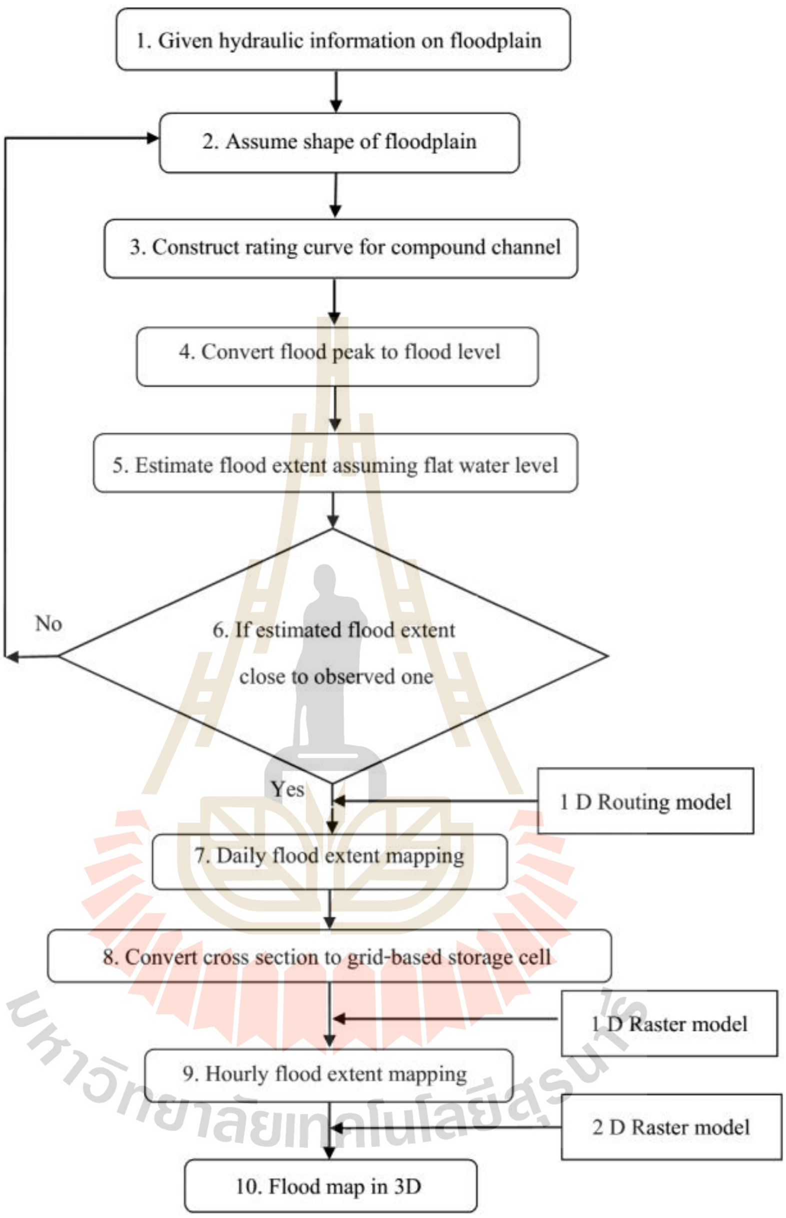
1. Given hydraulic information on floodplain
2. Assume shape of floodplain
3. Construct rating curve for compound channel
4. Convert flood peak to flood level
5. Estimate flood extent assuming flat water level
6. If estimated flood extent close to observed one
No
Yes
1 D Routing model
7. Daily flood extent mapping
8. Convert cross section to grid-based storage cell
1 D Raster model
9. Hourly flood extent mapping
2 D Raster model
10. Flood map in 3D

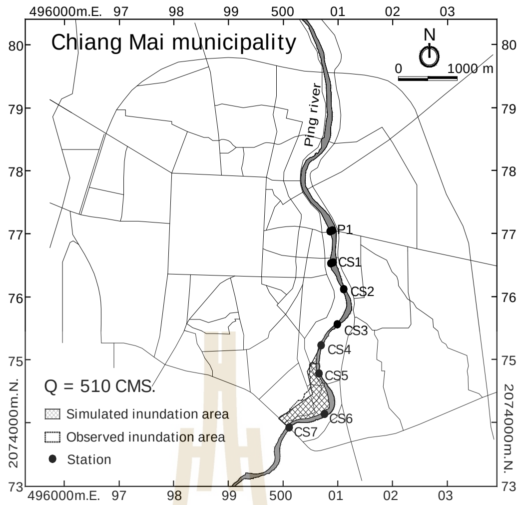
Chiang Mai municipality
496000m.E.
97
98
99
500
01
02
03
80
79
78
77
76
75
73
2074000m.N.
N
0
1000 m
Ping river
P1
CS1
CS2
CS3
CS4
CS5
CS6
CS7
Q = 510 CMS.
Simulated inundation area
Observed inundation area
Station

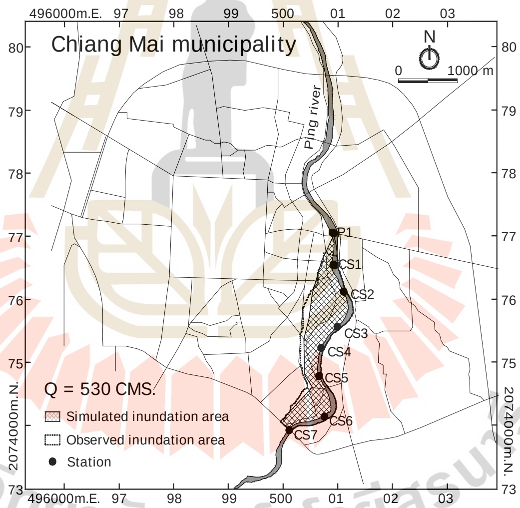
Chiang Mai municipality
496000m.E.
97
98
99
500
01
02
03
80
79
78
77
76
75
73
2074000m.N.
N
0
1000 m
Ping river
P1
CS1
CS2
CS3
CS4
CS5
CS6
CS7
Q = 530 CMS.
Simulated inundation area
Observed inundation area
Station

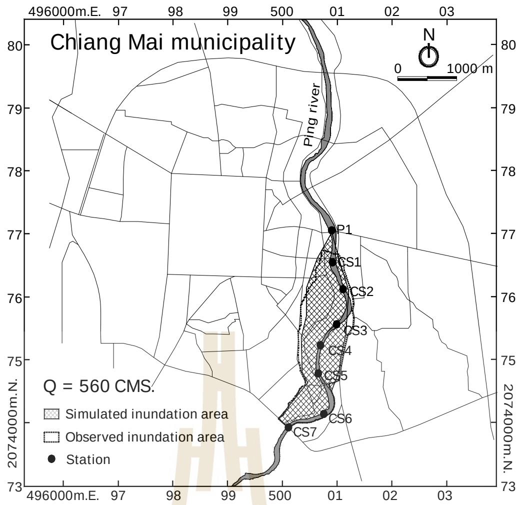
496000m.E. 97 98 99 500 01 02 03
Chiang Mai municipality
N
0 1000 m
Ping river
80
79
78
77
76
75
73
2074000m.N.
P1
CS1
CS2
CS3
CS4
CS5
CS6
CS7
Q = 560 CMS.
Simulated inundation area
Observed inundation area
Station

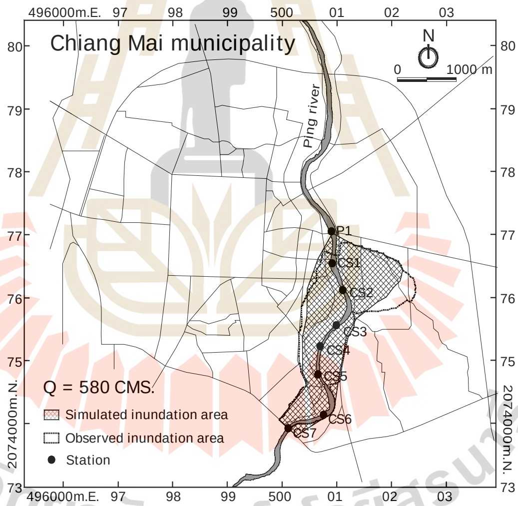
496000m.E. 97 98 99 500 01 02 03
Chiang Mai municipality
N
0 1000 m
Ping river
80
79
78
77
76
75
73
2074000m.N.
P1
CS1
CS2
CS3
CS4
CS5
CS6
CS7
Q = 580 CMS.
Simulated inundation area
Observed inundation area
Station

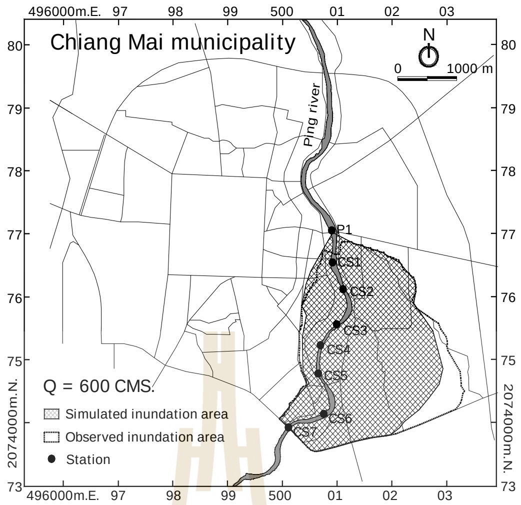
Chiang Mai municipality
Q = 600 CMS.
Simulated inundation area
Observed inundation area
Station
Ping river
P1
CS1
CS2
CS3
CS4
CS5
CS6
CS7
N
0
1000 m
496000m.E.
97
98
99
500
01
02
03
2074000m.N.
80
79
78
77
76
75
73

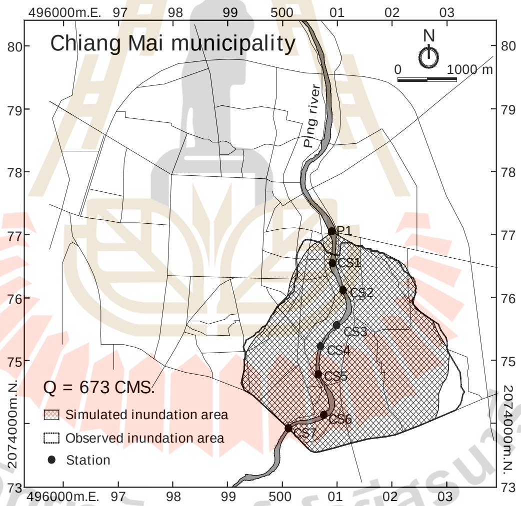
Chiang Mai municipality
Q = 673 CMS.
Simulated inundation area
Observed inundation area
Station
Ping river
P1
CS1
CS2
CS3
CS4
CS5
CS6
CS7
N
0
1000 m
496000m.E.
97
98
99
500
01
02
03
2074000m.N.
80
79
78
77
76
75
73

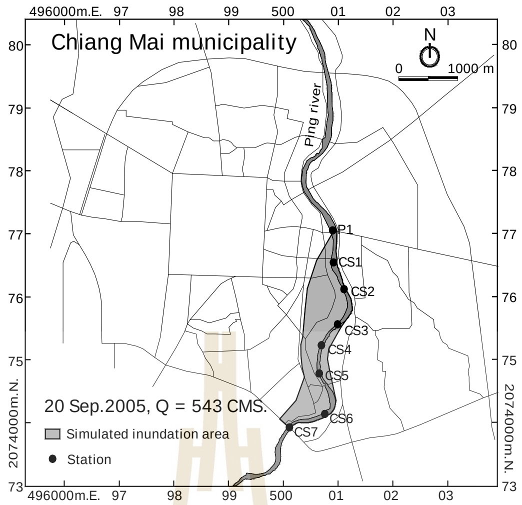
Chiang Mai municipality
Ping river
0 1000 m
N
P1
CS1
CS2
CS3
CS4
CS5
CS6
CS7
20 Sep.2005, Q = 543 CMS.
Simulated inundation area
Station
496000m.E.
2074000m.N.

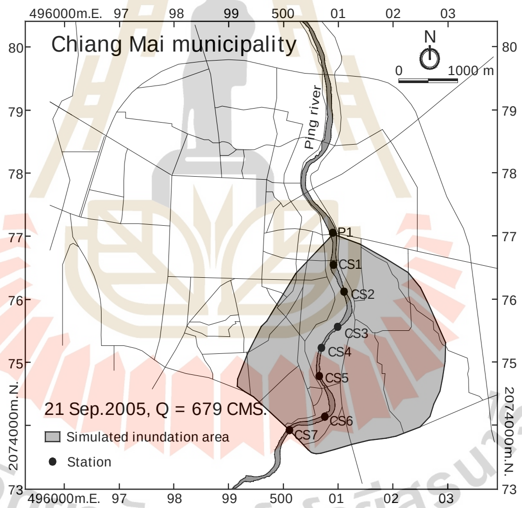
Chiang Mai municipality
Ping river
0 1000 m
N
P1
CS1
CS2
CS3
CS4
CS5
CS6
CS7
21 Sep.2005, Q = 679 CMS.
Simulated inundation area
Station
496000m.E.
2074000m.N.

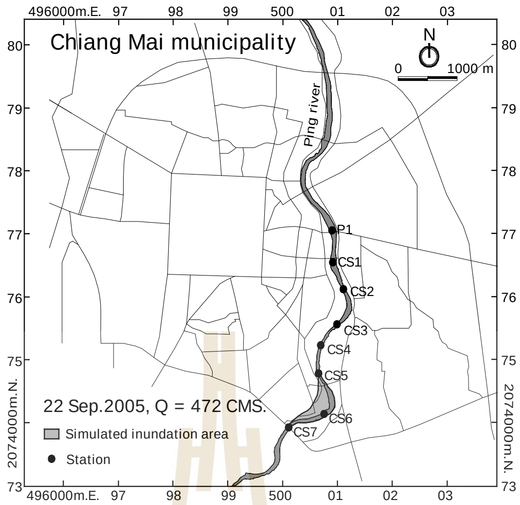
Chiang Mai municipality
496000m.E.
97
98
99
500
01
02
03
80
79
78
77
76
75
2074000m.N.
73
N
0
1000 m
Ping river
P1
CS1
CS2
CS3
CS4
CS5
CS6
CS7
22 Sep.2005, Q = 472 CMS.
Simulated inundation area
Station

For the first test, using u=1 ms^{-1}, ax=50 m, at=0.2 s, n=0.01 m$^{-1/3}$s to represent possible roughness on floodplain, total time=3,600 s and maximum water level=0.93 m, analytical solution from Equation 3.4 is presented in Figure 3.7a. Given initial condition, *h(t)* at x=0 from Equation 3.4, the diffusive and inertial models can generate the water surface curve almost fit to the curve from analytical solution. The inertial model performs better than the diffusive model.

For the second test, there is no direct analytical solution. The solution of Equation 3.3 can be obtained by numerical method using 4th order Runge-Kutta method. The common parameter values for this test similar to Test 1, but including S_0=10^{-3}, n=0.09 m$^{-1/3}$s, maximum water level=8.5 m, at=0.05 and 0.02 s for inertial and diffusive model, respectively. Maximum at is chosen to give no instability. Figure 3.7b shows estimated water surface elevation from the diffusive and inertial model compare to the numerical model.

For the third test, to investigate the simulation results from the whole cycle of flow reversals including rising front of flood waves during floodplain wetting and recession front during floodplain drying, a sinusoidal wave boundary condition is used at x=0, with wave amplitude 6.1 m period 4 hrs and S_0=10^{-3} for simulation period 7,200 s. There is no analytical solution for this test. Only the difference between the inertial and diffusive model is investigated (Figure 3.7c).

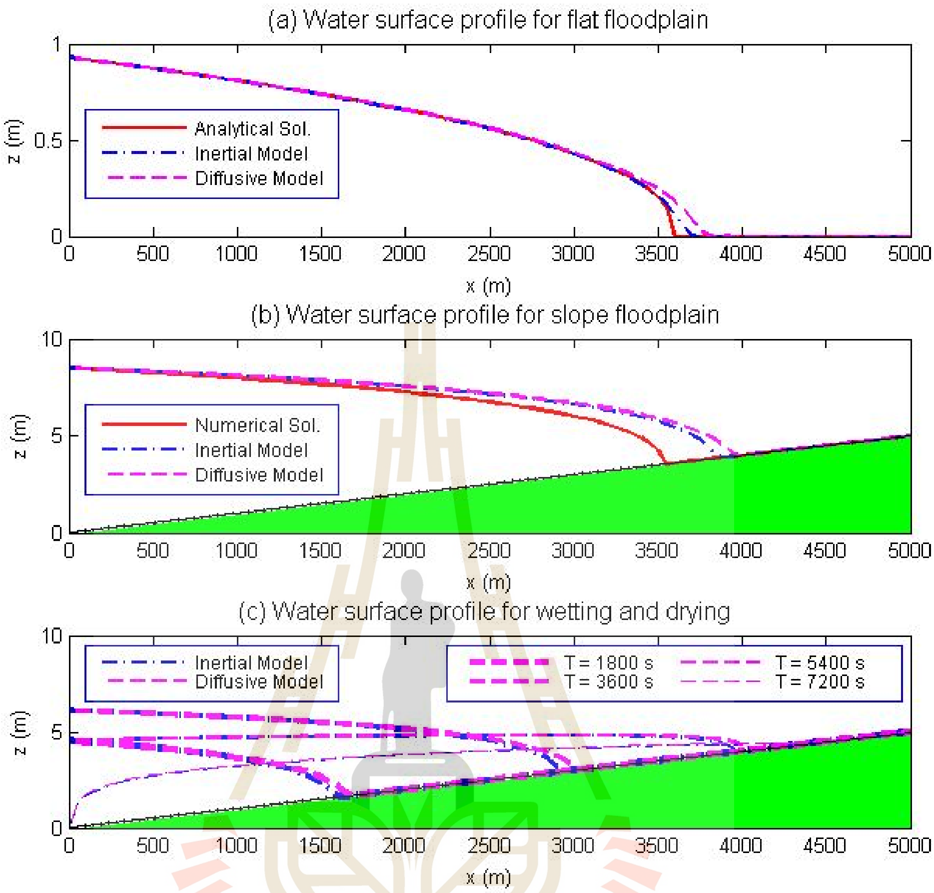
(a) Water surface profile for flat floodplain
Analytical Sol.
Inertial Model
Diffusive Model
z (m)
x (m)
(b) Water surface profile for slope floodplain
Numerical Sol.
Inertial Model
Diffusive Model
z (m)
x (m)
(c) Water surface profile for wetting and drying
Inertial Model
Diffusive Model
T = 1800 s
T = 3600 s
T = 5400 s
T = 7200 s
z (m)
x (m)

model.

(2) Simulation of one dimensional hourly flood extent

Test 1 to 3 are series of idealized case with increasing complexity. To demonstrate the numerical performance of the raster model working over complex topography, surveyed data at each cross-section is interpolate to grid-based storage cell with fine spatial resolution a*x*=50 m. A time series of observed flood hydrograph (during 20-21 September 2005) is interpolated for selected time step with smooth shape transition from daily to hourly or smaller time step. Receiving these input hydrograph, the inertial and diffusive model can be used to simulate a time series of water surface profile (Figure 3.8). For a longer duration (48 hrs), the diffusive model generates distance of flood extent longer than the inertial model. At a corner of steep river banks, simulated water levels likely encroached into the river banks. This unrealistic water profile can be minimized if the resolution of a*x* is decreased less than 50 m. The final step is the same as in Section 4.1, as the distance of inundation extent from all cross sections are combined to draw the map of time series of floodplain inundation extents, as shown in Figure 3.9.

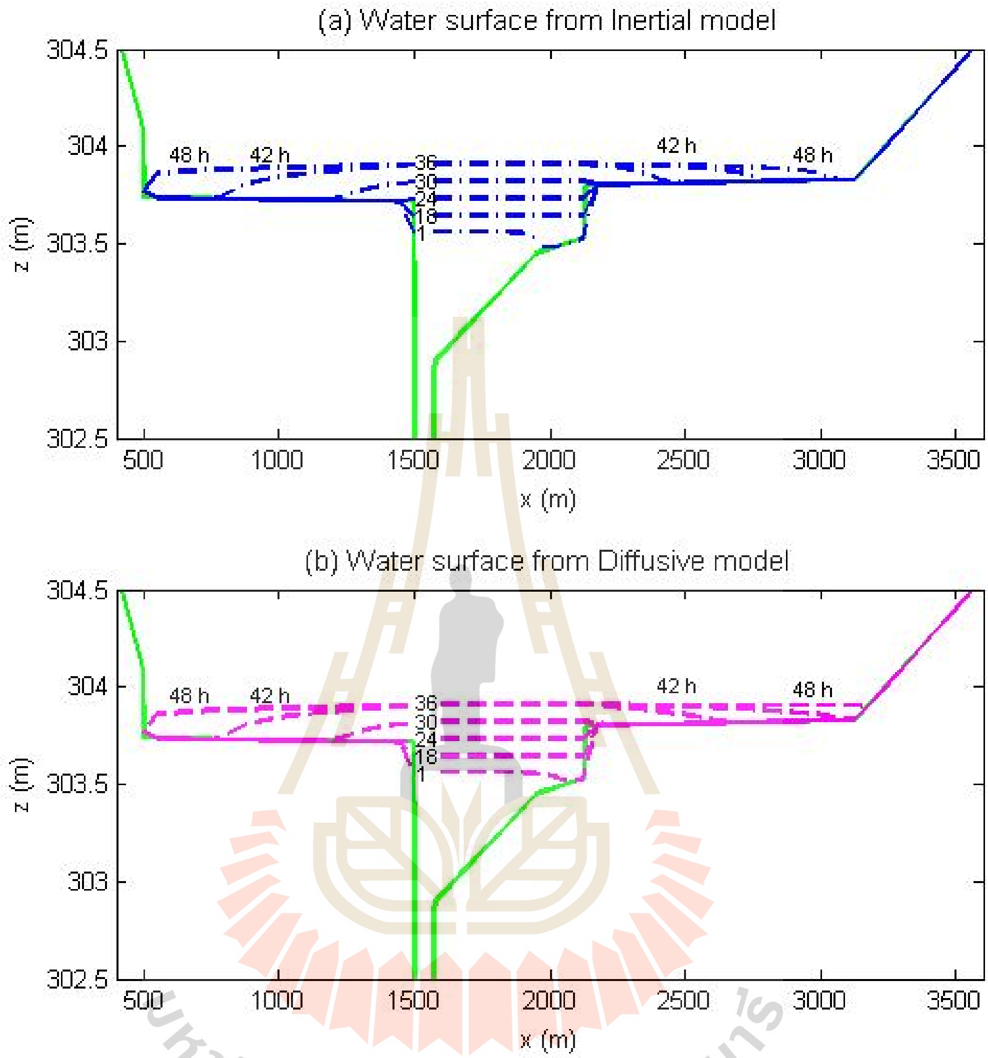
(a) Water surface from Inertial model
z (m)
x (m)
304.5
304
303.5
303
302.5
500
1000
1500
2000
2500
3000
3500
48 h
42 h
36
30
24
18
1
42 h
48 h
(b) Water surface from Diffusive model
z (m)
x (m)
304.5
304
303.5
303
302.5
500
1000
1500
2000
2500
3000
3500
48 h
42 h
36
30
24
18
1
42 h
48 h

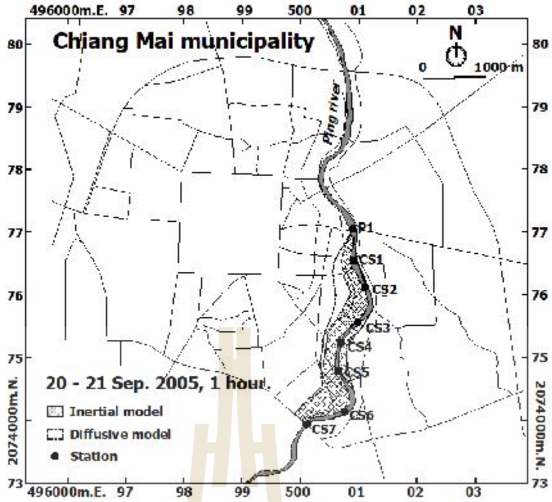

Chiang Mai municipality
Ping river
P1
CS1
CS2
CS3
CS4
CS5
CS6
CS7
20 - 21 Sep. 2005, 1 hour
Inertial model
Diffusive model
Station

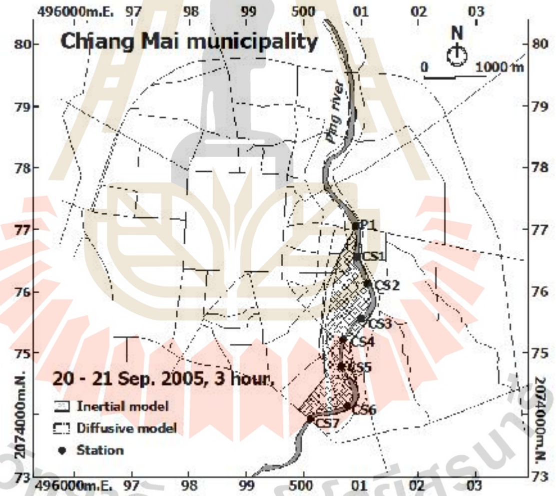

Chiang Mai municipality
Ping river
P1
CS1
CS2
CS3
CS4
CS5
CS6
CS7
20 - 21 Sep. 2005, 3 hour
Inertial model
Diffusive model
Station

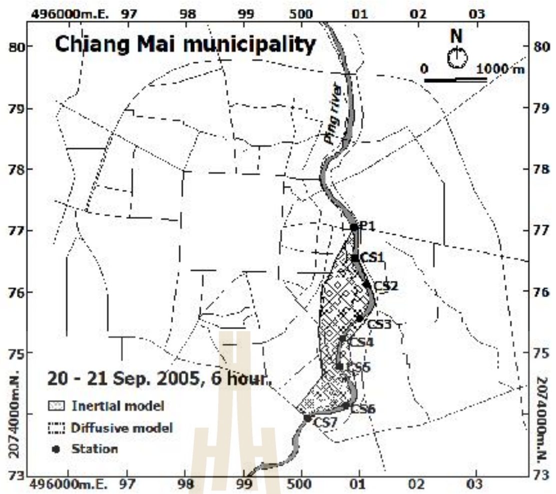
Chiang Mai municipality
496000m.E.
97
98
99
500
01
02
03
80
79
78
77
76
75
73
2074000m.N.
N
0
1000 m
Ping river
P1
CS1
CS2
CS3
CS4
CS5
CS6
CS7
20 - 21 Sep. 2005, 6 hour.
Inertial model
Diffusive model
Station

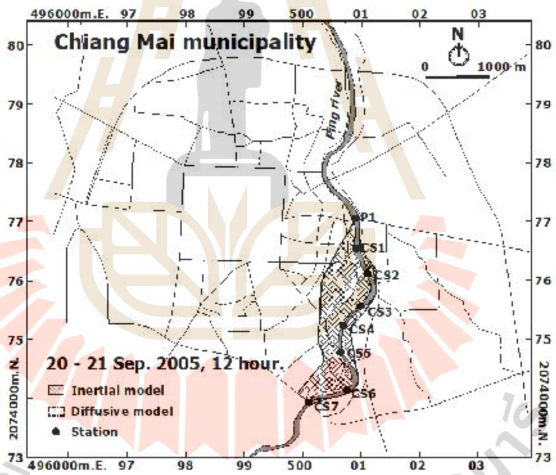
Chiang Mai municipality
496000m.E.
97
98
99
500
01
02
03
80
79
78
77
76
75
73
2074000m.N.
N
0
1000 m
Ping river
P1
CS1
CS2
CS3
CS4
CS5
CS6
CS7
20 - 21 Sep. 2005, 12 hour.
Inertial model
Diffusive model
Station

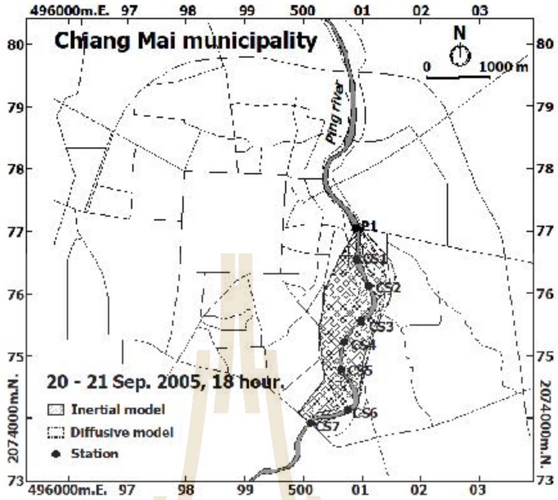
Chiang Mai municipality
Ping river
N
0 1000 m
P1
CS1
CS2
CS3
CS4
CS5
CS6
CS7
20 - 21 Sep. 2005, 18 hour
Inertial model
Diffusive model
Station
496000m.E.
2074000m.N.

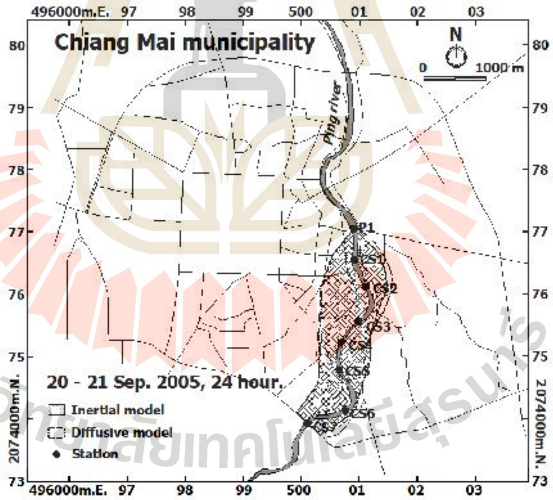
Chiang Mai municipality
Ping river
N
0 1000 m
P1
CS1
CS2
CS3
20 - 21 Sep. 2005, 24 hour
Inertial model
Diffusive model
Station
496000m.E.
2074000m.N.

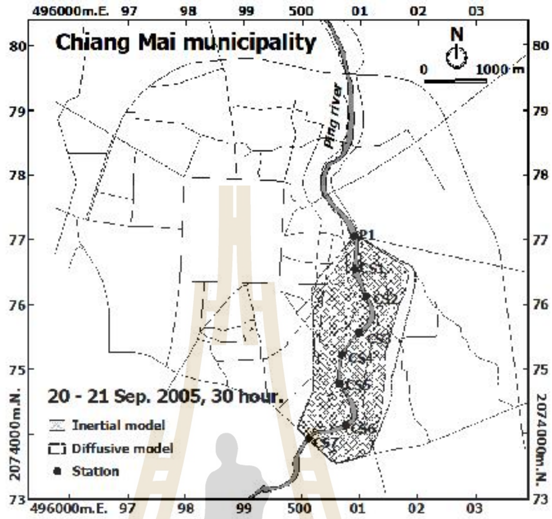
Chiang Mai municipality
N
0 1000 m
Ping river
P1
CS1
CS2
CS3
CS4
CS5
CS6
CS7
20 - 21 Sep. 2005, 30 hour.
Inertial model
Diffusive model
Station
496000m.E. 97 98 99 500 01 02 03
2074000m.N.

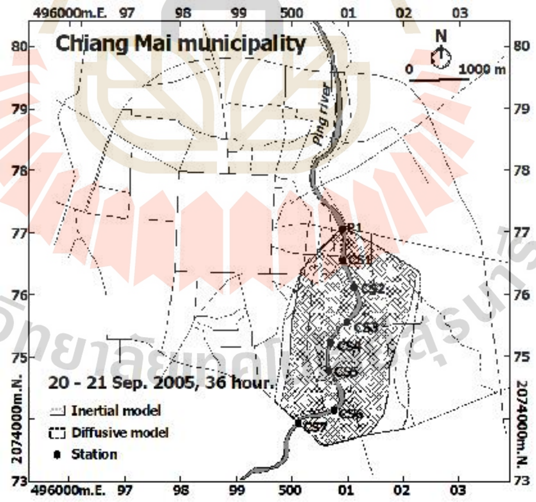
Chiang Mai municipality
N
0 1000 m
Ping river
P1
CS1
CS2
CS3
CS4
CS5
CS6
CS7
20 - 21 Sep. 2005, 36 hour.
Inertial model
Diffusive model
Station
496000m.E. 97 98 99 500 01 02 03
2074000m.N.

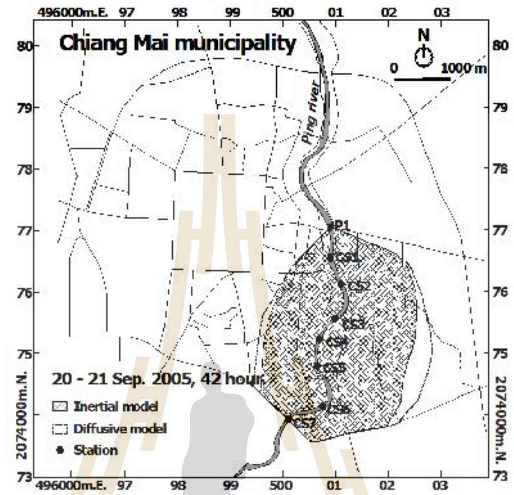
Chiang Mai municipality
496000m.E.
97
98
99
500
01
02
03
80
79
78
77
76
75
73
2074000m.N.
N
0
1000 m
Ping river
P1
CS1
CS2
CS3
CS4
CS5
CS6
CS7
20 - 21 Sep. 2005, 42 hour
Inertial model
Diffusive model
Station

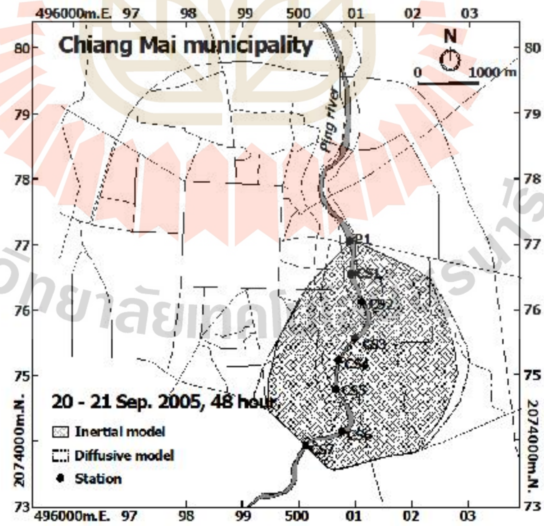
Chiang Mai municipality
496000m.E.
97
98
99
500
01
02
03
80
79
78
77
76
75
73
2074000m.N.
N
0
1000 m
Ping river
P1
CS1
CS2
CS3
CS4
CS5
CS6
CS7
20 - 21 Sep. 2005, 48 hour
Inertial model
Diffusive model
Station

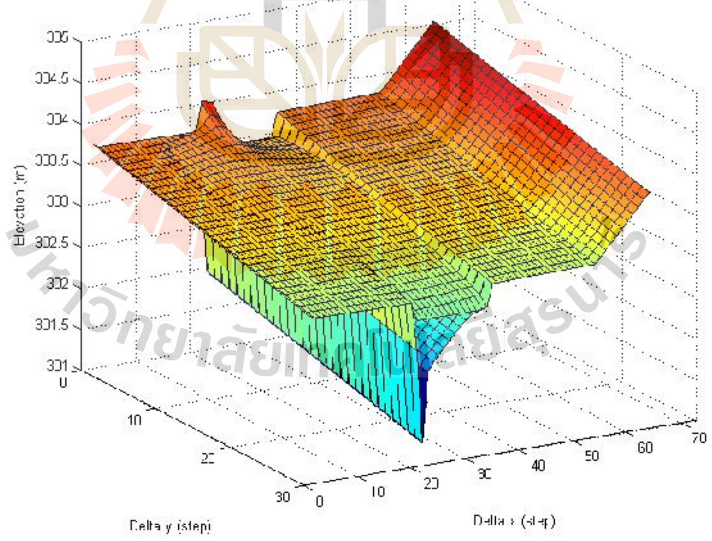
0 10 20 30 40 50 60 70

along the channel, slope = 0.0005, n = 0.09 $m^{-1/3}s$, a*x* = a*y* = 50 m, a*t* = 0.1 s.,

Running time = 3 hrs.

3.6 Conclusions

By using a synthetic rating curve for compound channel which includes the effect of trees and buildings distribution on floodplain, floodplain inundation model based on flat water surface assumption can be formulated with a number of selected channel cross sections. Although the vertical resolution of existing DEM (based on scale 1:50,000) for the floodplain of Chiang Mai Municipality is too low to represent any change of flood level, the assumed shape of floodplain can be defined and tested from a good fit between observed and simulated flood extent using the reverse engineering approach. This model can be used with confidence to construct a daily flood extent map.

To generate a time series of flood inundation maps from daily to hourly extents, a raster model consisting of diffusive and inertial formation are applied. The inertial model performs slightly better than the diffusive model for a horizontal floodplain and a slope floodplain, when compare to the analytical solution. The difference of simulated water level between the inertial and diffusive model become less pronounced for more complexity of floodplain topography and when receiving dynamic wetting and drying hydrograph. Inertial model can generate stable results with a time step larger than diffusive model due to increased stability with the addition of the inertial term. This study did not consider the computational performance and efficiency between different models.

If digital elevation data at a fine spatial resolution are available from an airborne laser altimetry survey or LiDAR data, then this data can be used to simulate more reliable inundation map and apply to the whole flooding area of Chiang Mai municipality, including the assessment of flood inundation extent from flood peaks with different exceedance probability or return period (Yin et al., 2013). The accuracy of flow patterns on floodplain depends on land surface characteristics and properties which can be interpreted from high resolution topographic information such as LiDAR data. This simplified floodplain inundation modeling are potential and alternative tools for developing countries where no spatial input data with high resolution are available.

3.7 Acknowledgement

The authors are grateful to Rajamangala University of Technology Isan (RMUTI) for financial support in form of a PhD Scholarship to the first author. We wish to acknowledge the Thai Meteorological Department, Royal Irrigation Department for providing field data. Special thanks go to Dr. Panya Polsan for his assistance to access hydrologic data.

3.8 References

Bates P. D. and De Roo A. P. J., 2000. A simple raster-based model for flood inundation simulation. In **Journal of Hydrology.** 236, 54-77.

Bates P. D., Horritt M. S. and Fewtrell T. J., 2010. A simple inertial formulation of the shallow water equations for efficient two-dimensional flood inundation modelling.

In **Journal of Hydrology.** 387, 33-45.

Bradbrook K. F., Lane S.N., Waller S. G. and Bates P.D., 2004. Two dimensional diffusion

wave modelling of flood inundation using a simplified channel representation.

In **International Journal River Basin Management.** 2(3), 211–223.

CENDRU (internet). General Information of the Upper Ping Basin (update 2013

April).Available from: **http://cendru.eng.cmu.ac.th/cmflood/** (in Thai).

Chatchawan S., 2005. Flood situation and flood protection report in Chiang Mai municipal

area 2005 (in Thai). Proceeding of the academic conferences: Towards society

harmony. In **Thai Development Research Institute Foundation**, Chon Buri,

Thailand, November 26-27, 2005.

Cook A. and Merwade V., 2009. Effect of topographic data, geometric configuration and

modeling approach on flood inundation mapping. In **Journal of Hydrology.** 377,

131-142.

De Kok J. L. and Grossmann M., 2010. Large-scale assessment of flood risk and the effects

of mitigation measures along the Elbe River. In **Nature Hazards.** 52, 143-166.

Ervine D. A. and MacLeod A. B., 1999. Modelling a river channel with distant floodbanks.

Proceedings of **the institute of civil engineers, Water maritime and energy,** 136(1), 21-33.

Fread D. L., 1993. Flow routing (Chap. 10). In **Handbook of applied hydrology**, D.R. Maidment, editor, MaGraw-Hill, New York, U.S.A.

Hagen E., Shroder Jr. J. F., Lu X. and Teufert J. F., 2010. Reverse engineered flood hazard

mapping in Afghanistan: A parsimonious flood map model for developing countries. **Quaternary International.** 226, 82-91.

Horritt M. S. and Bates P.D., 2002. Evaluation of 1D and 2D numerical models for predicting river flood inundation. In **Journal of Hydrology.** 268 (1-4), 87-99.

Hunter N. H., Bates P. D., Horritt M. S. and Wilson M. D., 2007. Simple spatially-distributed models for predicting flood inundation: a review. In **Geomorphology.** 90, 208-225.

Hunter N. H., Horritt M. S., Bates P. D., Wilson M. D. and Werner M. G. F., 2005. An adaptive time step solution for raster-based storage cell modelling of floodplain inundation. **Advances in Water Resources.** 28, 975-991.

Jothityangkoon C., Hirunteeyakul C., Boonrawd K. and Sivapalan M., 2013. Assessing the

impact of climate and land use changes on extreme floods in a large tropical catchment. In **Journal of Hydrology.** 490, 88-105.

Jothityangkoon C. and Sivapalan M., 2003. Towards estimation of extreme floods:

examination of the roles of runoff process changes and floodplain flows, In **Journal**

of Hydrology. 281, 206-229.

IPCC., 2007. Climate change 2007: **the scientific basis**, Cambridge University Press, Cambridge.

Merwade V.M., Olivera F., Arabi M. and Edleman S., 2008. Uncertainty in flood inundation mapping – current issues and future direction. **ASCE Journal of Hydrologic Engineering.** 13(7), 608-620.

Sarhadi A., Soltani S. and Modarres R., 2012. Probabilistic flood inundation mapping of ungauged rivers: Linking GIS techniques and frequency analysis. In **Journal of Hydrology.** 458-459, 68-86.

Tayefi V., Lane S. N., Hardy R. J. and Yu D., 2007. A comparison of one- and two-dimensional approaches to modelling flood inundation over complex upland floodplains. Hydrological Processes. 21(23), 3190-3202.

Yin J., Yu D., Yin Z., Wang J. and Xu S., 2013. Multiple scenario analyses of Huangpu River flooding using a 1D/2D coupled flood inundation model, In **Natural Hazards.** 66, 577-589.

Yu D. and Lane S.N., 2006. Urban fluvial flood modelling using a two-dimensional diffusion wave treatment, part 1: Mesh resolution effects. In **Hydrological Processes.** 20, 1541–1565.

CHAPTER IV

ASSESSING THE CLIMATE IMPACT ON FLOODPLAIN INUNDATION MAP IN THE CHIANG MAI MUNICIPALITY, UPPER PING RIVER BASIN OF THAILAND

4.1 Summary

Coupling of water balance model and floodplain inundation model is developed to receive projected rainfall time series from two types of regional climate model (RCM). Providing Regional Climates for Impacts Studies (PRECIS) and Meteorological Research Institute (MRI) are RCM with resolution 0.2 x 0.2 degree (grid size 20 x 20 km) daily time step, from year 2015-2044. They are generated from ECHAM 4 climate models. Empirical quantile mapping is used for bias correction of projection rainfall that its adjustment factors are estimated from comparison between observed and past projection rainfall from base-time period, year 1985-2014. A floodplain inundation model is applied based on 1D rating curve approach. This model receives peak runoffs as results from the water balance model, and generate flood extent in flood plain and draw flood inundation map of Chiang Mai municipality with different return periods. These expected results show the increase of flood inundation extent as a consequence of climate change.

4.2 Introduction

The impact assessment studies of climate change in various basins different part of the world indicate changes in the amount of precipitation, its frequency and intensity affecting the magnitude and seasonal pattern of streamflow. Sharma and Babel (Sharma and Babel, 2013) use the rainfall-runoff model (HEC-HMS) to receive time series of future projection rainfall from ECHAM4/OPYC general circulation model (GCM) for upper Ping river basin after they are improved by bias-correction and spatial disaggregation. Simulated results suggest a decrease of 13-19 % in annual streamflow and a shift in seasonal streamflow pattern. For regional and national scale studies, GCMs are a common tool to generate future projection climate variables at a coarse scale. For local scale such as basin level, many studies have applied different bias-correction and downscaling approaches to improve the local patterns of climate variables. Regional climate models (RCMs) are commonly used to transform coarse resolution GCM data to the local scale. Sharma and Babel (Sharma and Babel, 2013) use Gamma-Gamma distribution for rainfall intensity correction and use disaggregation model based on multiplicative random cascade approach for downscaling. To reduce bias of RCM simulation from Providing Regional Climates for Impacts Studies (PRECIS) and ECHAM4 climate models, Boonrawd and Jothityangkoon (Boonrawd and Jothityangkoon, 2015) use distribution mapping based on derived adjustment factors (AF), which is the ratio of observed and simulated rainfall depth for a given frequency of occurrence. They found that the combination of using seasonal AFs derived from monthly rainfall data for each month of all years, and AFs derived from all daily rainfall data and used to shift distribution of daily rainfall intensity provide the best improvement of simulated rainfall. Potential effect of both climate and land use change on the extreme flood for the upper Ping River Basin was studied by Jothityangkoon et al. (Jothityangkoon et al., 2013). A distributed rainfall–runoff model appropriate for extreme flood conditions is used to generate revised estimates of the Probable Maximum Flood (PMF). For mapping space-time flood extent of Chiang Mai floods, developed a coupling of a 1-D flood routing model and quasi 2-D floodplain inundation model to simulated temporal extent of flood area (Boonrawd and Jothityangkoon, 2015). This rainfall-runoff model and inundation model is used to receive future projection rainfall after bias correction and to delineate flood map in this study. Wuthiwongyothin et al. (Wuthiwongyothin et al., 2017) assessed the effects of climate change of the upper Ping River basin by using future projection rainfall from the ECHAM5 and the CCSM3 global climate model (GCM) They found that averaged discharge of inflow to Bhumibol dam increase to 17.3 % from 5.25 to 6.36 billion m^3 at the end of the 21th century (2016-2099). (Tangang, 2017) presents simulation output of more than ten CMIPS Global Climate Model (GCMs) from Southeast Asia Regional Climate Downscaling Experiment/ Coordinated Regional Climate Downscaling Experiment (SEACLID/CORDEX). Simulated results show a tendency of wetting in the northern area of equator by the increasing frequency of projected rainfall intensity 20 and 50 mm/day for near, mid, and end-of-century, and the increase of projected annual maxima for daily rainfall and daily rainfall intensity with 10 year return period. In contrast, the drying tendency is clearly increased such as the increase of projected consecutive dry day.

This chapter assesses the impacts of climate change on maximum annual discharges in the upper Ping River of Thailand and focusing on the future expansion of flood inundation in community area of Chiang Mai municipality and its vicinity, which is an initial step to develop possible flood hazard map (Osti et al., 2008).

4.3 Study area and RCM data

The Upper Ping River catchment is located in the north of Thailand. The river flows southward through the valley of Chiang Mai. The catchment area upstream of stream gauge station P1 (Navarat Bridge) and P68 (Ban Nam Tong) are 6,350 and 6,430 km^2, respectively. The flood study area covers about half of Chiang Mai municipality (40.2 km^2) and two districts (Pa Daet, 25 km^2 and Nong Hoi, 3.67 km^2) which lie on the floodplain of the Upper Ping River.

Observed flood inundation area

The observed flood inundation area from past floods was defined based on relationship between flood level at P1 and flood depth measured in the city during past flood events. Flood warning system for Chiang Mai city was set up in the form of flood hazard maps by Civil Engineering Natural Disaster Research Unit (CENDRU) (CENDRU, 2013). Inundation areas were divided into seven zones depending on upstream referenced water level at P1 (see Table 4.1 and Figure 4.1).

RCM data and observed rainfall

Two sets of time series of projection rainfall are generated from Providing Regional Climates for Impacts Studies (PRECIS) and Meteorological Research Institute (MRI) which receives input data from ECHAM4 climate models with resolution 0.2 x 0.2 degree (grid size 20 x 20 km.) daily time step, baseline period from year 1985-2014 (30 years) and future projection period from year 2015-2044 (30 years). The simulation covers the Intergovernmental Panel on Climate Change (IPCC)

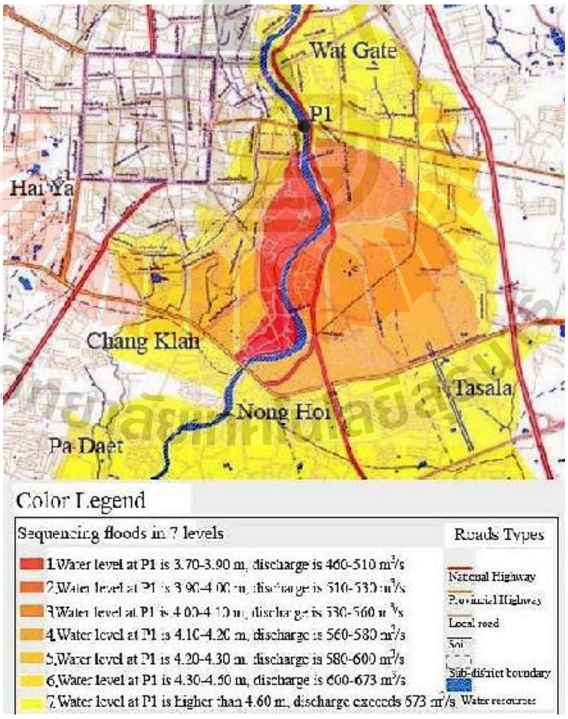
Wat Gate
P1
Hai Ya
Chang Klan
Tasala
Nong Hoi
Pa Daet
Color Legend
Sequencing floods in 7 levels
1.Water level at P1 is 3.70-3.90 m, discharge is 460-510 m³/s
2.Water level at P1 is 3.90-4.00 m, discharge is 510-530 m³/s
3.Water level at P1 is 4.00-4.10 m, discharge is 530-560 m³/s
4.Water level at P1 is 4.10-4.20 m, discharge is 560-580 m³/s
5.Water level at P1 is 4.20-4.30 m, discharge is 580-600 m³/s
6.Water level at P1 is 4.30-4.50 m, discharge is 600-673 m³/s
7.Water level at P1 is higher than 4.60 m, discharge exceeds 573 m³/s
Roads Types
National Highway
Provincial Highway
Local road
Soi
Sub-district boundary
Water resources

Table 4.1 Observed flood inundation area from past floods.

Observed flood (m^3/s)	Water level at P1 (m)	Inundation area (km^2)	Return period (year)
510	3.90	0.353	7.90
530	4.00	1.259	9.15
560	4.10	1.761	11.40
580	4.20	2.689	13.25
600	4.30	6.505	15.40
673	4.60	8.138	26.80

4.4 Methodology

To construct a map of floodplain inundation, the flowchart of 7 main steps is presented in Figure 4.2 and each step is explained in details in the following sub-section.

4.4.1 Derived AFs

The method of higher-skill bias corrected RCM data or empirical quantile mapping is operated based on derived adjustment factors (AF), which is the ratio between observed and simulated rainfall for a given frequency of occurrence. Correcting only the monthly mean precipitation can distort the relative variability of the inter-monthly precipitation distribution, and may adversely affect other moments of the probability distribution of daily precipitations. For bias correction test, the complexity of derived AFs is added in 5 method (Boonrawd and Jothityangkoon, 2015).

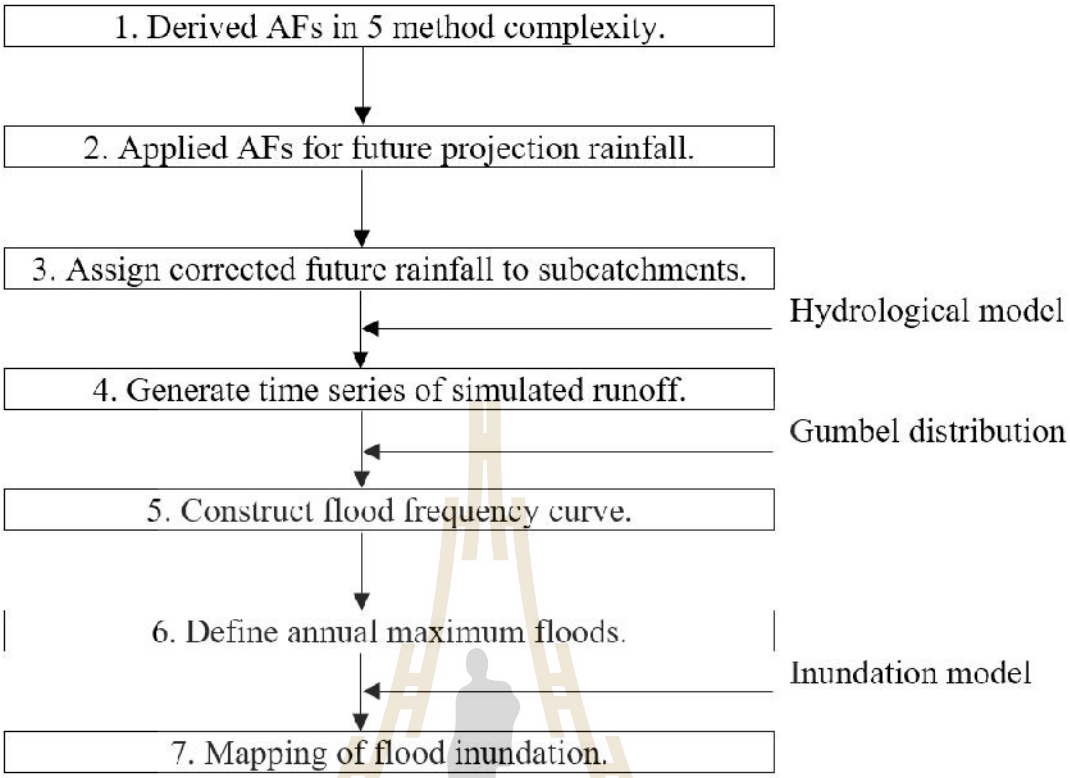
1. Derived AFs in 5 method complexity.
2. Applied AFs for future projection rainfall.
3. Assign corrected future rainfall to subcatchments.
Hydrological model
4. Generate time series of simulated runoff.
Gumbel distribution
5. Construct flood frequency curve.
6. Define annual maximum floods.
Inundation model
7. Mapping of flood inundation.

Method 4: seasonal AFs are derived from monthly rainfall data for each month of all years and used to shift distribution of monthly rainfall of each month (seasonal monthly AFs for monthly).

Method 5: is the combination of Method 4 for the first step and Method 1 for the second step (seasonal monthly AFs for monthly+ daily AFs for daily).

Boonrawd and Jothityangkoon, (2015) found that the Method 5 provides the best derived AFs compare to the other methods. An example of testing results from the Method 5 is shown in Figure 4.3 for PRECIS rainfall and Figure 4.4 for MRI rainfall. For calibration step, AFs are estimated from observed and simulated rainfall from RCM rainfall during 1982-1996 (15 years). For verification step, these estimated AFs are used to correct RCM rainfall during 1997-2011 (15 years) and compare to observed rainfall in the same verified period. For further testing in this study, the Method 5 is used to derive AFs for many locations of available observed rainfall. Finally, this method is used to derive AFs for every grids of RCM data.

4.4.2 Application of AFs for future projection rainfall

AFs are estimated again using the whole historical data (1982-2011, 30 years) for each grid. These AFs are used for bias correction of future projection rainfall at all grids of RCM data.

4.4.3 Assignment of corrected future rainfall to subcatchments

A time series of corrected future rainfall from a grid that give the shortest distance between the centroid of RCM grid and the subcatchment is assigned to the subcatchment.

4.4.4 Generation of time series of simulated runoff

A hydrological model used in this study is an adaptation of a sub-catchment based distributed water balance model developed by Jothityangkoon et al. (2013). The model has two components: a hillslope runoff generation model and a distributed flood routing model. The hillslope water balance model contains a number of parameters, which are measured or derived a priori from climate, soil and vegetation data or streamflow recession analyses. Based on the dynamics of water balance concept, discharges from each subcatchment are generated from 2 different runoff generation processes: saturation excess runoff and subsurface runoff. The catchment area upstream of P1 is divided into 62 subcatchments. The routing model based on a configuration of channel storages in parallel and series using constant averaged flow velocity (49.5 km/day) outlet at P1 estimated from time lag of observed hydrographs within the catchment. This model is applied to receive runoff from each subcatchment and route through river network to the outlet at P1.

4.4.5 Construction of flood frequency curve

Annual maximum of observed or simulated runoff is estimated from a time series of observed or simulated daily runoff and results from frequency analysis of the annual maximum are plotted in Gumbel distribution paper.

4.4.6 Defining annual maximum floods

The Extreme Value Type I distribution or Gumbel distribution is used to fit the observed or simulated annual maximum runoff. For a given specific return period, annual maximum flood can be estimated.

4.4.7 Mapping of flood inundation

Flood at specific return period is converted to flood level by using simulated rating curve for a compound channel developed by Jothityangkoon et al., (2013) Flat level of water surface is assumed and used to define intersection point between water surface and floodplain. At the same time, the shape or cross section of floodplain is estimated based on trial and error processes until assumed shape provides a good fit between estimated and observed flood extent in Figure 4.1. For each river cross section with estimated rating curve and the shape of floodplain, the distance of flood extent from the main channel for any flood magnitudes is calculated and use to draw flood map.

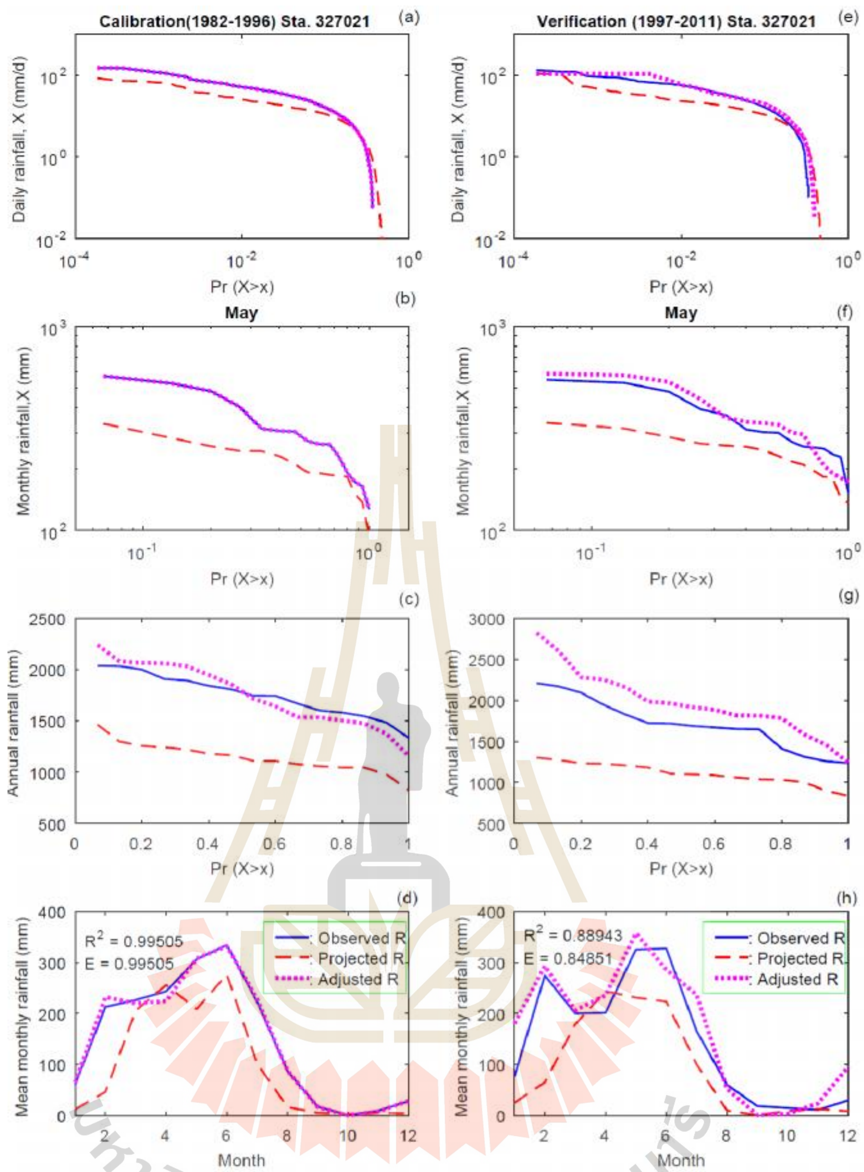

Calibration(1982-1996) Sta. 327021
(a)
Daily rainfall, X (mm/d)
Pr (X>x)
(b)
May
Monthly rainfall,X (mm)
Pr (X>x)
(c)
Annual rainfall (mm)
Pr (X>x)
(d)
Mean monthly rainfall (mm)
R^2 = 0.99505
E = 0.99505
Observed R
Projected R
Adjusted R
Month
Verification (1997-2011) Sta. 327021
(e)
Daily rainfall, X (mm/d)
Pr (X>x)
(f)
May
Monthly rainfall,X (mm)
Pr (X>x)
(g)
Annual rainfall (mm)
Pr (X>x)
(h)
Mean monthly rainfall (mm)
R^2 = 0.88943
E = 0.84851
Observed R
Projected R
Adjusted R
Month

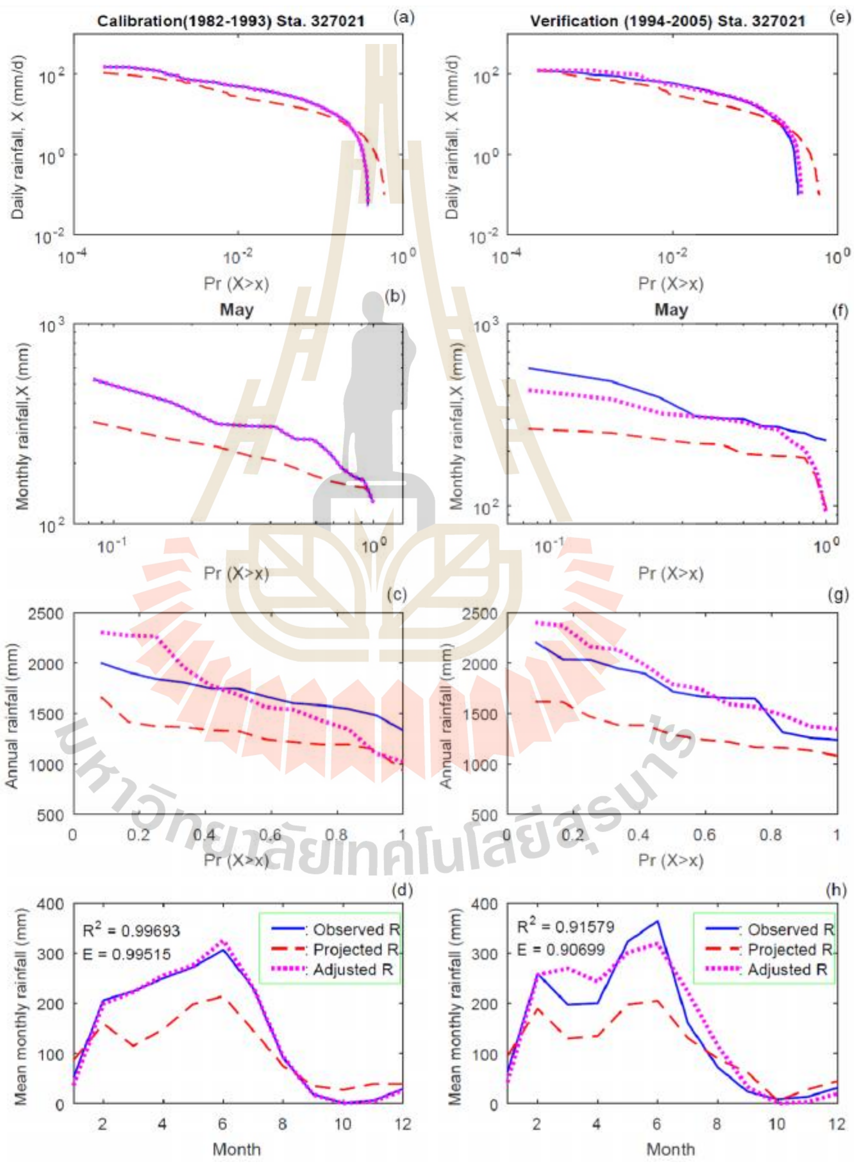

Calibration(1982-1993) Sta. 327021
(a)
Daily rainfall, X (mm/d)
Pr (X>x)
(b)
May
Monthly rainfall,X (mm)
Pr (X>x)
(c)
Annual rainfall (mm)
Pr (X>x)
(d)
R^2 = 0.99693
E = 0.99515
Observed R
Projected R
Adjusted R
Mean monthly rainfall (mm)
Month
Verification (1994-2005) Sta. 327021
(e)
Daily rainfall, X (mm/d)
Pr (X>x)
(f)
May
Monthly rainfall,X (mm)
Pr (X>x)
(g)
Annual rainfall (mm)
Pr (X>x)
(h)
R^2 = 0.91579
E = 0.90699
Observed R
Projected R
Adjusted R
Mean monthly rainfall (mm)
Month

and

adjusted rainfall at Sta. 327021, for calibrated results (a) to (d) and for

validated results (e) to (h), consisting of exceedance probability of

observed,

projected and adjusted data (daily, monthly annual and mean monthly

rainfall).

4.5 Results and Discussion

Return period of observed annual maximum flood in the fourth column of Table 4.1 shows that the return period of maximum observed flood for flood warning is about 27 years. By using derived AF based on Method 5 (combination of seasonal monthly AFs for monthly data and daily AFs for daily data), exceedance probability of annual and mean monthly projected rainfall are shifted close to observed rainfall (Figure 4.3, 4.4(b), (c), (f), (g)). For intra-annual variability, adjusted mean monthly rainfall has a good agreement with observed mean monthly rainfall for both PRECIS and MRI, calibration and validation period, coefficient of determination (R^2) > 0.89 and Nush-Sutcliffle efficient (E) > 0.84.

Figure 4.5 and Table 4.2 present observed and simulated annual maximum flood from different input rainfall. Simulated annual maximum flood from the water balance model with receiving observed rainfall similar to observed runoff for all return periods. Although, the time series of past projected rainfall from PRECIS and MRI are improved by bias correction using AFs, when the model receives past projected rainfall, simulated annual maximum is about 22-24 % for PRECIS and 31-35 % for MRI higher than simulated flood from observed rainfall.

Table 4.2 Annual maximum flood from different methods.

Return period (year)	Observed Max. Q (m^3/s)	Simulated annual maximum flood from (m^3/s)		
		Observed rainfall	Past projected R	
			PRECIS	MRI
10	524	542	649	696
25	663	664	806	869
50	754	754	923	998
100	843	844	1,038	1,125

Table 4.2 Annual maximum flood from different methods (cont.).

Return period (year)	Observed Max. Q (m^3/s)	Simulated annual maximum flood from (m^3/s)		
		Observed rainfall	Future projected R	
			PRECIS	MRI
10	524	542	706	1,014
25	663	664	866	1,298
50	754	754	985	1,509
100	843	844	1,103	1,718

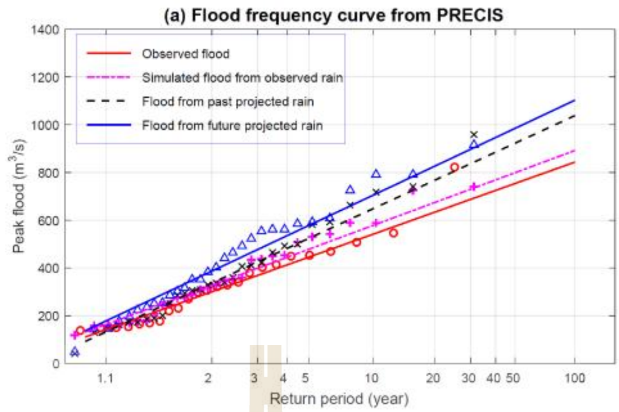
(a) Flood frequency curve from PRECIS
Observed flood
Simulated flood from observed rain
Flood from past projected rain
Flood from future projected rain
Peak flood (m³/s)
Return period (year)

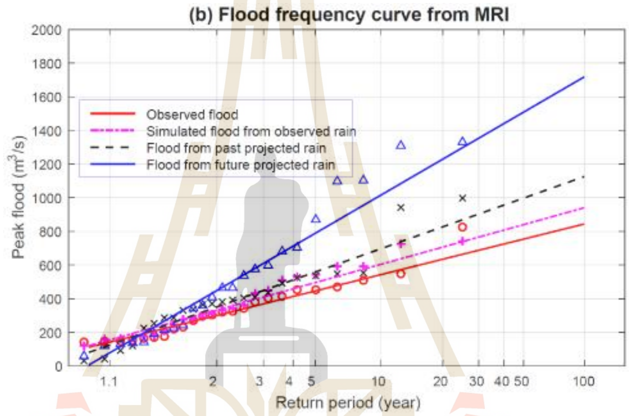
(b) Flood frequency curve from MRI
Observed flood
Simulated flood from observed rain
Flood from past projected rain
Flood from future projected rain
Peak flood (m³/s)
Return period (year)

Table 4.3 Flood inundation area.

Return period (year)	Flood inundation area (km^2)				
	Past floods	Future rainfall : PRECIS		Future rainfall : MRI	
		area	Increase (%)	area	Increase (%)
10	0.895	8.493	89.47	10.208	91.24
25	7.677	9.692	20.79	11.030	30.40
50	9.010	10.036	10.23	11.563	22.08
100	9.621	10.339	6.95	12.258	21.51

Due to climate change, if the model receives future projected rainfall, simulated annual maximum flood is about 31-35 % for PRECIS and 94-104 % for MRI, higher than simulated flood from observed rainfall (Table 4.2). In term of flood inundation area, future projected rainfall gives about 89.5, 20.8, 10.2, 7.0 % increase for PRECIS and 91.2, 30.4, 22.1, 21.5 % increase for MRI of inundation area compare to past flood area for 10, 25, 50 and 100 years return period, respectively (Table 4.3). Flood inundation maps and its boundary are presented in Figure 4.6 for PRECIS input and in Figure 4.7 for MRI input.

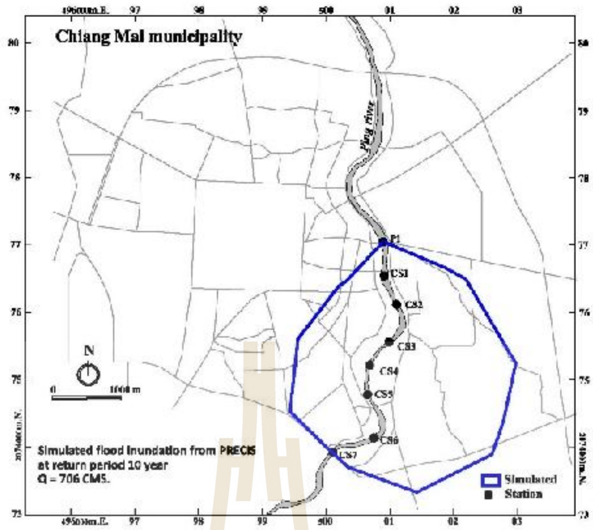
Chiang Mai municipality
Ping river
P1
CS1
CS2
CS3
CS4
CS5
CS6
CS7
N
1000 m
Simulated flood inundation from PRECIS
at return period 10 year
Q = 706 CMS.
Simulated
Station

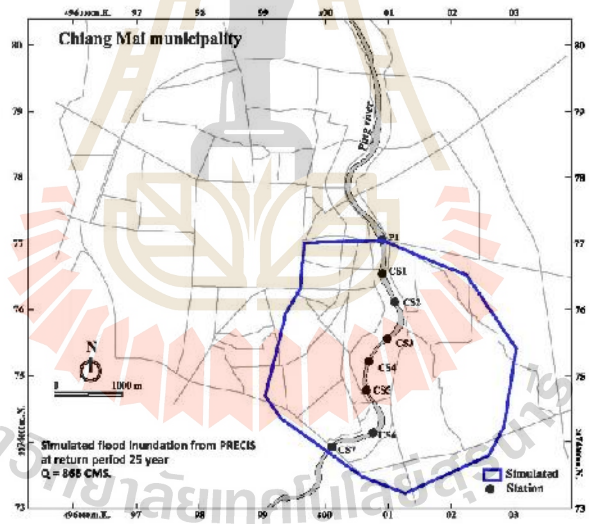
Chiang Mai municipality
Ping river
P1
CS1
CS2
CS3
CS4
CS5
CS6
CS7
N
1000 m
Simulated flood inundation from PRECIS
at return period 25 year
Q = 868 CMS.
Simulated
Station

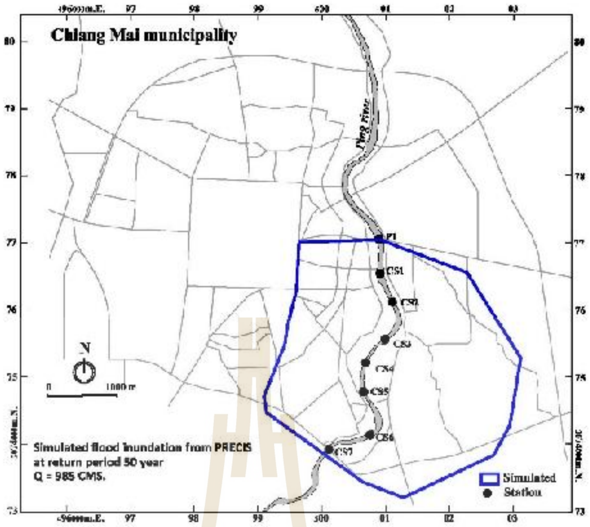
Chiang Mai municipality
Ping River
P1
CS1
CS2
CS3
CS4
CS5
CS6
CS7
N
0
1000 m
Simulated flood inundation from PRECIS
at return period 50 year
Q = 985 CMS.
Simulated
Station

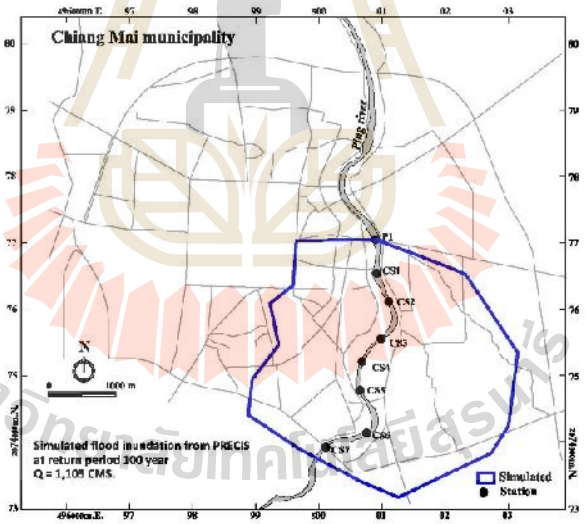
Chiang Mai municipality
Ping River
P1
CS1
CS2
CS3
CS4
CS5
CS6
CS7
N
0
1000 m
Simulated flood inundation from PRECIS
at return period 100 year
Q = 1,105 CMS.
Simulated
Station

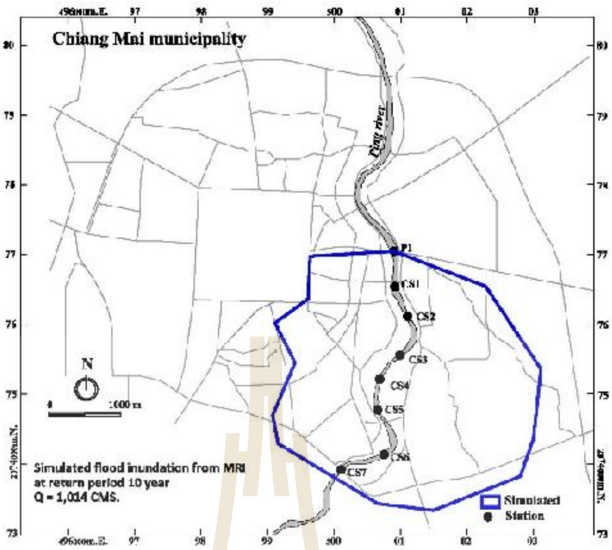
Chiang Mai municipality
Ping river
P1
CS1
CS2
CS3
CS4
CS5
CS6
CS7
N
1000 m
Simulated flood inundation from MRI
at return period 10 year
Q = 1,014 CMS.
Simulated
Station

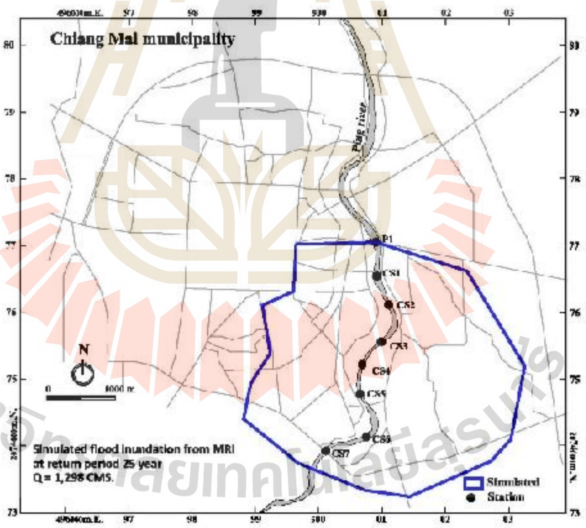
Chiang Mai municipality
Ping river
P1
CS1
CS2
CS3
CS4
CS5
CS6
CS7
N
Simulated flood inundation from MRI
at return period 25 year
Q = 1,298 CMS.
Simulated
Station

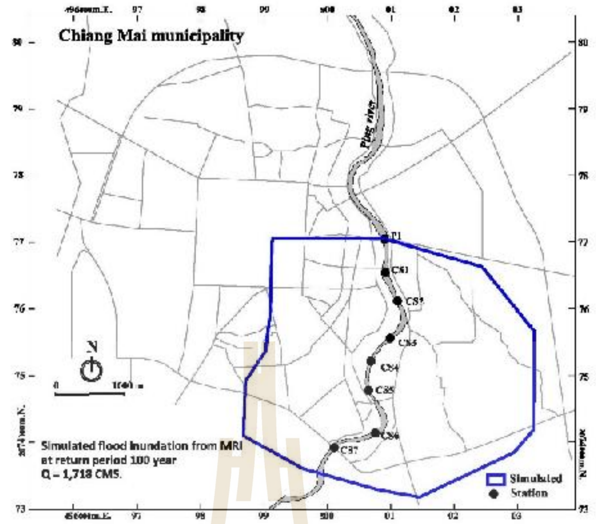
Chiang Mai municipality
Ping river
Simulated flood inundation from MRI
at return period 100 year
Q = 1,718 CMS.
Simulated
Station

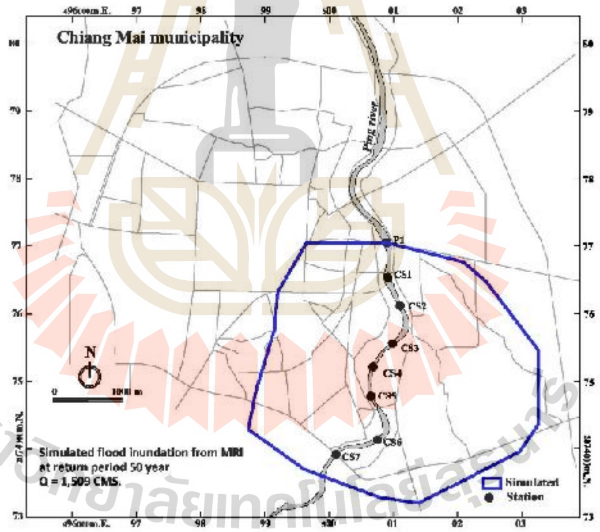
Chiang Mai municipality
Ping river
Simulated flood inundation from MRI
at return period 50 year
Q = 1,509 CMS.
Simulated
Station

4.6 Conclusion

To assess the impact of climate change, a time series of future projection rainfall from RCM rainfall models is used including PRECIS and MRI with bias correction. Combination of a water balance model and flood inundation model is linked to generate flood extent in flood plain and draw flood inundation map of Chiang Mai municipality. Simulated results show that the increase of flood inundation extent as a consequence of climate change. For bias correction method, adjustment factor based on empirical quantile mapping from a combination of seasonal monthly AF for monthly data and AFs for daily data is used to correct future projection rainfall from both PRECIS and MRI. By using a coupling of the distributed water balance model and floodplain inundation model to convert future projection rainfall from PRECIS to runoff and peak discharges and comparing to inundation area of past floods, the inundation area in Chiang Mai municipality is increased by 89.5, 20.8, 10.2 and 7.0 % with 10, 25, 50, 100 years return period, respectively. Similar trend occurs for MRI with higher percentage than PRECIS, increased by 91.2, 30.4, 22.1 and 21.5 % with 10, 25, 50, 100 years return period, respectively.

Limitation of this study is the use of projection rainfall from only two RCM outputs and using fixed landuse/ landcover. As being suggested by many studies of climate change impact, the use of more GCM, RCM and future IPCC scenario are required for decision-making processes in dealing with future uncertainty. However, it is expected that more RCM outputs are easily available in the future for this region. Integrated approach between climate change and land use change is recommended for future study.

4.7 Acknowledgements

This study was partly funded by the Institute of Research and Development, Suranaree University of Technology for the first author. Authors are grateful to Water Resources System Research Unit, Chulalongkorn University for providing MRI data.

4.8 References

Boonrawd K, Jothityangkoon C. Bias correction test of simulated rainfall from PRECIS using adjustment factors based on distribution mapping. In **Thai Hydrologist Association (THA) 2015 international conference on climate change and environmental management in Monsoon Asia**, 2015 January 28-30, Swissotel Concorde, Bangkok, Thailand, 2015.

Boonrawd K, Jothityangkoon C. Mapping temporal extent of Chiang Mai floods using coupled 1-D and quasi 2-D floodplain inundation models. In **Songklanakarin Journal of Science and Technology**, 2015;37 (2): 171-181.

CENDRU (internet). General Information of the Upper Ping Basin (update 2013 April).Available from: **http://cendru.eng.cmu.ac.th/cmflood/** (in Thai).

Jothityangkoon C, Hirunteeyakul C, Boonrawd K, Sivapalan M. Assessing the impact of climate and land use changes on extreme floods in a large tropical catchment.

In **Journal of Hydrology**, 2013; 490: 88-105.

Koontanakulvong S, Putthividhya A, Hoisungwan P, Suthitamnon C, Sakulthai S, Hanittinan P, Manajit A. Projected Change of Precipitation Extreme in River Basins in Thailand and China. In **The Thailand Research Fund (TRF)**, Project Code, RDG5530009; 2015.

Osti R, Tanaka S, Tokioka T. Flood hazard mapping in developing countries: problems and prospects, **Disaster Prevention and Management**, 2008;17(1): 104-113.

Sharma D, Babel MS. Application of downscaled precipitation for hydrological climate-change impact assessment in the upper Ping River Basin of Thailand, In **Climate Dynamics**. 2013;41:2589–2602, DOI 10.1007/s00382-013-1788-7.

Tangang F. Projected changes in mean precipitation, temperature and extremes over Southeast Asia region based on the multi-model simulations of SEACLID/CORDEX Southeast Asia. In **THA 2017. International Conference on Water Management and Climate Change Towards Asia's Water-Energy-Food Nexus**; 2017 January 25-27, Bangkok, Thailand, 2017.

Wuthiwongyothin S, Jang S, Ishida K, Kavvas ML. Assessment of Water Resources

During the 21st Century in Northern Thailand with Focus on Ping River Basin.

In **THA 2017 International Conference on Water Management and Climate Change Towards Asia's Water-Energy-Food Nexus;** 2017 January 25-27, Bangkok, Thailand, 2017.

APPENDIX A

FLOODPLAIN INUNDATION MAPPING WITHOUT HIGH RESOLUTION DEM

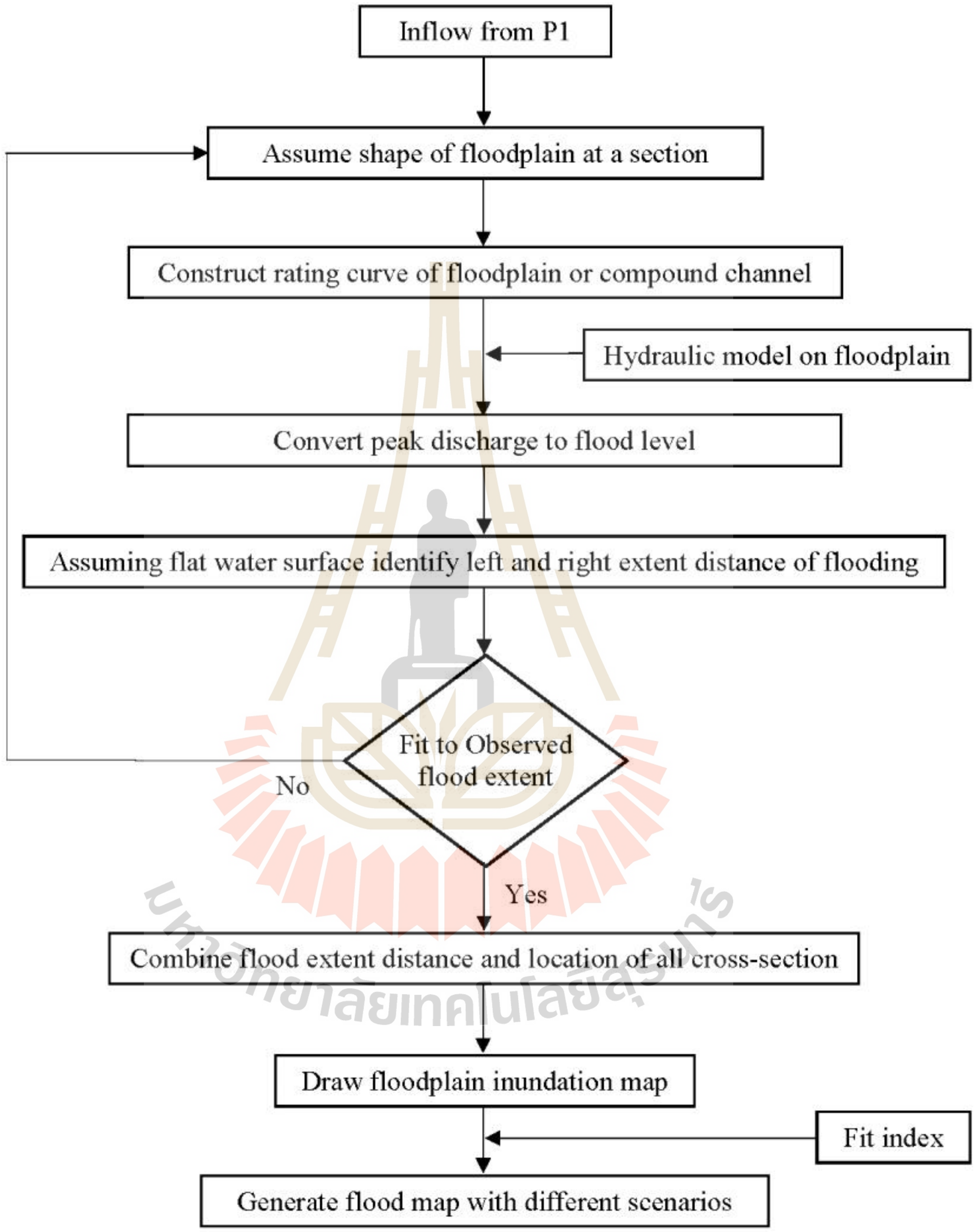
Inflow from P1
Assume shape of floodplain at a section
Construct rating curve of floodplain or compound channel
Hydraulic model on floodplain
Convert peak discharge to flood level
Assuming flat water surface identify left and right extent distance of flooding
Fit to Observed flood extent
No
Yes
Combine flood extent distance and location of all cross-section
Draw floodplain inundation map
Fit index
Generate flood map with different scenarios

Brief method on how to construct flood inundation map for the area without high resolution DEM is presented in Figure A 1

To draw the synthetic rating curve for compound channel, required parameters for each reaches are estimated from hydraulic properties, floodplain geometry and vegetation and building cover of compound channels (Figure A2). To solve the current problem of inadequate topographic input data for floodplain, the shapes of floodplain are defined by using fitting exercise based on the reverse approach between snap shot series of past and simulated inundation flood extent (Figure A3(c)) . These shapes are adjusted until the simulated and observed flood extents are similar and fit index is high enough. Mapping of daily flood can be generated relying on flat water levels.

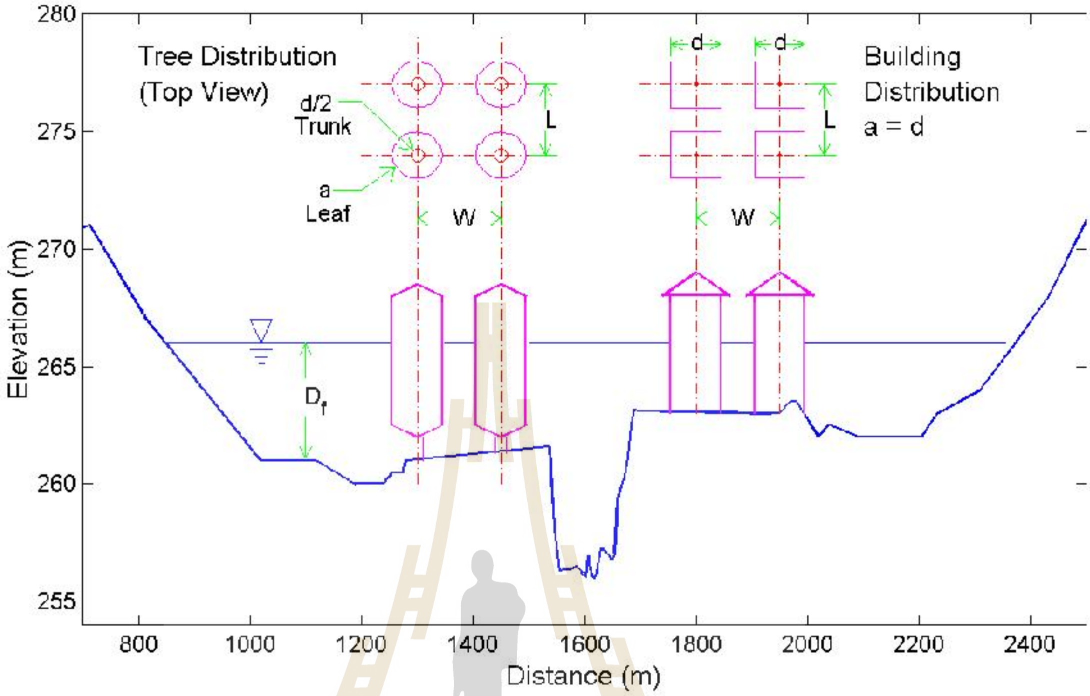

Tree Distribution
(Top View)
d/2
Trunk
a
Leaf
L
W
d
d
Building
Distribution
a = d
L
W
D_f
Elevation (m)
Distance (m)
280
275
270
265
260
255
800
1000
1200
1400
1600
1800
2000
2200
2400

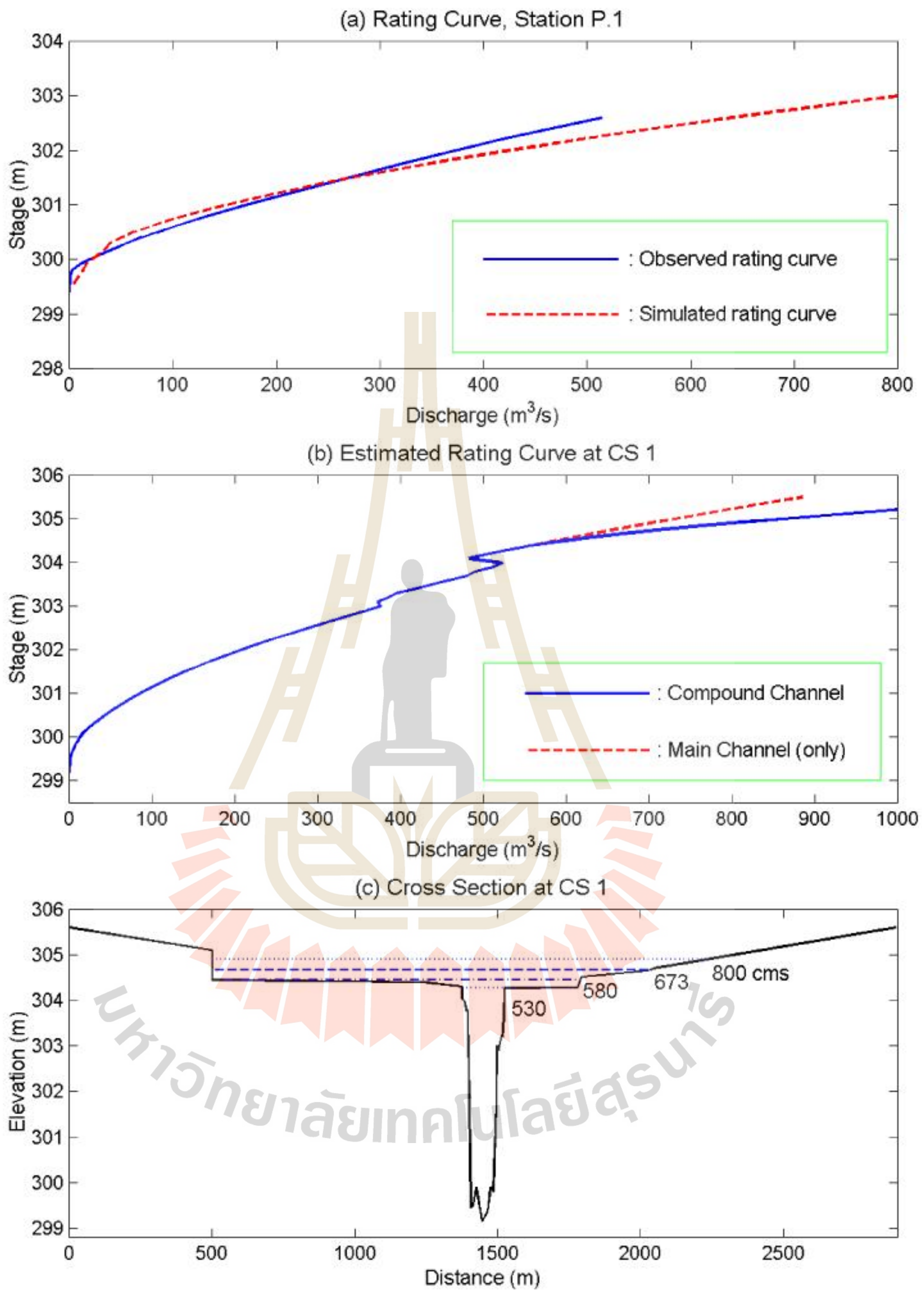
(a) Rating Curve, Station P.1
Stage (m)
Discharge (m3/s)
: Observed rating curve
: Simulated rating curve
(b) Estimated Rating Curve at CS 1
Stage (m)
Discharge (m3/s)
: Compound Channel
: Main Channel (only)
(c) Cross Section at CS 1
Elevation (m)
Distance (m)
530
580
673
800 cms

BIOGRAPHY

Mr. Kowit Boonrawd was born on October 1, 1975 in Pathumthani province, Thailand. He received his Bachelor of Science in Industrial Education (Civil Engineering) form Rajamangala Institute of Technology KhonKaen Campus in 1996. After graduation, he served in position of lecturer at Rajamangala Institute of Technology Sakonnakhon Campus in 1997, he received his Master's Degree in Civil Engineering (Water Resource Engineering) form KhonKaen University in 2004 and present he serve in position of lecturer at Rajamangala University of Technology Isan Sakonnakhon Campus. He continued with his Ph.D. graduate studies in the Civil Engineering Program, School of Civil Engineering, Suranaree University of Technology.